

**International
Journal of
Engineering
Technologies
(IJET)**

**Printed ISSN: 2149-0104
e-ISSN: 2149-5262**

**Volume: 3
No: 2
June 2017**

© Istanbul Gelisim University Press, 2017
Certificate Number: 23696
All rights reserved.

International Journal of Engineering Technologies is an international peer-reviewed journal and published quarterly. The opinions, thoughts, postulations or proposals within the articles are but reflections of the authors and do not, in any way, represent those of the Istanbul Gelisim University.

CORRESPONDENCE and COMMUNICATION:

Istanbul Gelisim University Faculty of Engineering and Architecture
Cihangir Mah. Şehit P. Onb. Murat Şengöz Sk. No: 8
34315 Avcilar / Istanbul / TURKEY
Phone: +90 212 4227020 Ext. 221
Fax: +90 212 4227401
e-Mail: ijet@gelisim.edu.tr
Web site: <http://ijet.gelisim.edu.tr>
<http://dergipark.gov.tr/ijet>
Twitter: [@IJETJOURNAL](https://twitter.com/IJETJOURNAL)


Printing and binding:

Anka Matbaa
Certificate Number: 12328
Phone: +90 212 5659033 - 4800571
E-mail: ankamatbaa@gmail.com

International Journal of Engineering Technologies (IJET) is included in:



**International Journal of Engineering Technologies (IJET) is
harvested by the following service:**

Organization	URL	Starting Date	Feature
 The OpenAIRE2020 Project	https://www.openaire.eu	2015	Open Access



INTERNATIONAL JOURNAL OF ENGINEERING TECHNOLOGIES (IJET)
International Peer-Reviewed Journal
Volume 3, No 2, June 2017 Printed ISSN: 2149-0104, e-ISSN: 2149-5262

Owner on Behalf of Istanbul Gelisim University
Rector Prof. Dr. Burhan AYKAC

Editor-in-Chief

Prof. Dr. Mustafa BAYRAM

Associate Editors

Prof. Dr. A. Burak POLAT
Assoc. Prof. Dr. Baris SEVIM
Asst. Prof. Dr. Ahmet AKTAS
Asst. Prof. Dr. Yalcin CEKIC
Asst. Prof. Dr. Ali ETEMADI

Publication Board

Prof. Dr. Mustafa BAYRAM
Prof. Dr. Nuri KURUOGLU
Prof. Dr. A. Burak POLAT
Asst. Prof. Dr. Ahmet AKTAS
Asst. Prof. Dr. Yalcin CEKIC
Asst. Prof. Dr. Mehmet Akif SENOL

Layout Editor

Asst. Prof. Dr. Ahmet AKTAS

Copyeditor

Res. Asst. Mehmet Ali BARISKAN

Proofreader

Asst. Prof. Dr. Ahmet AKTAS

Contributor

Ahmet Senol ARMAGAN

Cover Design

Mustafa FIDAN
Tarık Kaan YAGAN

Editorial Board

Professor Abdelghani AISSAOUI, University of Bechar, Algeria

Professor Gheorghe-Daniel ANDREESCU, Politehnica University of Timișoara, Romania

Associate Professor Juan Ignacio ARRIBAS, Universidad Valladolid, Spain

Professor Goce ARSOV, SS Cyril and Methodius University, Macedonia

Professor Mustafa BAYRAM, Istanbul Gelisim University, Turkey

Associate Professor K. Nur BEKIROGLU, Yildiz Technical University, Turkey

Professor Maria CARMEZIM, EST Setúbal/Polytechnic Institute of Setúbal, Portugal

Professor Luis COELHO, EST Setúbal/Polytechnic Institute of Setúbal, Portugal

Professor Filote CONSTANTIN, Stefan cel Mare University, Romania

Professor Furkan DINCER, Mustafa Kemal University, Turkey

Professor Mamadou Lamina DOUMBIA, University of Québec at Trois-Rivières, Canada

Professor Tsuyoshi HIGUCHI, Nagasaki University, Japan

Professor Dan IONEL, Regal Beloit Corp. and University of Wisconsin Milwaukee, United States

Professor Luis M. San JOSE-REVUELTA, Universidad de Valladolid, Spain

Professor Vladimir KATIC, University of Novi Sad, Serbia

Professor Fujio KUROKAWA, Nagasaki University, Japan

Professor Salman KURTULAN, Istanbul Technical University, Turkey

Professor João MARTINS, University/Institution: FCT/UNL, Portugal

Professor Ahmed MASMOUDI, University of Sfax, Tunisia

Professor Marija MIROSEVIC, University of Dubrovnik, Croatia

Professor Mato MISKOVIC, HEP Group, Croatia

Professor Isamu MORIGUCHI, Nagasaki University, Japan

Professor Adel NASIRI, University of Wisconsin-Milwaukee, United States

Professor Tamara NESTOROVIC, Ruhr-Universität Bochum, Germany

Professor Nilesh PATEL, Oakland University, United States

Professor Victor Fernão PIRES, ESTSetúbal/Polytechnic Institute of Setúbal, Portugal

Professor Miguel A. SANZ-BOBI, Comillas Pontifical University /Engineering School, Spain

Professor Dragan ŠEŠLIJA, University of Novi Sad, Serbia

Professor Branko SKORIC, University of Novi Sad, Serbia

Professor Tadashi SUETSUGU, Fukuoka University, Japan

Professor Takaharu TAKESHITA, Nagoya Institute of Technology, Japan

Professor Yoshito TANAKA, Nagasaki Institute of Applied Science, Japan

Professor Stanimir VALTCHEV, Universidade NOVA de Lisboa, (Portugal) + Burgas Free University, (Bulgaria)

Professor Birsen YAZICI, Rensselaer Polytechnic Institute, United States

Professor Mohammad ZAMI, King Fahd University of Petroleum and Minerals, Saudi Arabia

Associate Professor Lale T. ERGENE, Istanbul Technical University, Turkey

Associate Professor Leila PARSA, Rensselaer Polytechnic Institute, United States

Associate Professor Yuichiro SHIBATA, Nagasaki University, Japan

Associate Professor Kiruba SIVASUBRAMANIAM HARAN, University of Illinois, United States

Associate Professor Yilmaz SOZER, University of Akron, United States

Associate Professor Mohammad TAHA, Rafik Hariri University (RHU), Lebanon

Assistant Professor Kyungnam KO, Jeju National University, Republic of Korea

Assistant Professor Hidenori MARUTA, Nagasaki University, Japan

Assistant Professor Hulya OBDAN, Istanbul Yildiz Technical University, Turkey

Assistant Professor Mehmet Akif SENOL, Istanbul Gelisim University, Turkey

Dr. Jorge Guillermo CALDERÓN-GUIZAR, Instituto de Investigaciones Eléctricas, Mexico

Dr. Rafael CASTELLANOS-BUSTAMANTE, Instituto de Investigaciones Eléctricas, Mexico

Dr. Guray GUVEN, Conductive Technologies Inc., United States

Dr. Tuncay KAMAS, Eskişehir Osmangazi University, Turkey

Dr. Nobumasa MATSUI, Faculty of Engineering, Nagasaki Institute of Applied Science, Nagasaki, Japan

Dr. Cristea MIRON, Politehnica University in Bucharest, Romania

Dr. Hiroyuki OSUGA, Mitsubishi Electric Corporation, Japan

Dr. Youcef SOUFI, University of Tébessa, Algeria

Dr. Hector ZELAYA, ABB Corporate Research, Sweden

From the Editor

Dear Colleagues,

On behalf of the editorial board of International Journal of Engineering Technologies (IJET), I would like to share our happiness to publish the tenth issue of IJET. My special thanks are for members of editorial board, publication board, editorial team, referees, authors and other technical staff.

Please find the tenth issue of International Journal of Engineering Technologies at <http://ijet.gelisim.edu.tr> or <http://dergipark.gov.tr/ijet>. We invite you to review the Table of Contents by visiting our web site and review articles and items of interest. IJET will continue to publish high level scientific research papers in the field of Engineering Technologies as an international peer-reviewed scientific and academic journal of Istanbul Gelisim University.

Thanks for your continuing interest in our work,

Professor Mustafa BAYRAM
Istanbul Gelisim University
mbayram@gelisim.edu.tr

<http://ijet.gelisim.edu.tr>
<http://dergipark.gov.tr/ijet>

Printed ISSN: 2149-0104

e-ISSN: 2149-5262

International Journal of
Engineering Technologies
IJET

Table of Contents

	<u>Page</u>
<i>From the Editor</i>	<i>vii</i>
<i>Table of Contents</i>	<i>ix</i>
<ul style="list-style-type: none">• Evaluation of Optimal Economic Life of Cemented Carbide Tool Turning AISI4340 / <i>Olurotimi Akintunde Dahunsi, Olayinka Oladele Awopetu, Tunde Isaac Ogedengbe, Tiamiyu Ishola Mohammed, Taiwo Micheal Adamolekun</i>	37-43
<ul style="list-style-type: none">• Lessons Learned from Collapse of Zumrut Building under Gravity Loads / <i>Can Balkaya</i>	44-49
<ul style="list-style-type: none">• Engineering Material Selection for Automotive Exhaust Systems Using CES Software / <i>Ikpe Aniekan E., Orhorhoro Ejiroghene Kelly, Gobir Abdulsamad</i>	50-60
<ul style="list-style-type: none">• Conceptual Guideway Structural Design for MAGLEV High-speed Ground Transportation System / <i>Can Balkaya, W.J. Hall</i>	61-71
<ul style="list-style-type: none">• Optimum Insulation Thickness for the Exterior Walls of Buildings in Turkey Based on Different Materials, Energy Sources and Climate Regions / <i>Cenker Aktemur, Uğur Atikol</i>	72-82
<ul style="list-style-type: none">• Prominence of Hadfield Steel in Mining and Minerals Industries: A Review / <i>Chijioke Okechukwu, Olurotimi Akintunde Dahunsi, Peter Kayode Oke, Isiaka Oluwole Oladele, Mohammed Dauda</i>	83-90

International Journal of Engineering Technologies, IJET

e-Mail: ijet@gelisim.edu.tr

Web site: <http://ijet.gelisim.edu.tr>

<http://dergipark.gov.tr/ijet>

Twitter: [@IJETJOURNAL](https://twitter.com/IJETJOURNAL)

Evaluation of Optimal Economic Life of Cemented Carbide Tool Turning AISI4340

Olurotimi Akintunde Dahunsi[‡], Olayinka Oladele Awopetu, Tunde Isaac Ogedengbe,
Tiamiyu Ishola Mohammed and Taiwo Micheal Adamolekun

Mechanical Engineering Department, Federal University of Technology, P. M. B. 704, Akure, Ondo State, Nigeria.

(oadahunsi@futa.edu.ng, ooawopetu@futa.edu.ng, tiogedengbe@futa.edu.ng, timohammed@futa.edu.ng, tmadamolekun@futa.edu.ng)

[‡]Olurotimi Akintunde Dahunsi; First Author, Mechanical Engineering Department, Federal University of Technology, P. M. B. 704, Akure, Ondo State, Nigeria, Tel: +234 816 253 9990,
tundedahunsi@gmail.com

Received: 11.01.2017 Accepted: 02.05.2017

Abstract- As turning operation proceeds on a lathe machine, it is required that sufficiently good surface quality be achieved if all the affecting parameters, including tool geometry are held constant. In this paper, the effect of tool geometry variation due to wear in the case of C6 cemented carbide tool on AISI 4340, was studied. Using surface roughness as yardstick for estimating the point beyond which the maximum economic utilization derivable from the tool is hampered, it was realized that each insert should be replaced after ten minutes of turning operation to retain their optimum usefulness. The tool wear parameters were found to be in linear relationship with the cutting time, while the average surface roughness was modelled nonlinearly using an exponential function. A fourth degree polynomial approximated the trend for the cutting force. Sharp deflections were observed on the surface roughness and cutting force graphs after the tenth minute. Generally for the entire cutting time, the measured cutting force increased by about 33% while the flank wear width and crater wear width increased by 170% and 56% respectively. Surface roughness also increased by about 130%.

Keywords Carbide tool, AISI 4340, surface roughness, tool wear, tool geometry.

1. Introduction

Modern manufacturing technologies calls for simultaneous improvement in control of dimensional accuracy and surface textures of machined work pieces. Surface roughness specification is often necessary on several parts to properly fulfil their required functions. For example, fatigue life, bearing properties, and wear are three major factors that make the control of surface texture important. The basic objective of finish turning of hard metals is the achievement of the best surface quality possible at the most optimal and economic tool [1, 2, 3, 4].

While the surface roughness obtained from machining the workpiece on a lathe is dependent on the workpiece material and its hardness, it is also influenced by the cutting tool material used, cutting speed, feed rate and the tool geometry (particularly, tool nose radius), the rigidity of the

machine and the tool, as well as, the type and effectiveness of the cutting fluid used [5].

AISI 4340 belongs to a family of steel alloys classified as low-alloy steel, it is also refractory steel or heat resistant steel because it possess tremendous potentials for high temperature services like other refractory metals and alloys such as; Columbium, Tantalum, Tungsten, Molybdenum and so on. Finish turning process of AISI 4340 is gaining popularity because of increasing application of refractory and high hardness material. For example, hardened AISI 4340 is employed in constructing aircraft and automobile engine and transmission components. These includes; gears, cam shafts, axles and bearings. It is also employed in constructing tools, dies and molds for manufacturing operations [6, 7, 8, 9].

The economic benefits of the turning process over grinding process as finishing operation is substantial and includes; reduced cost, reduced machining time, process

flexibility, reduced energy consumption, good prospect for dry machining (which is good for reduction of environmental pollution), high material removal rate, better compatibility with thin wall sections and complex shapes, and comparable surface finish [6, 9, 10]. Taking advantage of this benefits is possible because of the availability of superior cutting tools [1, 11].

Refractory metals are usually more brittle and abrasive at room temperature [12], therefore their machining often result in more rapid tool wear and relatively shorter tool life. The exceptional tool performance of cemented carbide results from their high hardness and compressive strength. For example, the lowest hardness of cemented carbide is known to be approximately the same as the highest hardness available in tool steel [5]. Carbide tools are also capable of sustaining or retaining their properties at high temperatures, in fact, repeated cycling between high and low temperatures or sustained holding at high temperature has no tempering effect on the tool within its characteristic temperature range. The tool regains its original hardness when it returns to room temperature. It functions more efficiently at high speed but requires a lot of rigidity from the machine tool [6, 10, 13].

1.1. Failure and wear of cemented carbide tools

Single point carbide tools are generally preferred for high volume production machining even though they are susceptible to failure and wear, especially due to their brittle nature. Cemented carbide tools are largely used as cutting tool inserts. Such inserts interacts with chips and workpiece during cutting as shown in Figure 1 thereby resulting in the degradation of the tool.

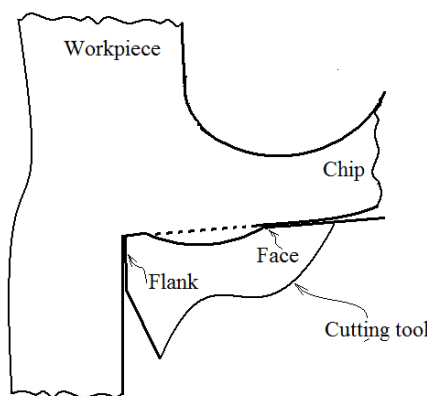


Fig. 1. Regions of tool wear in a single point cutting.

The failure of cemented carbide tools can be classified into the following two categories; failure mechanisms that brings the life of the cutting tool to an abrupt or premature end, and gradual tool wear that progressively develops on the tool flank surface (flank wear) or on the tool rake (crater wear) [1, 2, 5]. Tool failure is associated with breakdown of the cutting edge of the tool as a result of its direct contact with the workpiece. Wear could occur in these three main regions on the tool; face, flank and nose.

The wear that occurs on the tool surface over which the chip passes takes the form of a cavity and is called crater

wear. Its origin is usually a distance from the cutting edge. It is the most prominent form of tool wear. The flank is the portion of the tool that is in contact with the work at the point of chip separation. Flank wear usually begins at the cutting edge and grows into a wider contact area called wearland. The surfaces that are susceptible to tool wear during machining on a lathe are shown in Figure 2.

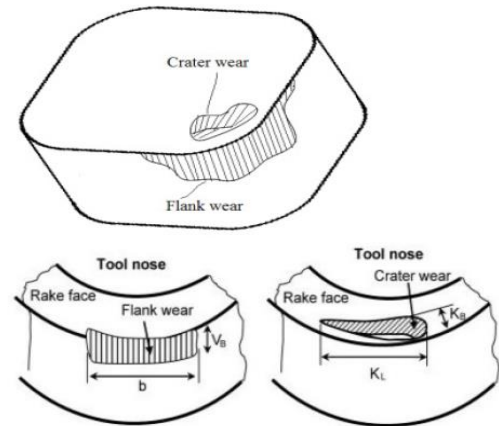


Fig. 2. Schematic of flank and crater wear and their measurements [1].

The nose wear is considered as part of the flank wear in many cases. Moreover, in operations like finish turning where the nose is in direct contact with the workpiece it is considered as a separate form of tool wear. At very high cutting conditions, as is frequently employed for cemented carbide cutting tools, the life of the tool is often determined by crater wear. If crater and flank wear occur concurrently in a balanced pattern, the tool geometry and life can be prolonged [14]. The intrinsic brittleness of cemented carbide tools make them quite susceptible to fracture and built-up-edge phenomenon being usually made with intricate geometries. Therefore, little wear affects the stability of the built-up-edge which in turn affects the surface quality and degrades efficient cutting before catastrophic failure [12].

1.2. Surface quality as criterion for determining tool failure

Surface roughness has been the prime criterion for surface quality and a guide for acceptable fatigue strength [5]. The ideal surface roughness usually represents the best possible finishing which may be obtained for a given tool shape and feed [12]. A specified surface roughness or a desired tolerance could be used to determine or rate the acceptability of a machined workpiece. This could however be related to the level or rate of wear of the tool used if built-up-edge, chatter, inaccuracies in machine tool movement and other negative factors are eliminated.

When the good surface roughness quality is the primary goal, the tool would be said to be worn-out when the desired surface roughness can no longer be achieved with the cutting tool. It is therefore highly desirable to put the cutting tool to optimum use to reduce machining cost.

Cutting force measurements has been employed in many documented works for tool condition monitoring [4, 15, 16].

Recent works has shown that good prospect exist for this when combined with monitoring of other parameters like acoustic emission and vibration magnitude measurements [4, 17, 18]. Cutting force measurements in this work has been employed as a tool to confirm the point of optimal economic utilization of the tool.

1.3. Cutting tool economic life

Prediction of tool life during machining is essential for cutting tool design and in determination of cutting conditions and tool change strategies. It is necessary to achieve an optimized metal cutting process in which there is balance of resources. Moreover, tool wear is an unavoidable consequence of the metal cutting operation, therefore the cutting tool wear is an important factor in the economic analysis of the operation. Tool wear and its retardation have a direct relationship with the attainment of several machining optimization criteria such as minimum cost, maximum production rate and maximum profit. Catastrophic tool failure should be avoided in turning process to eliminate its associated damages to the workpiece, cutting tool and the machine tool [2, 11]. Hence, estimation of the useful life of cutting tools is essential in finish turning process.

Usually, the tool life between tool re-sharpening or replacement is specified in one of the following ways:

1. Actual cutting time to failure,
2. Total time to failure – as with interrupted cutting process, for example, milling,
3. Length of work cut to failure,
4. Volume of metal removal to failure,
5. Number of components produced to failure, and
6. Cutting speed for a given time to failure.

Meanwhile, a cutting tool is taken to have failed when it is no longer capable of producing parts or workpieces within the required specifications. This is with little regard to the tool having justified cost before being regarded as having failed, especially for expensive tools like the carbide tools.

The point of failure and the amount of wear that caused the failure depends on the machining objective, thus, surface quality, dimensional stability, cutting forces and production rates are often used individually or in combination as criteria for establishing the point of tool failure [4, 11]. The machining cost increases due to increase in the number of operations involved.

It is however pertinent that tools be changed just when they attain an appropriate wear level to maintain the required level of surface finish. This must be done in a way that it result in reduced tool change time, loss in production time due to stoppage, as well as the overall machining cost. It is a general rule that on the production run, the higher cost of carbide tooling pays dividends, while on the short run, it may not be justified [4].

A cutting tool would be said to be worn-out at the point when it can no longer be used to obtain the surface roughness specification required. Cost of machining increases with

decrease in surface roughness of the machined product. The acceptable level of surface roughness is relative, therefore the focus of this work is to estimate the optimum life of the carbide tool employed in machining AISI 4340 workpiece in minutes.

2. Materials and Method

The finish turning experiment was performed using a three jawed self-centering Cholchester center lathe machine. The workpiece material was AISI 4340 steel with an initial diameter of 93.98 mm. the square shaped carbide tool used belonged to the ANSI classification of general purpose cutting tool, C6 with ISO equivalent P30. All the cutting parameters were held constant during the experiment. C6 is recommended by the American Society for Metals (ASM) for working on steel materials whose Brinnel hardness number reaches BHN 330 [5, 9, 19, 20]. The tool’s HRA hardness value and density are 91.3 Ra and 13.84 g/cm³ respectively and the tool angles were -6°, -6°, 6°, 6°, 15° and 0.6. The turning parameters are listed in Table 1 while the chemical composition of the tool is given in Table 2.

Table 1. Turning Parameters

Parameter	Value
Cutting speed	2.8 m/s
Feed	3 mm/rev
Depth of cut	1.30 mm
Cutting condition	Dry

Table 2. Chemical composition of the Carbide tool (wt%)

Chemical compound	CO	TiC	Tac	WC
Percentage content	3.0	3.0	7.0	82.0

The surface roughness, maximum flank wear width and maximum crater wear width were measured after every sixty seconds cutting time using the toolmaker’s microscope. The microscope was set to magnification factor x125 and x200 since it had the capacity of serving as a comparator whereby views could be superimposed. Kistler’s three component piezo-electric dynamometer mounted on the cross-slide of the lathe machine was used for the cutting force measurement. Measurements were made and recorded for twenty cutting operations (that is, twenty minute total cutting time and one minute for each cutting operation).

After the 13th minute, the cutting process started getting noisy having reached the galling stage where the material particles were welded to the machine surface signaling an onset of critical tool wear. When working on AISI 4340 steel, C6 is not recommended for more than 3 mm depth of cut [20]. The chemical composition of the work material is presented in Table 3.

Table 3. Chemical composition of AISI 4340 steel (wt%)

Alloy elements	C	Mn	Si	Cr	Ni	Mo	Fe
Percentage content	0.40	0.75	0.28	0.80	1.80	0.20	Remainder

3. Results and Discussion

3.1. Statistical analysis

Significant impact of cutting speed, feed rate and depth of cut on the surface roughness and tool wear during turning process has been established in previous works [3, 12, 19, 21 - 23]. These parameters were held constant in this work to enable a relationship to be established between the rate of tool wear, cutting force and workpiece surface roughness.

Mathematical model relating the parameters were obtained using regression analysis in MINITAB 14 and Microsoft Excel 2007 with the Solver tool. The relationship between the cutting parameters is as given in Equation 1.

$$S = f(F, VB, KT) \tag{1}$$

where S represents workpiece surface roughness measurements in millimeters, F represents the average

resultant cutting force measured in Newtons, VB represents flank wear measured in millimeters and KT represents the crater wear measured in millimeters as well. A summary of the regression statistical output is presented in Table 4 and 5.

Table 4. Summary of the general regression analysis output data

Regression parameter	Value
R ²	0.8955
Adjusted R ²	0.8759
Standard error	0.0006
Significance of F	4.5341 x 10 ⁻⁸
Number of observations	20

Table 5. Other regression analysis output data

	Coefficients	Standard error	t - stat	P - value	Lower 95%
Intercept	-1.1114 x 10 ⁻²	3.23 x 10 ⁻³	-3.4478	3.3086 x 10 ⁻³	-1.7985 x 10 ⁻²
Cutting force, F	1.5362 x 10 ⁻⁴	3.211 x 10 ⁻⁵	4.7840	2.0285 x 10 ⁻⁴	8.5548 x 10 ⁻⁵
Flank wear, VB	-6.7590 x 10 ⁻²	9.7736 x 10 ⁻²	-0.6916	0.4991	-0.2748
Crater wear, KT	3.6566 x 10 ⁻²	3.0121 x 10 ⁻²	1.2139	0.2423	-2.7290 x 10 ⁻²

Equation 2 is computed from coefficients in Table 5, while a graph comparing the measured and predicted surface roughness measurement is presented in Figure 3. Residuals resulting from the comparison in Figure 3 are shown in Figure 4. Except for the first cutting operation where the residual was large the others were within a range of about $\pm 6 \times 10^{-4}$ mm.

$$S = 1.1114 \times 10^{-2} + 1.5362 \times 10^{-4} F - 6.7590 \times 10^{-2} VB + 3.6566 \times 10^{-2} KT \tag{2}$$

3.2. Surface roughness

Figure 5 presents an exponential trend relationship between the surface roughness of the machined workpiece and the cutting time. The trend is also mathematically by $R_a = 3.642 \times 10^{-3} + 4.776 \times 10^{-5} e^{0.2403t}$. The curve began to deflect upwards around the tenth minute signifying a sharp increase in the rate of change of the surface roughness from the eleventh minute onwards.

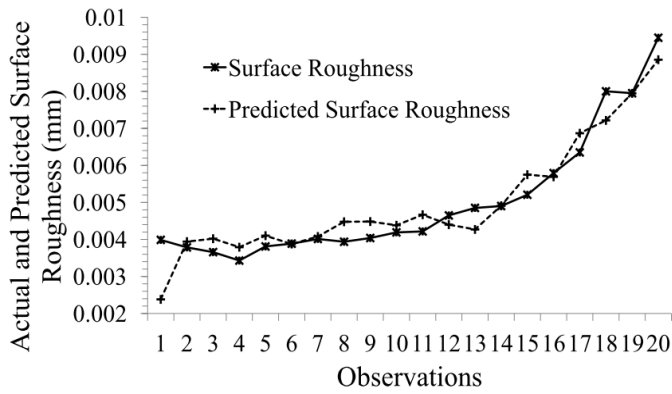


Fig. 3. Measured and predicted machined surface roughness.

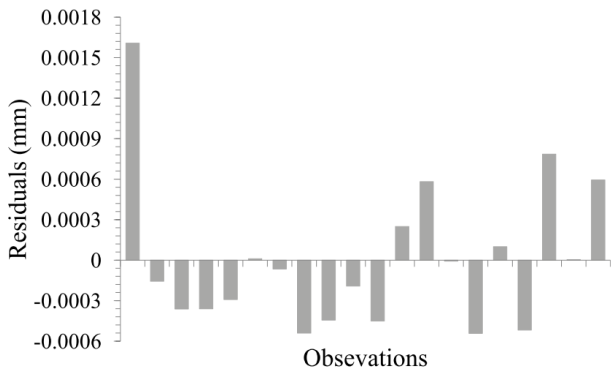


Fig. 4. Deviation of the predicted surface roughness values from the measured values.

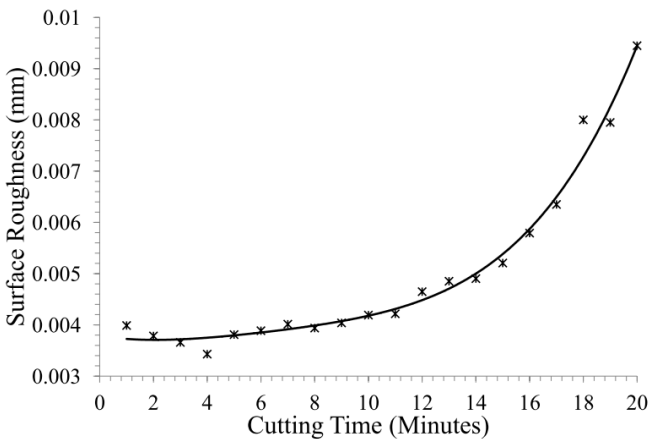


Fig. 5. A graph of surface roughness against time.

The surface roughness of a work material primarily depends on the feed and cutting tool geometry, but since a constant feed was used in this experiment, the change in the geometry of the tool as a result of wear must be responsible for the change in the surface roughness of the work material. Consequently, if surface roughness is considered as the primary factor in assessing the tool life in this experiment it would be economical to have changed the cutting tool at the tenth minute of the cutting operation even though it was yet far from the maximum permissible wear values prescribed in standards.

3.3. Flank and crater wear

Flank and crater wear progressed in linear trends as shown in Figure 6. The pattern and range of values are normal and expected. Moreover, the ratio of the highest value measured for the maximum flank wear width to the lowest was about 2.75, while the flank wear grew at a rate of about 0.0014 mm/min. The ratio of the highest value measured for crater wear to the lowest was about 1.56 and the wear parameter grew at a rate of 0.005 mm/min.

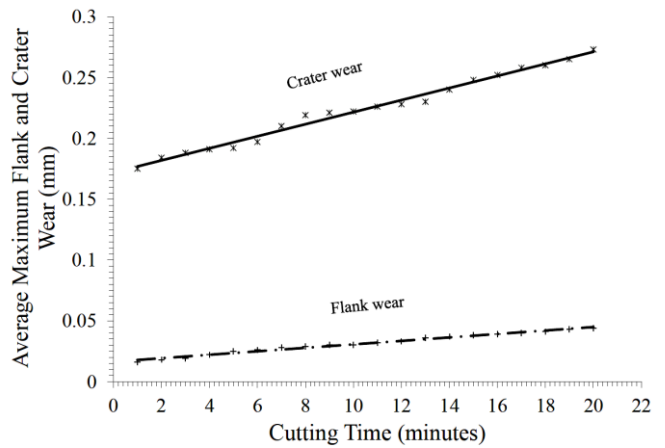


Fig. 6. Progress of maximum flank and crater wear with the cutting time.

When the cutting edge of the carbide tool insert used was compared with the cutting edge of a new tool under the toolmaker’s microscope, a maximum flank wear depth of 0.013mm and a maximum crater wear depth of 0.01mm was revealed in the used tool, this shows a ratio of 1:3 in favour of the flank wear.

The maximum flank wear and the maximum crater wear measured were however found to be significantly less than the stipulated maximum permissible wear of 0.55mm and 0.25mm respectively [11, 22, 24] but the rate of surface degradation started to get serious at about the 10th minute of the experiment. Figure 6 also shows that crater wear was more dominant. This signifies that the principal tool wear process was diffusion between the cutting tool and the chips. Composition of the carbide tools has been known to make them readily predisposed to diffusion wear [1, 2, 19, 22].

Moreover, this is corroborated by Zhang and others [25] as well as Aslantas and others [1] in their work which made case for coated ceramic tool inserts. Chemical reactions (related to diffusion wear) and high temperature (due to low thermal conductivity of the cutting tool) combined with high stress values in the cutting region combined to give rise to the crater wear formation [11]. With further deterioration, the crater wear reaches the tool tip and fracture occurs, thereby modifying the tool geometry as shown in Figure 7.

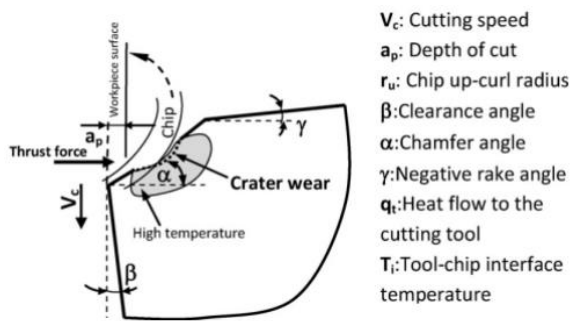


Fig. 7. Crater wear favoured chip curling pattern [1].

3.4. Cutting Force

Although the trend for the cutting force could best be modelled with a fourth degree polynomial given by,

$$y = -0.0012x^4 + 0.0662x^3 - 1.1169x^2 + 6.8907x + 49.419 \quad (3)$$

as shown in Figure 8. Its increase can be said to approximately correlate with the increase in surface roughness of the workpiece linearly as shown in Figure 9. This was achieved with a coefficient of determination, R^2 of 0.9644. The prominence of the second turning point which occurred at about the 11th minute also approximately agree with the observation of 10th minute turning point in Figure 5.

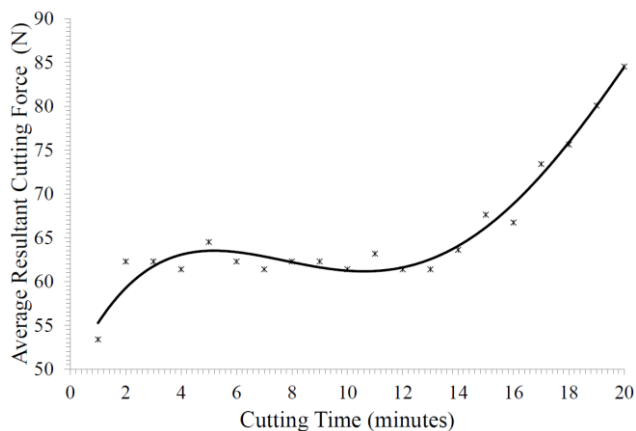


Fig. 8. Average resultant cutting force.

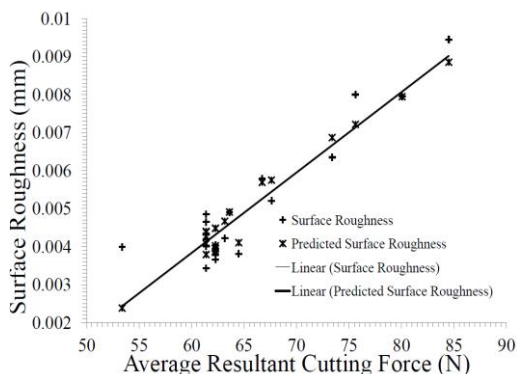


Fig. 9. Correlation of surface roughness with the cutting.

4. Conclusion

In-process tool monitoring and measurement has been employed in determining the optimal economic life of the cemented carbide tool turning AISI4340. The trend for the increase in the flank and crater wear was linear while the trend for the surface roughness followed an exponential growth in conformity with documented patterns in the literature. The workpiece surface roughness was found to deteriorate beyond acceptable level after the 10th minute of the turning process.

Acknowledgements

The authors wish to acknowledge the immeasurable assistance received from Mr M. L. Olawuyi as well as the University of Detroit, Michigan.

References

- [1] Aslantas, K., Uzun, I., and Cicek, A.: Back Propagation Algorithm: The Best Algorithm Among the Multi-Layer Perceptron Algorithm, *International Journal of Computer Science and Network Security IJCSNS*, 9, 442–451, 2009.
- [2] Astakhov, V. P. and Davim, J. P.: Tools (Geometry and Material) and Tool Wear, in: *Machining Fundamentals and Recent Advances*, edited by Davim, J. P., Springer Verlag Publisher, London, 2008.
- [3] Mandal, N., Doloi, B., and Mondal, B.: Predictive Modeling of Surface Roughness in High Speed Machining of AISI4340 Steel Using Yttria Stabilized Zirconia Toughened Alumina Turning Insert, *International Journal of Refractory Metals and Hard Materials*, 38, 40–46, 2013.
- [4] Kayhan, M. and Budak, E.: An Experimental Investigation of Chatter Effects on Tool Life, *Journal of Engineering Manufacture – Proceedings of the Institute of Mechanical Engineering (IMEchE)*, 223, 1455–1463, 2009.
- [5] Lyman, T.: *Metals Handbook*, American Society of Metals, Metals Park, Ohio 44073, 8th edn., 1997.
- [6] Shihab, S. K., Khan, Z., Mohammad, A., and Siddiquee, A.: A Review of Turning of Hard Steels Used in Bearing and Automotive Applications, *Production and Manufacturing Research: An Open Access Journal*, 2, 24–49, 2014.
- [7] Josh, A. and Rampal, R.: Effect of Cutting Parameters on Tool Wear of Coated Carbide Tool in Hard Turning of AISI4340, *International Journal of Engineering Sciences and Research Technology*, 3, 112–117, 2014.
- [8] de Lima, J., de Avila, R. F., and Abrao, A. M.: Turning of Hardened AISI 4340 Steel Using Coated Carbide Inserts, *Proceedings of Institution of Mechanical Engineering: Engineering Manufacture*, 221, 1359–1366, 2007.
- [9] Suresh, R., S. Basavarajappa, V. N. G., and Samuel, G. L.: Machinability Investigations on Hardened AISI 4340 Steel Using Coated Carbide Insert, *International Journal*

- of Refractory Metals and Hard Materials*, 33, 75–86, 2012.
- [10] Coelho, R. T., Ng, E., and Elbestawi, M. A.: Tool Wear When Turning Hardened AISI 4340 with Coated PCBN Tools Using Finishing Cutting Conditions, *International Journal of Machine Tools and Manufacture*, 47, 263–272, 2007.
- [11] Arsecularane, J. A., Zhang, L. C., 10 and Montross, C.: Wear and Tool Life of Tungsten Carbide, PCBN and PCD Cutting Tools, *International Journal of Machine Tools and Manufacture*, 46, 482–491, 2006.
- [12] Wilson, F. W.: *Fundamentals of Tool Design*, Prentice-Hall of India Private Limited, New Delhi, India, 1997.
- [13] Johnson, J. L., Runyon, G., and Morton, C.: Powder Power, *Cutting Tool Engineering*, 60, 112–117, 2008.
- [14] Astakhov, V. P.: The Assessment of Cutting Tool Wear, *International Journal of Machine Tools and Manufacture*, 44, 2004.
- [15] Ezugwu, E. O., Olajire, K. A., and Bonney, J.: Modelling of Tool Wear Based on Component Forces, *Tribology Letters*, 11, 55–60, 2001.
- [16] Awopetu, O. O., Dahunsi, O. A., and Aderoba, A. A.: Selection of Cutting Tool for Turning _ - Titanium Alloy BT5, *Assumption University Journal of Technology*, 9, 46–52, 2005.
- [17] Bhuiyan, M. S. H., Choudhury, I. A., and Dahari, M.: Monitoring the ToolWear, Surface Roughness and Chip Formation Occurrences Using Multiple Sensors in Turning, *Journal of Manufacturing Systems*, 33, 476–487, 2014.
- [18] Yaldiz, S. and Unsacar, F.: A Dynamometer Design for Measurement the Cutting Forces on Turning, *Measurement*, 39, 80–89, 2006.
- [19] Sahoo, A. K. and Sahoo, B.: Experimental Investigation on Machinability aspects in Finish Hard Turning of AISI4340 Steel Using Uncoated and Multilayer Coated Carbide Inserts, *Measurement*, 45, 2153–2165, 2012.
- [20] Davies, J. R.: *Metals Handbook*, American Society of Metals, Metals Park, Ohio 44073, desk edn., 1998.
- [21] Hughes, J. I., Sharman, A. R. C., and Ridgway, K.: The Effect of Cutting Tool Material and Edge Geometry on Tool Life and Workpiece 30 Surface Integrity, *Journal of Engineering Manufacture: Proceedings of the Institute of Mechanical Engineers*, 220, 93–107, 2006.
- [22] Li, B.: A Review of Tool Wear Estimation Using Theoretical Analysis and Numerical Simulation Technologies, *International Journal of Refractory Metals and Hard Materials*, 35, 143–115, 2012.
- [23] Babu, B. V. and Karthik, S.: Genetic Programming for Symbolic Regression of Chemical Process Systems, *Engineering Letters*, 14, 1–14, 2007.
- [24] Werner, K. A.: In-Process Monitoring of Cutting Tool Forces, *Biennial International Machine Tool Technical Conference*, 4, 11.83–11.99, 1984.
- [25] Zhang, S., J. F. Li, J. X. D., and Li, Y. S.: Investigation on Diffusion Wear During High-Speed Machining Ti-6Al-4V Alloy With Straight Tungsten Carbide Tools, *International Journal of Advanced Manufacturing Technology*, 44, 17–25, 2009.

Lessons Learned from Collapse of Zumrut Building under Gravity Loads

Can Balkaya*‡

*Department of Civil Engineering, Faculty of Engineering and Architecture, Istanbul Gelisim University, Istanbul, Turkey
(cbalkaya@gelisim.edu.tr)

‡Corresponding Author; Can Balkaya, Department of Civil Engineering, Istanbul Gelisim University, Istanbul, Turkey
Tel: +90 212 422 7020, Fax: +90 212 422 7401, cbalkaya@gelisim.edu.tr

Received: 08.03.2017 Accepted: 05.06.2017

Abstract- The 11-story reinforced concrete Zumrut Building in Konya, Turkey collapsed on February 2, 2004. Ninety-two people died. This study was conducted to determine the mechanism of the collapse and identify lessons learned to avoid future disasters. Using structural drawings, material samples, and soil information obtained from the site, reasons for the collapse were investigated. A three-dimensional (3-D) structural model and analyses were performed using ETABSV8.11, and various possible critical cases were studied. The step-wise nonlinear analysis used to obtain the collapse mechanisms was an example of forensic structural engineering and revealed that the progressive collapse of the building was torsional, caused by decrease in structural system's capacity to redistribute gravity load after failure of a column. The lessons learned include the importance of project controls to reduce design and construction errors, ensure that construction and repairs are consistent with design intent, and changes are checked for safety and included in drawings. The importance of integrating architectural and structural systems to form 3-D continuous structural frames to reduce the probability of progressive collapse is also discussed.

Keywords Zumrut Building, Progressive collapse, Collapse mechanisms, 3-D finite element analysis, Failure of structure.

1. Introduction

Construction began on the Zumrut residential apartment building in 1994. The 11-story reinforced concrete building was located in the Selcuklu area of Konya, Turkey. At the time, the area was considered to be a "no seismic" zone, and structural designer calculations were performed considering gravity loads and wind forces only. The building survived just five years after the completion of construction. Progressive collapse of the building under gravity loads caused a sudden and total collapse on February 2, 2004 (Fig. 1), killing 92 people. The progressive collapse was started by a possible local failure in the ground-level columns. The first dynamic mode of the structure is the torsion mode. This causes a rotational/torsional motion and progressive collapse of columns in that story level and then progressive collapse of upper story levels results in total collapse of the building.

Most of Turkey lies within active earthquake regions, and building collapses, and damage due to earthquakes are fairly common. The damaged and collapsed buildings are typically restored or removed before evidence can be collected for a detailed investigation. But in the case of

Zumrut Building, a team of experts from Middle East Technical University (METU) was able to begin investigating the disaster during the removal of debris, after requesting the public prosecutor in Konya. The author was the head of the investigative team.

The investigation revealed that there were four main causes of the collapse of Zumrut Building [1]: 1) construction errors 2) project errors 3) lack of control of construction and projects and 4) different construction and repairs not shown in structural project.

A 3-D structural model of the building was developed to identify the possible progressive collapse mechanisms using the general structural analysis program ETABSV8.11 [3]. The 3-D modelling of Zumrut Building was then analysed using step-wise nonlinear analysis. When a structural element reached its capacity, it was crushed. Analysis of the structural systems continued until the collapse mechanisms of Zumrut Building were identified. After studying many possible critical paths, the progressive collapse was found to be a torsional rotation collapse.



Fig. 1. Progressive collapse of Zumrut Building.

The lessons learned from this case emphasize the importance of appropriate structural systems, design approaches for gravity and lateral loads, and detailing in reinforced concrete buildings. They also emphasize the importance of control mechanisms during design and construction, construction quality and material quality, selection of a foundation system, and the effects of integrated architectural and structural systems in preventing progressive collapse.

2. Investigation of Collapse Reasons of Zumrut Building

2.1. Construction Errors

The sudden collapse of the 11-story reinforced concrete building was mainly due to poor construction and some design alterations that deviated from best practices for structural projects of this kind. The workmanship was not good. Concrete strength was lower than the project and code requirements for a reinforced concrete building. To determine the concrete quality used in the construction, many samples were taken on site after the collapse of the building. These samples were tested in the METU Department of Civil Engineering Material Lab, as shown in Fig. 2. The approved design compressive strength for the reinforced concrete was 160 kgf/cm^2 (C14). Test results of concrete cylinders taken from the site revealed a compressive strength of 80 kgf/cm^2 (C8). Since the samples were taken only from undamaged structural members, the compressive strength of damaged members is unknown.



(a) Structural Element



(b) Compressive Strength Test of Samples

Fig. 2. Concrete core samples.

Based on material testing and site investigation, it was observed that the concrete gradation in the Zumrut Building was not uniform. The gradation did not satisfy Turkish or ASTM Standards. The quantity of the sand present was more than that of the gravel. Some aggregates were very big, as shown in Fig. 3, which does not comply with standards. Sand and gravel were taken partly from a river and were probably unwashed.



Fig. 3. Concrete gradation and cover.

Stirrup spacing, reinforcement cover, and replacements were also did not comply with code requirements. Small and large reinforcement material samples were taken from the site and tested in the METU Material Lab. Reinforcement types were found to be of the StI type (2200 kgf/cm^2). Stirrups were not increased near the beam–column connection regions. In some locations, stirrup spacing was too large in some columns, as much as 40–50 cm with an average of 35 cm.

Reinforcement cover varied significantly, it was found to be 5 cm in some columns. However, in some locations the

reinforcements were replaced very close to the surface or inside the section (Fig. 3). On the other hand, the main longitudinal reinforcement of beams were replaced so closely that there was no enough space between the rebars for concrete. Beam dimensions in the approved structural design were 20/50 cm. This small concrete beam sections, as well as use of reinforcement type StI (2200 kgf/cm²) instead of StIII (4200 kgf/cm²), resulted in a large amount of reinforcements in the beam design. In such cases, reinforcements must be replaced in layers rather than as a single bottom reinforcement layer (Fig. 4) in order to form bonding between concrete and reinforcement. On Zumrut Building, placement of the large amount of reinforcements as a single bottom layer resulted in no bond or a very weak bond of reinforcement in the concrete. Thus, most of the beams did not properly transfer the forces due to the lack of a strong bond during collapse of building.



Fig. 4. Bond between concrete and reinforcement.

2.2. Project Errors

The Zumrut Building was modelled in 3-D using the analysis program ETABSV8.11 to check the existing structural project and design calculations. During the structural design calculation check, only the original project was considered; other repairs not shown in the structural drawings were not considered (repairs were only shown in architectural revised drawings). When the project was prepared, Konya was not considered as an earthquake region according to Turkish Earthquake Codes. For this reason, only vertical gravity loads (dead loads, live loads) and additional lateral loads (wind loads and their combinations) were considered in the design and control of the RC structural design calculations.

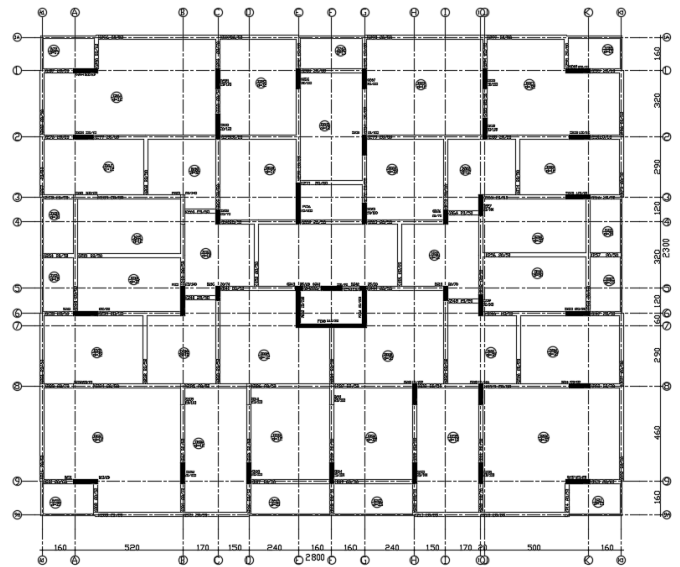


Fig. 5. Typical structural floor level of RC Zumrut Building.

The 11-story Zumrut Building was approximately 36 m high. The ground floor was 5.6 m high to accommodate shops, and the residential floors were 3 m high. Columns dimensions were generally 20/100 cm, 20/70 cm, and 25/100 cm (25/70 cm at the basement and ground floor levels). Beam dimensions were generally 20/50 cm. Reinforced concrete slabs were 12 cm. The rigidity center was at the right of the mid-part of the floor plan due to the shear walls of the elevator as shown in Fig.5.

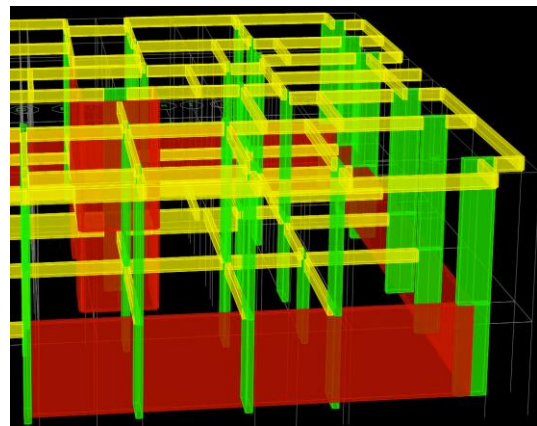


Fig. 6. Console part and beams located at out of frames at façade.

The floor areas were extended 1.5 m outside the frames all around the façade except at the ground level, as shown in Fig. 6. Between the columns around the exterior part of building, there are no beams. This may be due to architectural views as shown in Fig. 5 and Fig. 6. Thus, the frames were effectively not working, due to the lack of beams in the frame axes. The beams were connected to the frame columns using a cantilever beam and were located at the outer perimeter of the plan. This also resulted in the exterior frame column being subjected to large console load effects in the out-of-frame elevation. Corner columns were more critical. The outer parts of the building frames were working not effectively under lateral loads to transfer the loads when the stability of the building changed. Thus, the

torsional resistance of the building was very low. On the other hand, there were discontinuities in the structural frame systems in both directions. Most of the frames, as shown in the structural plan (Fig. 5), were single-span frames especially in the short direction of the building. There was no direct connection between the frames; they were discontinuous in both directions. Some of them were not even located in the same line as that of the axes. There were four flats on each floor, but as seen in the floor plan in Fig. 5, the layout was not symmetric, and flats had different construction areas. When the author asked why the four flats were not symmetrically located in the floors, the reason was given as the consideration of the percentage sharing of the landowners. All columns between the B and J axes in the plan shown in Fig. 5 were located in the same direction as strong directions.

Existing reinforced concrete design calculations were checked. The calculations considered allowable stress design but included conceptual design errors. For example, the project designers used higher allowable concrete stresses for the concrete by considering the critical load case as the combination of gravity loads plus lateral wind forces (DL, LL, WL), which resulted in the selection of small column and beam dimensions. However, when considering the primary gravity loads, it was observed that this resulted in large structural sections in this load case. All combinations must be considered in structural design. In particular, basement and ground floor column dimensions must be 25–45% larger than the project calculations.

As noted above, the structural frame system was discontinuous in both directions. The frame system in the basement and on the ground floor became all the more critical because of project errors and structural irregularities such as beams that were not located in the frame axes between the columns, reinforcement detailing mistakes, small column and beam sizes due to design calculation mistakes, and soft story irregularity due to the 5.6 m height of ground floor columns. Discontinuous frames were connected to other frames using primary and secondary beams. Maybe for architectural reasons, the beam dimensions were 20/50 cm for the console, and there was large frame spacing. Thus, these beams became more critical. Since the beam sections were small, more reinforcements were required and replaced in the beams with no or less bonding.



Fig. 7. Continuous foundation system in both directions.

The building foundation was a continuous foundation system in both directions, constructed in a grid system with shear walls around the perimeter of the basement (Fig. 7 and Fig.8). No damage was observed in the foundation after removal of the debris.

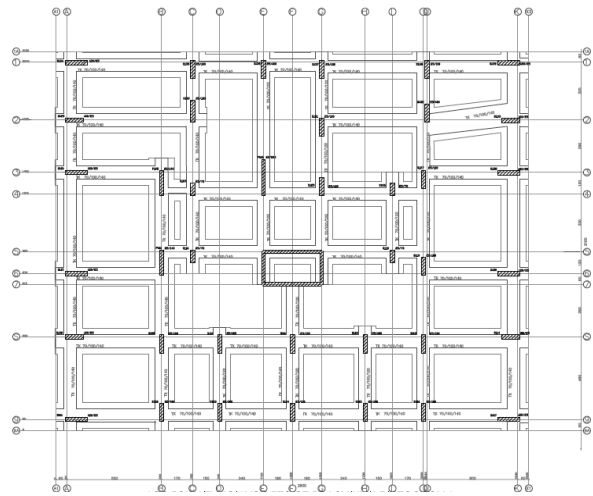


Fig. 8. Foundation plan.

Soil samples were taken during the site investigation (Fig. 9). The soil in the project site was silty clay, and no groundwater and settlement problems were observed after the collapse of the building. Thus, it was concluded that the soil and foundation system did not have any major effect on the collapse of Zumrut Building.



Fig. 9. Soil samples and foundation depth.

2.3. Different Construction and Repairs without Checking Structural Safety

Construction and repairs were not shown or different than structural projects. It was observed from the collapsed building that the ground floor level (of shops) and roof level were constructed as ribbed slabs of 32 cm rather than reinforced concrete slabs of 12 cm, as shown in the approved structural drawings. The ribbed slabs were approximately two times heavier than the 12 cm of reinforced concrete slab. This substitution was not shown in the structural drawings, and structural calculations were not performed for ribbed slabs constructed at the two floors. In addition, two U80 steel profiles with lengths of 5 m were found at the right side of the back of the building. They may have been used under beams in the ground floor level because the ground floor was 5.6 m high (0.6 m beam depth). Approved architectural drawings showed an internal floor level of +3.00 with beams between the ground floor and first floor. But these alterations shown in the architectural drawings were not shown in the

structural drawings as well as not checked for structural safety. During the removal of debris, a column of variable dimensions was also found at the ground floor (Fig. 10). The cross-section of the column size varied from 25/70 cm at the top to 25/40 cm at the bottom. This variation was probably to provide more spacing.



Fig. 10. Column found in debris with variable cross-section (Bottom part 25/40 cm, upper part 25/70cm) at the ground level.

2.4. Lack of Control of Construction and Projects

Project and construction errors, and some construction and repairs those were not shown in the structural project drawings indicated that the supervision of construction and the control of the project were inadequate. Most probably, it was considered as a mere formality. Although a RC building with a height of 36 m can be considered as a low to medium high-rise building in Konya, the control mechanisms on these buildings require much more specific attention.

3. 3-D Nonlinear Finite Element Analysis and Collapse Mechanism

3-D modelling of Zumrut Building (Fig. 11) was analysed using step-wise nonlinear analysis [2]. Column capacities were calculated by using material quality obtained from test results. When a structural element reached its capacity, it was crushed, and analysis continued until the collapse mechanism was determined. The progressive collapse of the building was a torsional collapse (Fig. 12). Possible local failure mechanisms would cause a progressive failure of the story columns due to excess capacity on neighbouring structural elements. This story collapse resulted in a torsional motion. To obtain the torsional motion evidenced by the original collapse of Zumrut Building, many alternative potential collapse paths for the columns were studied.

The study revealed that if a column was crushed, the neighbouring column faced additional loads of 20%. Since most of the columns were near capacity—due to project and construction errors, and low-quality concrete—these additional loads caused progressive collapse of adjacent columns.

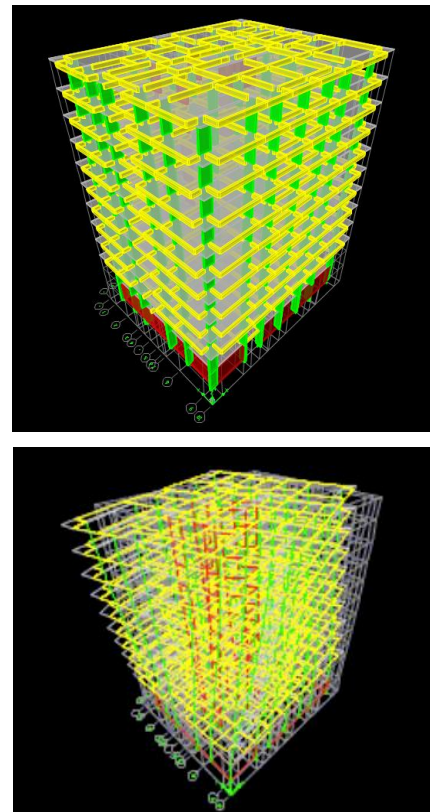


Fig. 11. 3-D finite elements modeling of RC Zumrut Building.

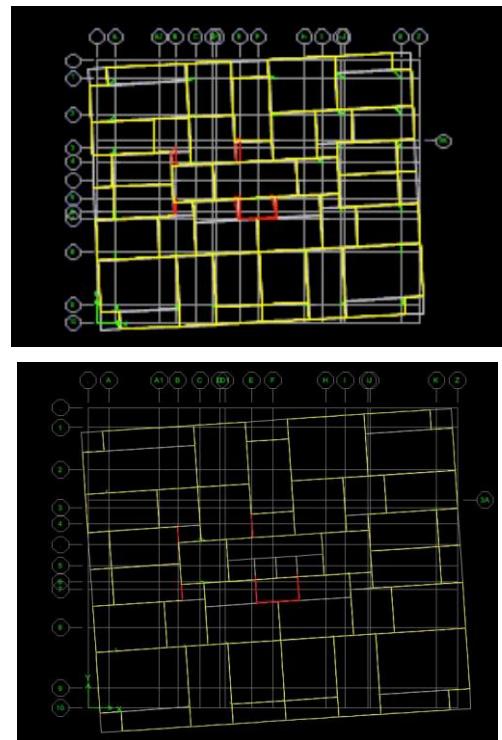


Fig. 12. Rotational/torsional collapse of Zumrut Building in plan view.

The building torsional capacity was very low, and structural frames were not continuous in both directions; discontinuities in the 3-D structural framing, and very low bonds in the RC beams, result in improperly redistribution of

the forces. The result was collapse of story level, progressive collapse of the upper stories and total collapse of Zumrut Building.

Thus, progressive collapse of Zumrut Building occurred due to loss of gravity load capacity to redistribute the load after the failure of a column. This was caused by a lack of frame continuity, capacity, and other mechanisms. Removal or crushing of a single column from a building such as this would cause it to collapse. To obtain the original collapse torsional rotation, many critical load paths were applied to the model. Depending on the column that was removed or failed the torsional rotation direction and collapse angle and mechanism were different. Each column was removed alternately from each level, and then capacity checks and load distributions were done for the new situation. In this manner, the progressive collapses of each floor level were obtained. After considering many alternative cases, the reason for the collapse of Zumrut Building was obtained in the analysis. This was a forensic structural engineering study to investigate and determine the causes of structural failure by using 3-D nonlinear finite element analyses.

4. Lessons Learned from Zumrut Building Collapse

Unexpected loads may occur after construction of a high-rise building due to events such as terrorist attacks, gas explosions, blasts, fires, or accidental collisions (e.g., with a truck or plane). Repair and reduction of structural element capacity or an increase in the design loads due to new usage are also factors, as new façades that impose additional gravity loads. Increased seismic loads and wind forces may also arise. However, the Zumrut Building disaster occurred entirely under gravity loads. Zumrut Building in Konya, Turkey was collapse due to the combination of the following reasons: construction errors, project errors, different construction and repairs without checking structural safety and lack of control of construction and projects.

To prevent progressive collapse of buildings, lessons learned from the collapse of Zumrut Building are:

- In the structural design, the first rule will be life safety; the structure must first be safe under gravity loads, and then the design must consider lateral loads for life safety.
- In a building design, torsion is not a desired mode of dynamic behaviour of the building. International standards and codes consider the bending mode to be the preferred first mode; structural engineering design should prevent torsion from becoming the first mode.
- To prevent total collapse, the design of high-rise buildings must implement after studying the overall strength and stability of the 3-D structural system by assuming a local failure.
- To increase the structural performance of building structures, the use of indeterminate systems, 3-D behaviour, and 3-D continuous structural framing systems in both directions in the design will reduce the probability of progressive collapse and prevent the total failure of the building.

- Some architectural needs will reduce the overall torsional rigidity or discontinuity of structural systems or less redundant systems due to architectural reasons. In such cases, a new structural system or revised architectural system is required for safety.
- Locating floor areas in the console in some or all of the façade of a building is very common in Turkey to gain construction area above the ground level according to permissions in municipalities construction law. In such cases, frames do not properly transfer the forces under lateral loads or in cases of torsion due to a lack of beams between the columns. If these beams exist, they will probably pass through the rooms and corridors. For the structural continuity and transfer the forces alternative structural floor systems can be used, such as ribbed floors or flat-plate floor systems to integrate the architectural and structural system requirements. Otherwise, beams should be placed between the columns in the frame or the column lines should be put under console beams to construct a new frame at the exterior console part without closing the ground level from foundation to the top (not allowed in Turkey).
- If architectural changes done after construction of the building affect the structural system, whether through additional load or new load transferring, the structural system must be checked for structural safety.

5. Conclusion

In a local failure, redistribution of additional forces may exceed the capacity of neighbouring structural elements, causing local buckling or crushing of structural column elements. Local buckling or crushing may lead to local failure or even progressive collapse, as shown in the collapse of Zumrut Building. Therefore, a structure should be designed to provide capacity with continues structural systems allowed re-distribution of additional loading and stability. Selection of continuous 3-D structural system will prevent progressive collapse and primary collapse of the whole structural system due to redistribution of excess forces by creating a 3-D system of adequate strength and stability that accounts for the probability of local failures due to unexpected or accidental loads.

References

- [1] C. Balkaya, "Collapsed reasons of Zumrut Building in Konya" (in Turkish). TMMOB Union of Chambers of Turkish Engineers and Architects, *J. Teknik Guc*, No: 135, 2004.
- [2] C. Balkaya, "Investigation of collapsed Zumrut Building in Konya and progressive collapse mechanisms" *8th International Congress on Advances in Civil Engineering*, Famagusta, North Cyprus, 2008.
- [3] ETABSV8.11. "Structural and Earthquake Engineering Software" Computers and Structures, Inc. Berkeley. California, USA, 2002.

Engineering Material Selection for Automotive Exhaust Systems Using CES Software

Ikpe Aniekan E. ^{*‡}, Orhorhoro Ejiroghene Kelly ^{**}, Gobir Abdulsamad ^{*}

^{*}Department of Mechanical Engineering Coventry University, Priory Street, CV15FB, West Midlands, UK

^{**}Cemek Machinery Company Technology Incubation Centre, Federal Ministry of Science & Technology
Benin City, Edo State, Nigeria

(ikpeaniekan@gmail.com, kelecom@yahoo.com, abdulsamad.gobir@gmail.com)

[‡]Corresponding Author: Ikpe Aniekan, Swan court Flat 11, Coventry, CV24NR. Tel: +447586821646,
ikpeaniekan@gmail.com

Received: 32.12.2016 Accepted: 05.06.2017

Abstract-This report reviews the automotive exhaust system with respect to its in-service conditions and selection of suitable materials for exhaust manifold, downpipe silencer/ muffler box and tail pipe which comprises the exhaust system. The functions of each component were discussed, highlighting how they function as part of the exhaust and Cambridge Engineering Software (CES) software was employed in the material selection process. Mass, cost, high temperature (>800°C for exhaust manifold and >400°C for downpipe silencer/ muffler box and tail pipe) and high corrosion resistance were used as basic criteria for the material selection. Variety of materials including Nickel-based superalloys, stainless steel, Nickel-chromium alloys were obtained in the material selection route for exhaust manifold. Similarly, low alloy steels, stainless steel, grey cast iron, Nickel-based superalloys, Nickel-chromium alloys were obtained in the material selection for downpipe silencer/ muffler box and tail pipe. Nickel-based superalloys and Nickel-chromium alloys possess suitable properties for this application, but were not considered due to their high densities and high cost. Low alloy steels were not selected because they tend to exhibit poor corrosion resistance when exposed to salt on the road surface and condensate from the exhaust system. Grey cast iron has low tensile strength and elongation and therefore not exhibit enough toughness required to withstand the severe working conditions. However, stainless steel (Ferritic stainless steel and Austenitic stainless steel) was considered as a better choice of material for automotive exhaust systems due to its considerable price and density, acceptable strength at elevated temperatures and excellent corrosion resistant it possesses as a result of the protective film of chromium oxide which forms on the surface of the metal.

Keywords Material, Cost, Exhaust system, Temperature, Corrosion, Mass, Service life.

1. Introduction

Automobile exhaust systems are integral parts of the overall chain of functions in an automotive system. The significance of exhaust systems has evolved to cover various functional processes in an automobile. Owing to this revolution, material selection prior to manufacturing of automotive exhaust systems has been very crucial. A typical automotive exhaust system incorporates piping system that directs hot reaction gases away from the combustion chamber of an internal combustion engine of automobile systems [10]. In other words, the exhaust system which comprises one or more exhaust pipes conveys burnt toxic and noxious gases through one or more exhaust pipes away from the engine, and depending on the exhaust design, the burnt gases may be expelled through the Catalytic converter to minimise air pollution, resonator, tailpipe etc.

In principle, the exhaust pipes connects the exhaust manifold, resonator, muffler and catalytic converters together for effective exhaust flow, minimal noise, and emission levels. Exhaust systems operate at relatively high temperature and such operating condition usually necessitate the use of

materials with high resistance to heat property, in order to prevent thermal corrosion from limiting the service life of the exhaust material. Furthermore, due to the effects of CO₂ emissions on the environment, Green House Gas (GHG) emission taxes incurred by automobile manufacturers and the ongoing fight against reduction of GHG emissions by United Nations and by IPCC and other environmental protection agencies, manufactures in recent times have conducted researches on possible ways of ensuring that emission of toxic and/or noxious gases into the environment is minimised and the use of suitable materials is one of such [16]. To this revolution, material selection during manufacturing process of automobile exhaust system has been very important. Initially, combustion systems were used to reduce noises produced by high-pressure exhaust gases that were emitted in large amounts by first generation automobiles [5].

The evolution of functioning systems in automobile exhaust, advances in technology and material science have made tremendous significance in the production of the best materials and designs for automobile exhaust systems. As regards material selection and design, there are many factors that must be put into consideration [3, 6]. Illustration by

Precision Automobile [14] shows that a typical automotive exhaust system is made up of the exhaust manifold, a flexible joint, a catalytic converter, a muffler box, tail pipe etc. as

shown in Fig. 1. Each of these sections has distinct functions that are significant in the operational gymnastics of the automobile exhaust system [2].

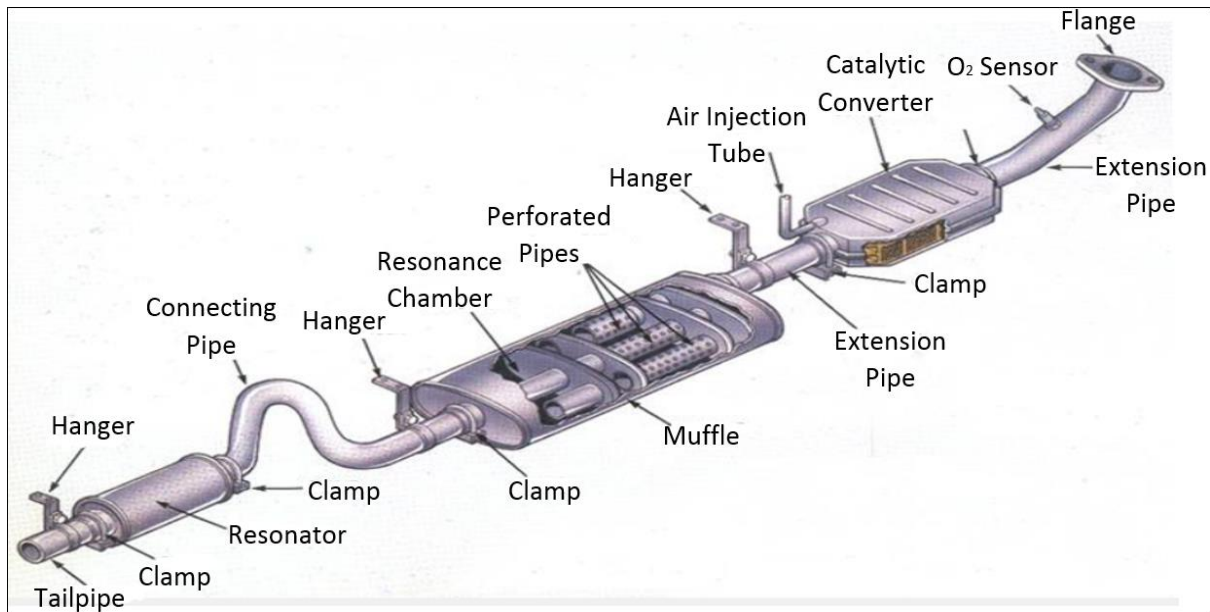


Fig. 1. Typical view of an Automotive Exhaust System [14].

1.1. Exhaust Manifold

The Exhaust manifold are units of pipes made of special material that collect exhaust gases from the engine outlets (through valves) and channel them into a common exhaust pipe. The nature and appearance of the exhaust manifolds depend largely on not only the engine but also the nature of the exhaust materials to be transported. Studies in thermodynamics provide the exact operational temperatures for each conversion in the engine that helps in the determination of important parameters that aid in material selection [6].

The exhaust manifold is installed adjacently to the engine part where the exhaust outlet is situated. At the end of the exhaust stroke of a normal automobile engine, the exhaust valve opens, and the exhaust gas that was filled in the cylinder escapes at high pressure into the exhaust manifold.

As a result of the pressure and the velocity in which the exhaust gases are emitted by the engine through the exhaust valve, the exhaust materials gas possess high temperatures [13]. However, as the exhaust materials are transported through the exhaust manifold, divergent pressure reduction and equalization activities happen that not only reduces the pressure content, but also the velocity of the gases. Therefore, material selection for the exhaust manifold of the automobile exhaust system should incorporate the consideration of all these factors. Essentially, the material should be able to withstand the high pressures exhibited by the exhaust gases as they are thrust out through the exhaust valve. Also, the nature of the gases emitted by each engine is largely dependent on the fuel the engine operates on.

Fundamentally, there are diesel and petrol engines, each of which emits different types (by composition) of exhaust

gases. Therefore, the material chosen should not react with any chemical component in the exhaust mixture. This is because reactions between the material and the exhaust gases will not only corrode the exhaust manifold, but also reduce its durability drastically. Moreover, the operating temperature (700-800°C) of the exhaust gases should also be a guiding factor in the selection of the most appropriate material. Logically, each engineering material has a unique threshold temperature point above which the qualities of the material are affected. During operation, exhaust materials can be exposed to ambient temperature level up to 800°C or even higher under certain severe conditions.

The exhaust system during operation is also exposed to a number of various chemical conditions such as road salt, alkaline and acidic exhaust condensate within the exhaust system. Based on these factors, materials selected for manufacturing of exhaust system must possess not only sufficient strength and fatigue resistance but also excellent corrosion resistance against varieties of operational conditions.

While metals generally form a protective oxide layer on the surface, variety of mechanisms can affect this oxide layer and gradually expose the metal substrate to degradation. Some failure mechanisms that can easily hamper the service life of exhaust system material during its in-service condition as follows;

- i. High temperature corrosion (dry hot corrosion)
- ii. Condensate and salt corrosion (wet corrosion)
- iii. Elevated temperature mechanical failure
- iv. Stress corrosion cracking
- v. Intergranular corrosion

1. 2. Muffler Box

The muffler box is positioned in between the centre pipe and the tail pipe. It functions as a damper of exhaust noise by suppressing it to an acceptable level before passing out to the environment through the last outlet called the tail pipe which is visible to the human eye in an automotive. The internal combustion engines generate high intensity pressure waves which are propagated along the engine exhaust parts.

Fundamentally, the noise produced inside the engine is transported in the form of pulses. Therefore, the main function of the muffler box is to suppress these pulses and reduce them to a frequency that would not cause exorbitant pollution to the environment. Additionally, these pulses can cause vibrations that could be transmitted to other parts of the automobile [12]. Therefore, the material selected should incorporate a sound absorbing material that is within the range of the sounds propagated from the specific engine that it is used. Given that sound is transmitted in a form of pulses and waves. As a matter of fact, mufflers used in modern vehicles use reactive silencers that reflect the propagated sounds back to the sources and inhibit their propagation (in the original frequencies) to the environment through the tail pipe.

Technically, the muffler box has important aspects that tie it with the tail pipe; a choice of the material for design for the muffler box directly affects the choice of materials for the tail pipe. The muffler box is structured in a way that it should not have anything in its interior that would interrupt the flow of exhaust gases.

1. 3. Tail Pipe

The tail pipe is coupled with the muffler box and lies adjacently to the tail of the muffler box. The main function of the tail pipe is to relay sound and excessive exhaust gases from the automobile exhaust system. This is virtually the end part of the whole exhaustive system.

2. Loading Conditions

The mechanical loading condition in which an automotive exhaust system operates under are highlighted as follows;

2.1 Thermal Loading

This arises due to uneven expansion of some areas on the exhaust pipes especially when the material is exposed to high temperature. This uneven expansion can initiate crack or can superimposed on existing crack to extend the crack length [15].

The thermal stress is given by

$$\sigma_T = E\alpha (T_2 - T_1) \tag{1}$$

Where

σ_T is the stresses due to uneven expansion
 E is the Young's Modulus of the material
 α is the coefficient of thermal expansion
 $(T_2 - T_1)$ is the temperature gradient.

Material Characteristics for the major components in a typical vehicle exhaust are presented in Table 1.

Table 1. Material Characteristics for Vehicle exhaust system Components [10]

Criteria	Exhaust Manifold	Muffler Box	Tail Pipe
Service Temperature	750-900°C	100-400°C	100-400°C
Required Properties	- Resistance to High temperature - Thermal Fatigue life - Oxidation resistance	- Corrosion resistance - Oxidation resistance	- Corrosion resistance - Oxidation resistance

2.2. Residual Stress

The residual stress is induced due to vibration on the exhaust system as a result of loading condition when the car is in operation. If these vibrations are close to the natural frequency of the material, resonance may occur. Such high vibration frequency can initiate crack.

2.3. Fracture Toughness (K_{1c})

The position of the exhaust system exposes its parts to frequent vibrations and knockings that usually result in crack initiation over time. Therefore, it is important to look inward for materials that possess high fracture toughness to resist crack propagation from existing cracks and to reduce the effect of residual stresses caused by vibrations and other loading effects. Material index to optimise fracture toughness and resistance to Stress Corrosion Cracking (SCC) for the exhaust system components [11] is given as

$$K_{1c} = \sigma(\pi c)^{0.5} \tag{2}$$

Where

K_{1c} is the fracture toughness
 σ is the stress distribution and
 c is a very small crack.

$$K_{1c} = \frac{wl}{A} (\pi c)^{0.5} \tag{3}$$

$$A = \frac{wl}{K_{1c}} (\pi c)^{0.5} \tag{4}$$

$$m_3 = \frac{wl}{K_{1c}} (\pi c)^{0.5} l\rho \tag{5}$$

$$m_3 = wl^2 (\pi c)^{0.5} \left(\frac{\rho}{K_{1c}} \right) \tag{6}$$

In order to optimize performance indices $m_3 = m_1$

To minimize mass, $\frac{K_{1c}}{\rho}$ should also be maximized.

3. Methodology

Material selection is a very important part of engineering processes as far as the design of systems is concerned. Generally, effective material selection process implies selecting materials with optimal costs with good performance that meets the component designed service life. Based on the above material requirements and materials indices, a search was carried out using the Cambridge Engineering Selector (CES) software Level 3 to select suitable materials for automotive exhaust manifold. Since the service temperature considered for a typical automotive exhaust system is about 800°C and above, a minimum temperature of 800°C was set to filter off materials whose service temperature is below this value.

Moreover, fracture toughness is one of the most important factors that determine the longevity of the exhaust system under such severe condition. Therefore, a minimum value of 15Mpa.m^{0.5} was used to filter off materials with fracture toughness below this value. Similarly for muffler box and tail pipe, a minimum service temperature of 400°C and fracture toughness > 15Mpa.m^{0.5} were used in the material selection process. Applying the above parameters in each material selection process generated the following graphs. The objective of the material selection process is to minimise cost, maximize Thermal Strength and minimise Mass.

Materials selected at the end of each process must possess certain characteristics that meets the following criteria;

- i. High Melting point due to high temperature gases passing through the exhaust system. High Service temperature above 800°C for exhaust manifold and above 400°C for Muffle box and tailpipe.
- ii. High resistance to corrosion. Internal and external-different environments specify
- iii. Oxidation considering hot water vapour of exhaust gas.
- iv. Low density which can improve fuel economy.
- v. High young modulus in order to withstand vibration from the engine.
- vi. High thermal conductivity in order to allow even spreading of heat along the whole component.
- vii. High fracture toughness to resist crack propagation from an existing crack.
- viii. High resistance to thermal fatigue considering high temperature of above 800°C for exhaust manifold and above 400°C for Muffle box and tailpipe.
- ix. High yield strength to withstand the thermal stresses.

Fig. 2 presents the criteria for limits applied in the material selection for the Exhaust Manifold.

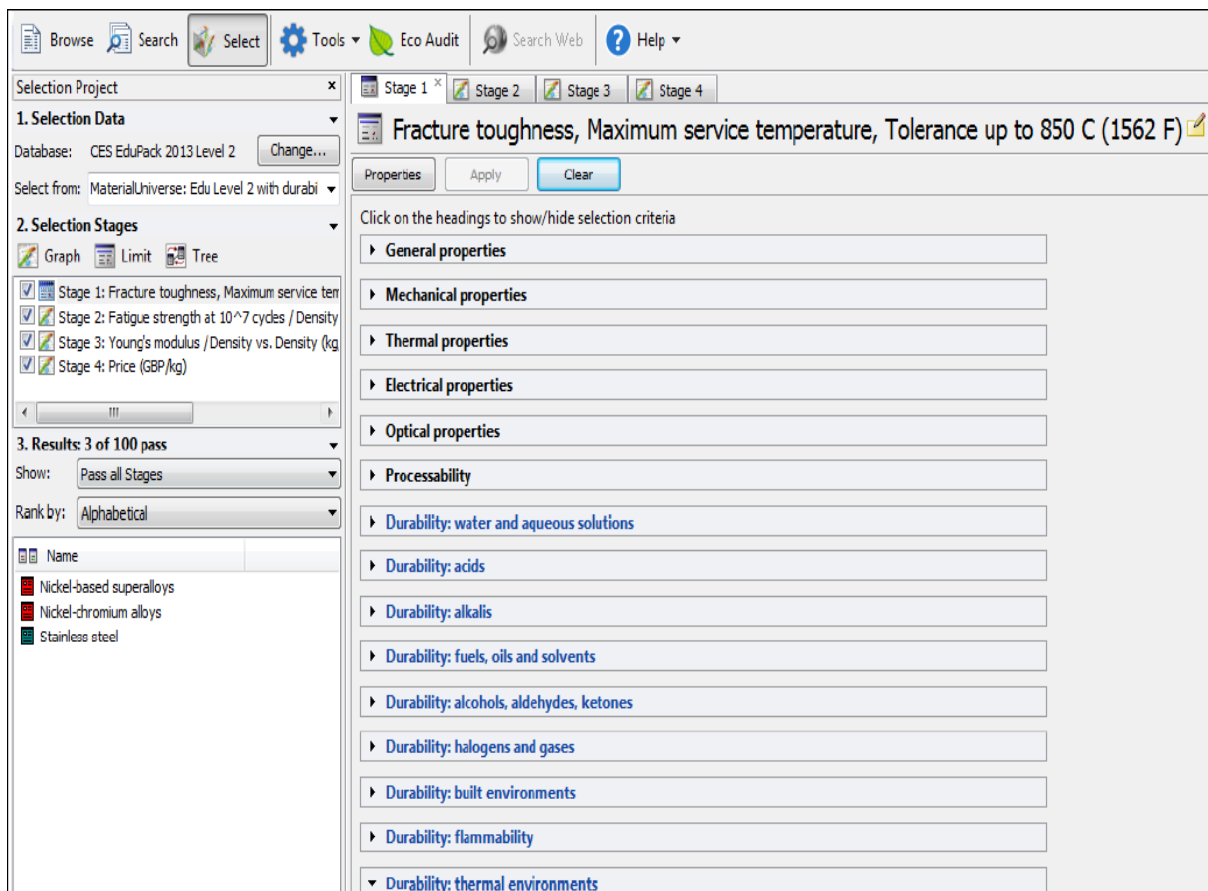


Fig. 2. Chart of Limits Applied in Material Selection for Exhaust Manifold.

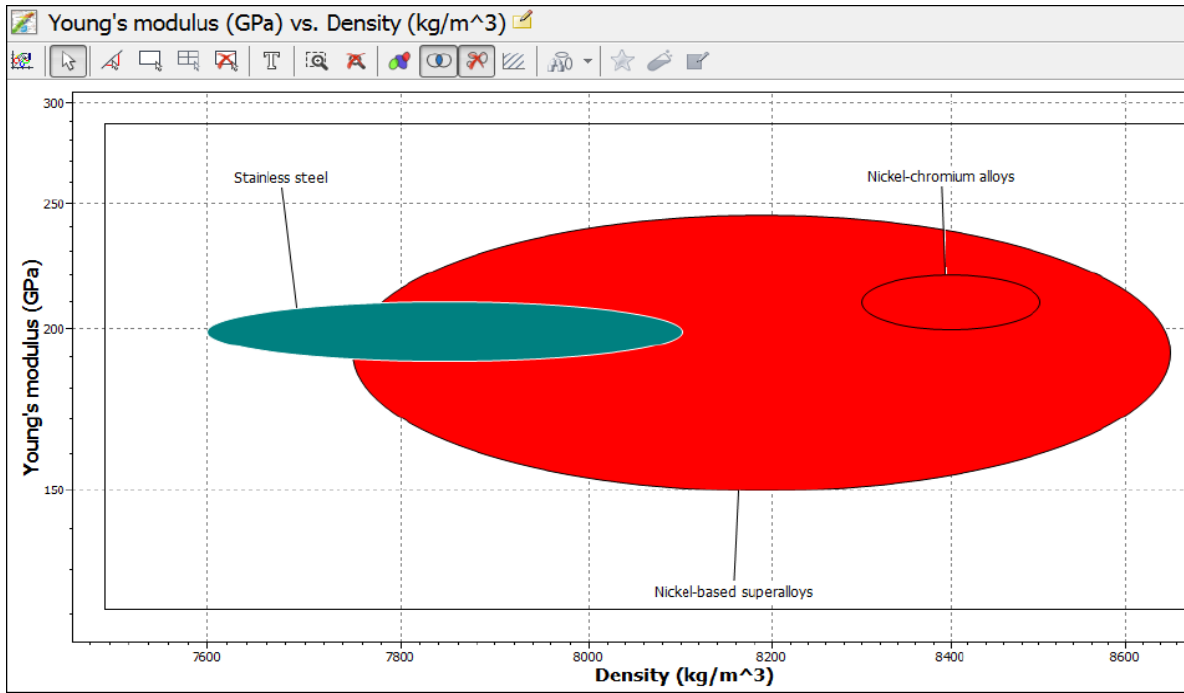


Fig. 3. Graph of Specific Young’s Modulus (GPa) against Density (kgm^{-3}).

The graph above demonstrates the materials young’s modulus (GPa) against density (kg^{-3}). The material shown in Fig. 3, stainless steel, nickel-chromium alloys and nickel-based alloys have high young modulus which provides the required stiffness but stainless steel has a moderately low

density which makes it a better choice of material for automotive exhaust than nickel. Fig. 4 represents a Graph of Fatigue strength at 10^7 cycles/Density (kgm^{-3}) plotted against Thermal expansion coefficient ($\mu\text{strain}/^\circ\text{C}$).

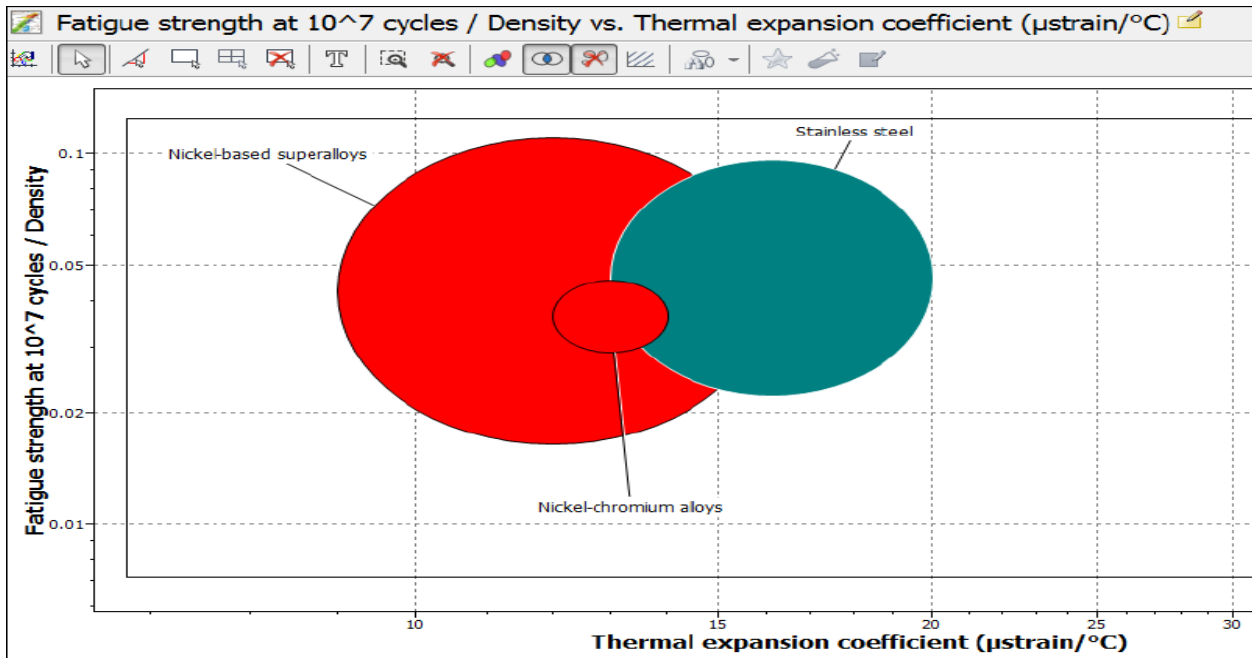


Fig. 4. Graph of Fatigue strength at 10^7 Density (kgm^{-3}) against Thermal Expansion Coefficient ($\mu\text{strain}/^\circ\text{C}$).

From the material selection chart shown in Fig. 4, Nickel alloys and stainless steel possess better fatigue strength and coefficient of thermal expansion that qualifies both materials

as potential material for automotive exhaust system. Fig. 5 is a graphical representation of Thermal conductivity ($\text{W/m}^\circ\text{C}$) against Maximum service temperature ($^\circ\text{C}$).

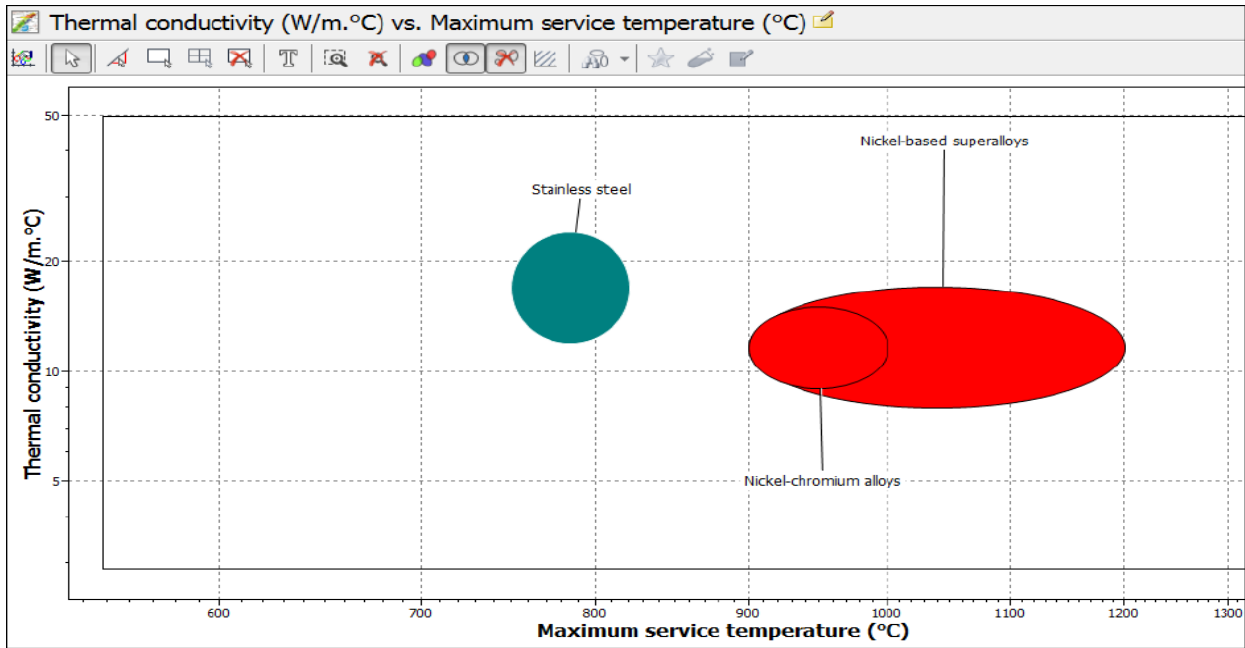


Fig. 5. Graph of Thermal Conductivity (W/m°C) against maximum service temperature (°C).

Fig. 5 presents materials potential materials with high thermal conductivity at the required service temperature. Nickel alloys may operate in a temperature level that

outmatches stainless steel, but stainless steel equally have the thermal conductivity required for optimum performance and longevity of exhaust systems.

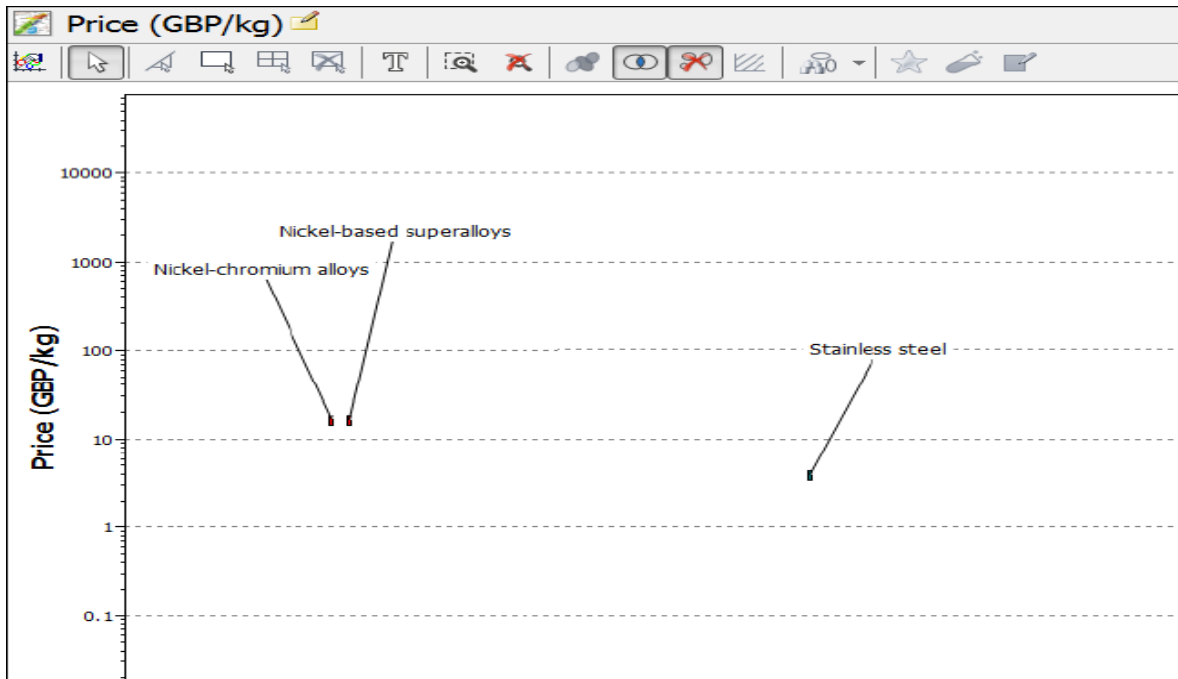


Fig. 6. Graph of Unit Price (GBP/Kg).

As shown in Fig. 6, stainless steel is comparably cheaper than nickel and its alloys. Since cost is one of the primary consideration that determines the feasibility of components production, stainless steel may be a better choice of material for automotive exhaust systems due to its good corrosion resistance property which can improve the material performance and longevity of the product.

3.1. Muffler Box and Tail Pipe

The material selection for both the muffler box and tail pipe were done at once as they have similar service conditions and loading properties. Fig. 7 presents the criteria for limits applied in the material selection for the muffler box and tail pipe.

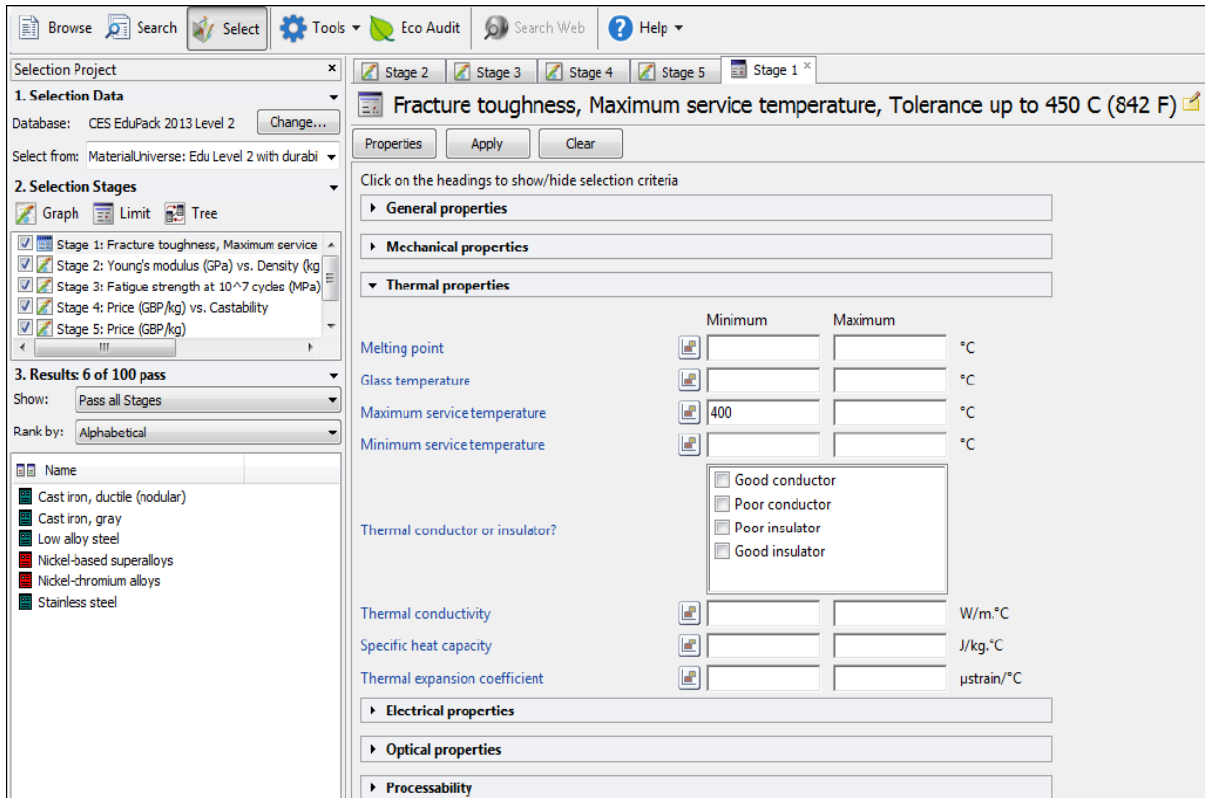


Fig. 7. Chart of Limit Applied in Material Selection for Muffler Box and Tail Pipe.

Once the conditions in Fig. 7. was applied, the following materials passed; gray cast iron, low alloy steel, nickel-based

super alloy, nickel-chromium alloy and stainless steel as shown in Fig. 8.

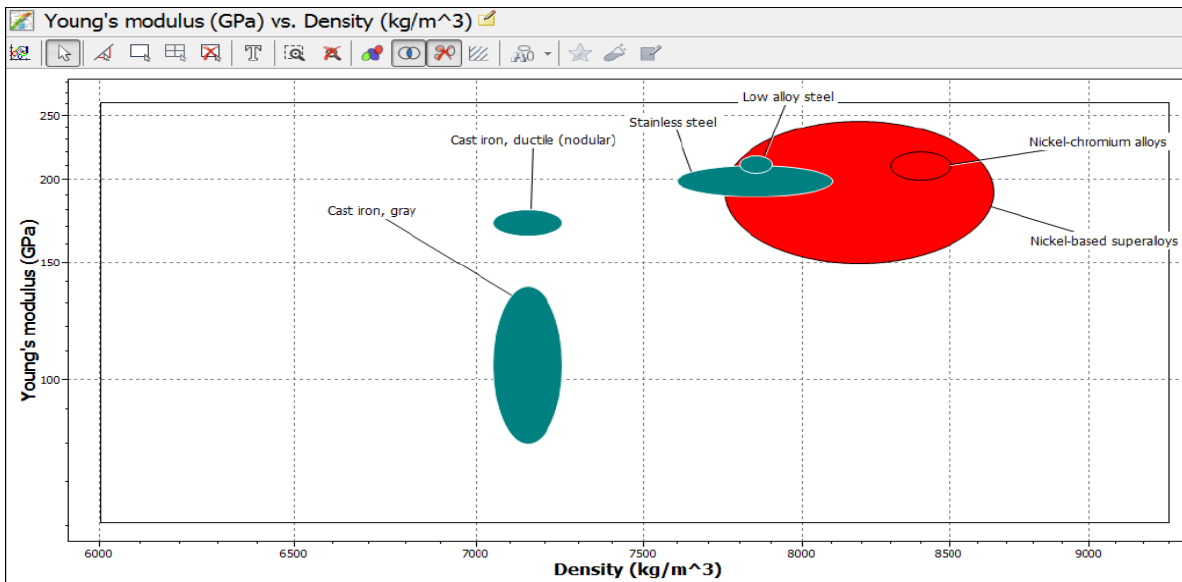


Fig. 8. Graph of Young's modulus (GPa/kgm⁻³) against specific yield strength (MPa/kgm⁻³) for Muffler Box and Tail Pipe.

Fig. 8 presents the potential materials for muffler box and tail pipe and these includes such as high carbon steel, stainless steel, cast iron and nickel alloys. Compared to the other three materials cast iron has low toughness and does not possess the strength needed to withstand the adverse conditions the muffler box and tail pipe is exposed to. Nickel alloys has the required strength but its density is relatively

high for this application. Stainless steel and low carbon steel possess the required strength and stiffness to withstand vibration, but stainless steel is costlier and has better corrosion resistant property than low carbon steel. Fig. 9 shows a graph of fatigue strength at 10⁷ Density (kgm⁻³) against thermal expansion coefficient (μstrain/°C).

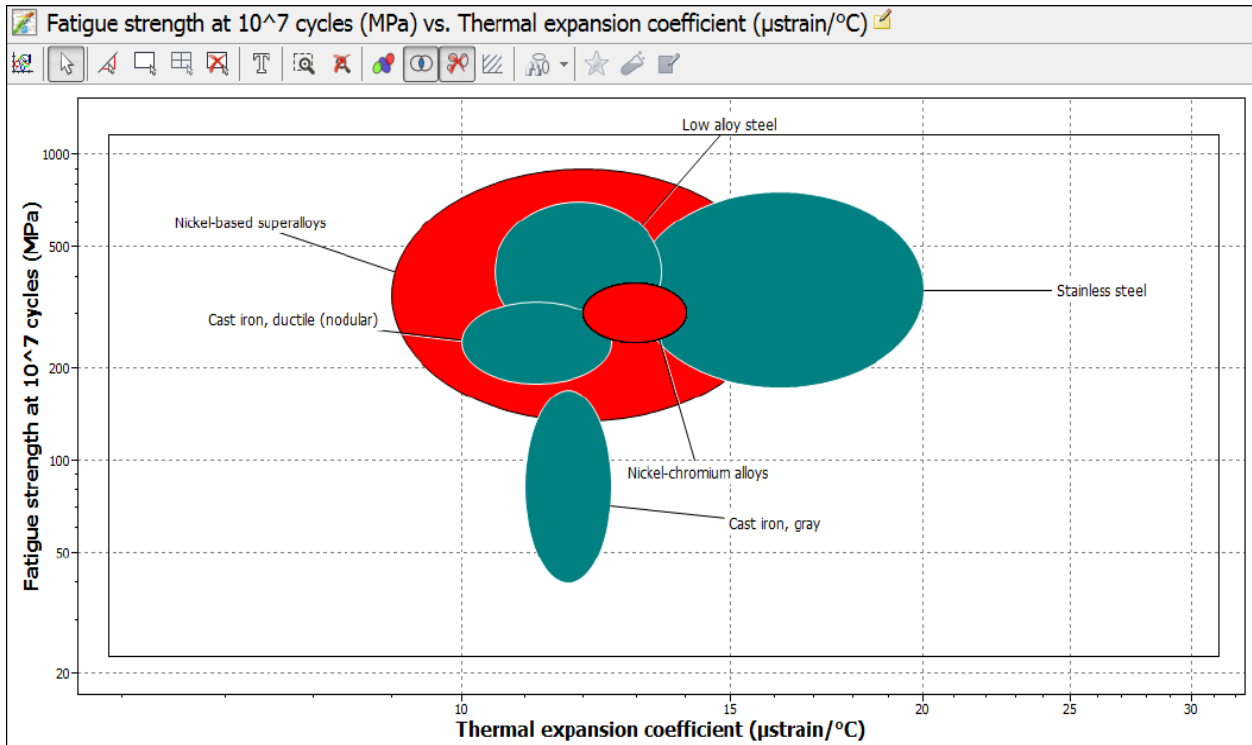


Fig. 9. Graph of Fatigue strength at 10⁷ Density (kgm⁻³) against Thermal Expansion Coefficient (µstrain/°C).

Nickel alloys can withstand relatively high temperature than other materials shown in Fig. 9. Stainless steel can also be a better material that can suit muffler box and tail pipe in automotive exhaust system application. However in real automotive applications, cast iron also possesses good

coefficient of thermal expansion that can equally perform suitably as potential automotive exhaust material. Fig. 10 shows a graph of thermal conductivity (W/m°C) against thermal expansion coefficient (µstrain/°C).

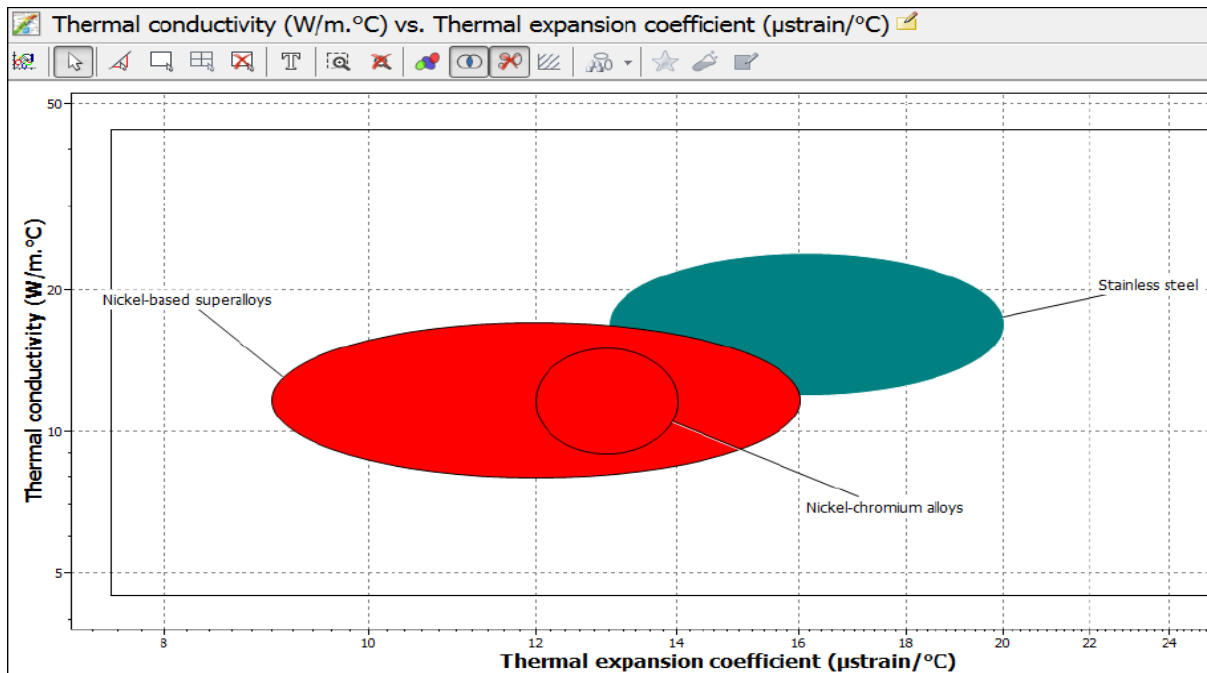


Fig. 10. Graph of Thermal conductivity (W/m°C) against thermal expansion coefficient (µstrain/°C).

As shown in Fig. 10, both materials can withstand the high temperature condition needed for this application. Fig. 11

shows the graph of price for different materials suitable for muffler Box and tail pipe of an automotive exhaust system.

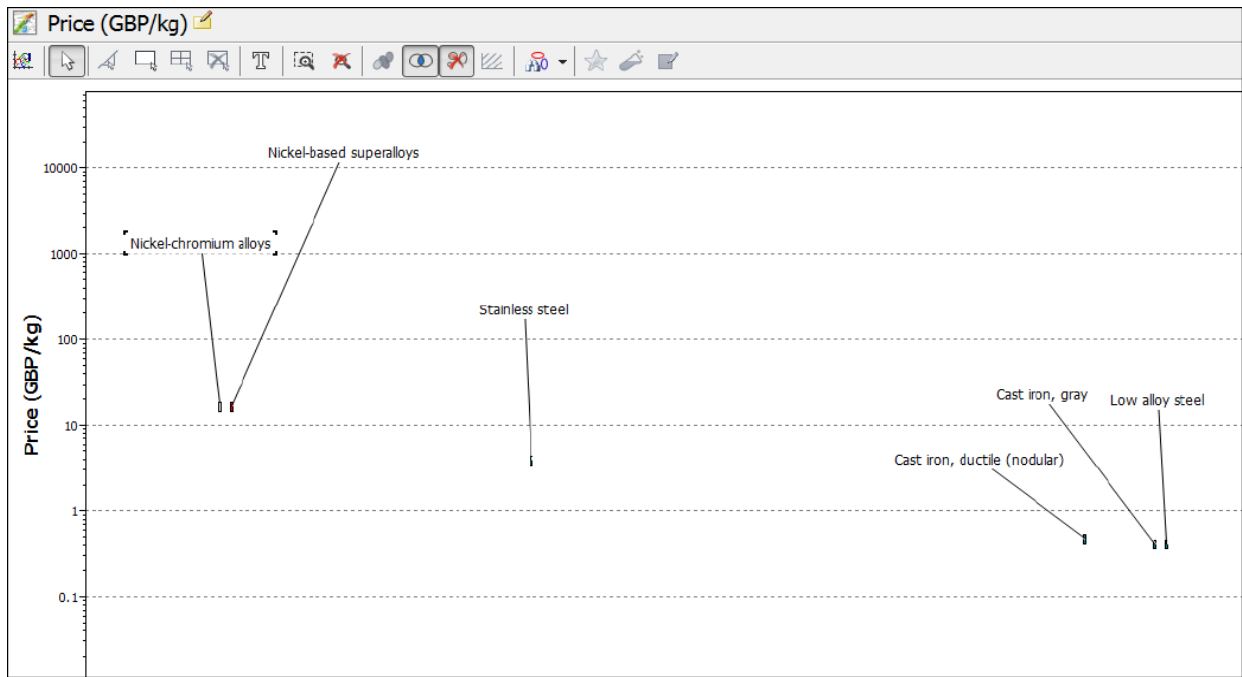


Fig. 11. Graph of Price (GBP/ Kg).

From the graph shown in Fig. 11, cast iron is obviously cheaper than stainless steel, nickel alloys and low alloy steel whereas, stainless steel is comparably more expensive than low alloy steel. However, nickel alloy is relatively more expensive than all the materials in Fig. 11, considered for muffler box and tail pipe of an automotive exhaust system.

4. Discussion

Fundamentally, a study of the different parts of the automobile with respect to the exhaust system reveals that it is exposed to various chemical and physical environments that must be accounted for by the choice of material, as well as the design. The position of the exhaust system exposes its parts to frequent vibrations and knockings that require the materials used in processing the parts to be hard as well as flexible. Additionally, the chemical composition of the exhaustive gases brings about the probability of reactions and corrosion between the parts, for example, condensate corrosion and salt corrosion. While starting a car engine in the cold conditions, exhaust system remains at ambient temperature. Condensed moisture content in the exhaust gases accumulates on the muffler and after-treatment system as well as the walls of the tubes. This phenomenon is known as condensate corrosion, and the condensate is sometimes composed of certain compounds such as CO_3^{2-} , NH_4^+ , SO_4^{2-} , NO_3^- , Cl^- and organic compounds [8]. Also, alloys used in manufacturing exhaust components usually undergo instances where high temperature exposure takes place after the alloys must have been exposed to acidic substances such as road-defrosting salt. This phenomenon is known as salt corrosion, in which the defrosted salt contends halides such as chlorides which can be very aggressive on stainless steel materials, and can act as flux agent that removes the protective oxide layer over time.

In the material selection process shown in Fig. 2-11, stainless steel seems to be a more suitable material for most exhaust system components considered in this paper due to its high corrosion resistant property, stiffness, resistant to high temperature above 400-1000°C working condition of typical automotive exhaust system. Also, the exhaust gases can condense and stick on the interior surface of the manifold. This is also one of the reasons why stainless steel is chosen for this application because it prevents condensation of exhaust gases onto its surfaces [9]. Considering the various types of stainless steel materials available, the two most importantly applicable stainless steel materials on automotive exhaust systems are the Ferritic stainless steel, and Austenitic stainless steel.

In addition to chromium and carbon, austenitic stainless steels generally contain nickel between 6 and 35%. The role of nickel is to stabilize austenite phase, improves mechanical properties fabrication and welding characteristics. Addition of nickel to steel can result in movement of the eutectoid point to the left and also increase the critical range of temperatures. Chromium is usually combined with nickel to achieve required ductility and toughness offered by nickel and the hardness and wear resistance provided by chromium. Sufficient addition of carbon to austenitic grades than ferritic grades can significantly increase the material strength at high temperatures. However, the application of austenitic stainless steels in exhaust system manufacturing attracts considerably higher as a result of the high percentage of nickel content, thus limiting it to applications where a suitable ferritic stainless steel is not available for use.

The application of austenitic stainless steel in automotive exhaust systems offer a refined surface finishing and are usually applicable to higher priced luxury cars and a more demanding applications.

One of the lower cost austenitic stainless steel often considered for automotive exhaust application is the type 304, but residual stresses in the material and its exposure to road salt makes this material grade highly susceptible to stress corrosion cracking (SCC) as well as intergranular corrosion if welded as a result of its relatively low nickel content. Compared to Type 304 alloys, austenitic stainless steels such as Type 316 alloys exhibits high resistance to material defects such as stress corrosion cracking and corrosion attack, and are sometimes considered as a better automotive exhaust material due to its higher nickel contents. Type 316L alloys also offer better resistance to intergranular corrosion defect over Type 316 but at the expense of some loss of strength, whereas, Type 316Ti offers almost the same strength as Type 316 alloys and also improved resistance to intergranular corrosion. Moreover, the Type 316 alloys tend to corrode rapidly when exposed to high temperatures and are not usually recommended for applications with temperature exceeding approximately 650°C.

However, the quantity of ferrite and austenite phases in a steel can be controlled through the percentage concentrations of nickel and chromium [1]. Ferritic stainless steel contains about 30% chromium in composition and less than 0.12% carbon and traces of nickel. Although the low carbon percentage reduces high temperature strength, this may not be too much of a concern in many exhaust system applications. Nickel is soluble in ferrite phases and does not form carbides or oxides, whereas, the addition of chromium to steels can result in the formation of variety of very hard carbides of chromium, yet the resulting steel material remains more ductile compared to steel of similar manufactured by simply increasing the percentage composition of carbon. Addition of chromium can also refine the material grain structure, with improved degrees of toughness and hardness. Moreover, it can also increase the critical range of temperatures by moving the eutectoid point to the left. The resultant moderately ductile, excellent resistance to corrosion attack and relatively low cost requirement have made the Ferritic stainless steel a well-known and widely used material for exhaust systems. A commonly used stainless steel grade such as Type 409 developed in the early 1960's for mufflers is a chromium ferritic stainless steel with over 11% chromium content stabilized with titanium. Higher chromium steels are commonly used nowadays because they offer greater oxidation and corrosion resistance. While 409 served as a good automotive exhaust material, more demanding applications generally require the use of ferritic grades such as 439 which can offer adequate oxidation and corrosion resistance at higher temperatures [4]. Thin double wall pipes in recent times are becoming common for automotive exhaust application, with austenitic stainless steel applicable at the inner pipe in some designs.

Materials generally used for manufacturing exhaust pipes, mufflers as well as other parts of exhaust system comprises ferrous alloys. Aluminium alloys in some cases are also used as a coating on ferrous alloys to provide more resistance corrosion effect. Furthermore, nonferrous nickel and titanium alloys are sometimes applicable in exhaust

system parts, particularly when very high performance is required. Ceramics have also had limited application in components of exhaust system to adequately benefit from its insulating properties. Ferrous alloys are primarily dependent on iron-carbon alloys such as stainless steel, carbon steel, alloy steels, cast iron etc. and their performance when used as material for exhaust systems depends on alloying elements are added for the following reasons [16];

- i. To provide solid solution strengthening of ferrite,
- ii. To cause alloy carbides precipitation instead of cementite Fe_3C ,
- iii. To improve material resistance against corrosion attack and other unique reasons.

Material choices for exhaust system is driven by several factors such as performance, cost, durability and reliability, warranty requirements and legislated and customer satisfaction. Mild carbon steel has been the choice of material for producing exhaust system components for several decades, due to the fact that the application of iron oxide served as coating on the exhaust system that to some extent protected it from atmospheric corrosion. Generally, it tends to exhibits poor corrosion resistance when exposed to salt on the road surface and condensate from the exhaust system. Consequently, exhaust systems manufactured from Mild carbon steel possessed very short service life when exposed to various environmental conditions by vehicles designed with such exhaust material. The effect of corrosion attack on carbon steel can minimised by means of using a hot dipped aluminium coating generally known as aluminized steel [7].

One of the most widely used ferrous alloy alloying element is chromium, which sufficient addition of it results in stainless steel. If the temperature of stainless steel is raised, the chromium content forms a protective chromium oxide layer that prolongs oxidation rate. The minimum quantity of chromium required to passivate the surface and to classify a given material as stainless steel is about 10.5%. As long as the oxide layer constantly remains stable, the metal substrate is remains protected against corrosion attack on the material which in turn prolongs the component service life. More preference was given to stainless steel in the mid-1990s as the principal material for components of exhaust systems downstream (than plain carbon and low alloy steels) such as the exhaust manifold or turbocharger. In recent times, this transition has taken precedence due to customer's demands for extended warranties and emission tax. Over the years, technologies to meet highly stringent emission polices has raised exhaust temperatures which in turn has made the task of meeting strength and performance requirements very challenging. In the early 21st century, requirements including several alloying elements used in stainless steel have experienced an extensive rate in price fluctuations. As a result of this, stainless steel manufacturers have included an adjustable alloy surcharge to account for these price variations. Many manufactures have invested on research studies to reduce the sensitivity of the finished product's price to these alloy surcharges [10].

5. Conclusion

In conclusion, material selection is a factor of numerous aspects of a component's design. The choice of the material is governed by very many factors as shown in the study above. One interesting factor is that the more challenges a component is exposed to in its in-service life, the higher requirements to improve the material performance and the wider the research needed to understand the challenges bedevilling the component prior to carrying out the material selection. High temperature and corrosion attack were spotted at as the primary defects that hampers the service life of an automotive exhaust system, and stainless steel (Ferritic stainless steel and Austenitic stainless steel) was selected as a choice of material suitable enough to withstand this challenges, and this is not too different from the conventional exhaust materials.

Acknowledgement

The authors of this manuscript would like to express their gratitude to Coventry University for providing the tools used in achieving the objectives of this paper.

References

- [1] N. Arlt, Korrosions-und hitzebeständige Stähle in Abgassystemen. CTI Exhaust Materials Forum 21-22.11.2007, Frankfurt, Germany, 2007.
- [2] D. Askeland and P. Pradeep, The Science and Engineering of Materials. Thomson Engineering, 2005.
- [3] M. Ashby, H. Shercliff, and D. Cebon, Materials Engineering, Science, Processing and Design. USA, Butterworth-Heinemann, 2007.
- [4] ATI, Stainless Steels Type 439/AL 439 HP. ATI Allegheny Ludlum Corporation Blue Sheet Technical Data, Pittsburgh, Pennsylvania, USA, 1999.
- [5] W. Callister, Materials Science and Engineering. New York, John Wiley & Sons, 2007.
- [6] D. Gaskell, Introduction to the Thermodynamics of Materials. Taylor and Francis Publishing London SW1P 1WG, 1995.
- [7] M. S. Chattha, J. Perry, R. L. Goss, C. R. Peters, H. S. Gandhi, Corrosion of aluminized low carbon steel exhaust system in vehicles equipped with three-way catalytic converters and development of a protective polymeric coating, Ind. Eng. Chem. Res., 29 (7), 1438-1442, 1990.
- [8] P. Gumpel and C. Hoffmann, Corrosion resistance of stainless steels to wet condensates in automotive exhaust systems. Proceedings of the 6th European Stainless Steel Conference, Helsinki, 2008.
- [9] D. Green, R. Hannink and M. Swain, Transformation Toughening of Ceramics. Boca Raton: CRC Press, 1989.
- [10] Y. Inoue and M. Kikuchi, Present and future trends of stainless steel for automotive exhaust system", Nippon Steel Technical Report No. 88, 2003.
- [11] A. E. Ikpe, I. Owunna, P. O. Ebunilo and E. E. Ikpe, Material Selection for High Pressure (HP) Turbine Blade of Conventional Turbojet Engines. American Journal of Mechanical and Industrial Engineering 1 (1), 1-9, 2016.
- [12] P. Lewis, K. Reynolds and C. Gagg, Forensic Materials Engineering: Case Studies. Boca Raton: CRC Press, 2003.
- [13] F. Mathews and R. Rawlings, Composite Materials: Engineering and Science. . Boca Raton: CRC Press, 1999.
- [14] Precision Automobile, exhaust system [online] available at <http://www.precisionautosales.com/exhaust.php>, 2000.
- [15] J. Shackelford, Material Science for Engineers. Prentice Hall: Upper Saddle River, 2000.
- [16] K. Zimmermann, Lightweight design in exhaust systems using tailored products. 9th International CTI Forum Exhaust Systems, January 26, 2011, Stuttgart, Germany, 2011.

Conceptual Guideway Structural Design for MAGLEV High-Speed Ground Transportation System

Can Balkaya*[‡], W.J. Hall**

*Department of Civil Engineering, Faculty of Engineering and Architecture, Istanbul Gelisim University, Istanbul, Turkey

**Department of Civil and Environmental Engineering, University of Illinois at Urbana-Champaign, Urbana, IL, USA.

(cbalkaya@gelisim.edu.tr, wjefhall@comcast.net)

[‡]Corresponding Author; Can Balkaya, Department of Civil Engineering, Istanbul Gelisim University, Istanbul, Turkey

Tel: +90 212 422 7020, Fax: +90 212 422 7401, cbalkaya@gelisim.edu.tr

Received: 27.04.2017 Accepted: 21.06.2017

Abstract- The conceptual guideway structural designs for MAGLEV (magnetic-levitation) high-speed ground transportation system are discussed by considering four different guideway designs of Bechtel, Magneplane, Grumman and Foster-Miller. The important aspects of the conceptual designs as well as some of the apparent shortcomings that will need attention in the design studies are emphasized. In this context the technical assessments and design observations may be considered for the guideway conceptual designs are given in this study.

Keywords Guideway, MAGLEV, Structural design, High-speed, Transportation system

1. Introduction

High-speed rails were mainly constructed on guideway structures with fast progress of train technology as MAGLEV (magnetic-levitation) for ground transportation system. The assessment studies have involved detailed review of four major conceptual designs namely those by Bechtel Corporation [2], Magneplane International Inc. [3], Grumman Aerospace Corporation [4], and Foster-Miller Inc. [5]. The assessment observations center on major issues addressed in the conceptual design reports. The evaluation has been prepared purposely to emphasize the positive aspects of the conceptual designs, as well as some of the apparent shortcomings that will need additional attention in design studies in the years ahead [6]. In this context the assessments may be considered to be somewhat general in nature at this point in time, for in almost all cases for the guideway conceptual designs presented, the technical details provided were, at most, of a 'general nature'.

With respect to the technical observations arising from these studies, authors offer the following observations. Four major conceptual design studies considered with

concentration on subtopics in five major areas, namely (1) route; (2) environmental concerns; (3) design criteria and preliminary design; (4) vehicle-system interface; and (5) maintenance/repair.

For the most part, as would be expected and is appropriate, major attention has been devoted to the guideway, and various factors that affect the guideway design, including operation and maintenance of the guideway system, vary between the various studies, and admittedly are difficult to quantify until such time as specific route is selected. It is safe to say that this area of the system design studies, namely the guideway system, is going to require a great deal more effort in the years ahead as the approaches in US an operating maglev high-speed ground transportation system.

2. Technical Assessment and Design Observations

2.1. Route

All of the conceptual designers gave considerable attention to a hypothetical route in the sense of looking at system requirements generally, and then specifically

alignment, curvature, tilt, and related factors pertaining to the routing and operation of the MAGLEV system, especially as it would relate to the performance of the vehicles.

With reference to 'best ride' assessment, the Magneplane designers concentrated on banking angle, curve layout, power requirements, and performance profiles. Consideration of the vehicle and guideway concepts as briefly summarized in the four alternatives, will reveal that the Magneplane design lends itself to being the easiest geometry for banking.

From an overall basis it can be noted that with respect to vertical geometry, as it applies to guideway design and performance, essentially it is not treated in any of the designs. Also, the authors have gleaned, from comments made in the studies here and there that are unlikely that the guideway will follow any highway right-of-way for any extended distance, primarily because of the tight turns that occur on highways. The high speeds of the MAGLEV system will require large radius turns, with provision for banking (super elevation); this latter topic received little attention in the conceptual design studies, except for Magneplane. As might be expected, Magneplane pointed up its vehicle/guideway system geometry in terms of advantage for banking on turns.

Route factors that would impact construction are being looked at in detail as a part of a separate study under the ongoing U.S. Army CERL assessment program. Indeed, in many cases, in evaluating 'route type' factors, it would be difficult to be more specific until a specific route was chosen, but some general observations can be made, and these follow in this section.

2.2. Existing Routes

Certain of the conceptual designs suggested that the routing might be along the median of interstate highways or other corridors, for example railroad rights-of-way. On the other hand, there is a reason to believe that although some of these corridors might be viable under certain circumstances, as noted earlier herein in this section of the summary report, in most cases the curvatures associated with turns on these routes would be totally unacceptable for a high speed vehicle. Most high speed ground transportation systems would be unable to follow existing highway-railway routes other than possibly when it is convenient (or necessary) through congested urban areas.

2.3. Rivers and Tunnels

The route studies would need to give special attention to the crossing of rivers, estuaries, and soft ground, in the sense of not only long-term performance (settlement and stability) of the piers (and guideway) under such situations, but also in the sense of safety measures for egress of people in the event of emergencies. Wetlands received special attention in the Magneplane design.

Likewise, tunnels will necessary have to receive special attention in the sense of adequate clearance for vehicles, airflow and acoustic effects, to prevent difficulties with the

vehicle systems as they traverse tunnels. In the case of air flow around vehicles in a tunnel, Magneplane, Grumman, and Foster-Miller each made mention of the importance of the problem, especially for high speed vehicles. Guideway support systems in the vicinity of rivers and streams, and factors associated with the use of tunnels, are going to require a great deal more attention as design progresses.

2.4. Grade Level/Overhead Guideway Plan

For some designs vehicles tilting will be required on curves. The maximum tilt of the vehicle for the various designs is noted in parentheses followed by the maximum bank angle: Bechtel (15 deg./30 deg.); Grumman (9 deg./ 24 deg.); Foster Miller (12 deg./28 deg.); and Magneplane (no tilt by virtue of the design vehicle-guideway system/ 45 deg.).

2.5. Horizontal Geometries

Among the various designs, Bechtel studied the matter of limiting horizontal geometries, and noted further that fiber reinforced plastic (FRP) tendons might be required in the long term in switching systems. Foster-Miller noted that glass reinforced plastic (GRFP) tendons may be needed in the long term on switches. The other designers made particular note of the requirements and singled it out for the future studies.

2.6. Aesthetics

As would be expected in a conceptual design, only a limited amount of attention was directed to aesthetics. It became obvious when reviewing the conceptual designs that the geometry of the columns was a big factor in overall aesthetics. For an aboveground facility such as the one contemplated, the matter of aesthetics will be a major concern with regard to the public and governmental entities that are concerned with the location of the facilities and guideways, as well as the overall operation. Probably the two most attractive column systems were the Bechtel canted double-column and cap arrangement, and the Grumman single pedestal. The other two designs called for parallel double columns. Also of importance is the spacing of the columns; in most cases even though some design exercises were undertaken to explore girder depth and span, versus column spacing along the guideway, baseline designs varied greatly. The Bechtel design called for a column spacing of 25m, whereas the Grumman baseline was 18m. The Magneplane design appeared to have columns at about a 9m spacing, namely quite close, which would seem to pose an aesthetic, if not a cost, concern.

Of equal importance will be attention to the effect that these systems will have on the surrounding land, facilities, housing developments, and industries, in the neighborhood of systems, both from an aesthetic appearance point of view as well as a noise point of view.

In the light of the above-ground power line systems strung across the specific route, much less recent attention to possible electromagnetic effects on people and animals, it

seems likely MAGLEV will come under intense scrutiny for similar considerations, especially noise and electromagnetic effects on people, both those on vehicles as well as those living and working near such systems.

2.7. Power Supply

An aspect of operation and safety that needs attention is the matter of loss of power and measures to handle emergencies loss of power would shut down the system and may require the need for quick egress. What is not so clear from the conceptual designs is whether or not there will be redundant power sources. Propulsion power 'pulsing' were it to occur, could lead to undesirable oscillations of the vehicles during travel; there was modest mention of that possibility in one or more of the MAGLEV designs. Additionally, there is the matter of power cabling; will this cabling be run along or within the guideway, or exterior to the guideway? The security of such a system, much less considerations of magnetic fields associated therewith, will be a consideration. It is realized that these topics are partly operational problems, but the guideway design necessarily will have to include consideration of such matters.

2.8. Personnel Safety/Emergency Stop

The matter of safety of personnel (passengers and operating crew) in the event of an emergency stop is one of great concern. Magneplane, Grumman and Foster-Miller give some attention in the conceptual design to walkway concepts, for use in emergencies. Grumman and Magneplane focused attention on a central walkway between the vehicle guideways, although this design raises questions about its viability in the sense of protection for keeping people from falling off the central walkway, including downward egress to exit the system especially in difficult terrain, over water, or in inclement weather. Foster-Miller exhibited a downward (beneath vehicle) exit arrangement. Clearly, safety concepts with regard to passengers are a matter that is going to require a great deal of additional attention.

2.9. System versus Environment

Another factor with regard to the route that will need attention is the differing climates through which the system would necessarily operate, perhaps from warm through cold climates. In such cases, the route will need to be evaluated for its ability to accommodate the varying types of weather and environments that it may encounter. For example, Bechtel noted that icing could create problems for its vehicle/guideway design. Magneplane studied and problem, and especially debris related matters. Grumman considered weather as no problem, probably because of the large gap maintained between the guideway and vehicle. In the case of Foster-Miller, the open part of the bottom of the guideway serves to eliminate much of the problem with weather. It is apparent that all designers were quite conscious of the problem that might exist, for they gave great attention to sensors for monitoring such effects.

In some respects the Magneplane designs will preclude some of the difficulties with inclement weather, because of its open truss design, although the details of the 'trough' area as yet not clear. At the other extreme, the Foster-Miller design suggests major problems because of the vertical sidewall and the extreme small clearance between the sidewall and vehicle, measured in centimeters apparently.

2.10. Environmental

All of the designers gave consideration to the environment to some degree, some in more detail than others, and especially with regard to the operation of the system. Among the environmental effects requiring attention are such factors as earthquakes (seismic effects), wind (straight winds up through tornadoes), rain, ice, snow, lightning, dirt, debris, and flooding, and their affiliated effects, including such items as slope stability and liquefaction. Detailed design criteria will need to be developed to cover these and other factors.

External vehicle/system factors include effects of noise on passengers and route environs, as well as vibrations/motions of the vehicle as it would affect ride quality need investigation. Similar comments pertain to electromagnetic field effects, as they may possibly affect passenger comfort and health.

2.10.1. Wind

Certain of the designers, but in varying degrees addressed high winds. It is perceived that for some of the vehicle guideways systems were the vehicle to stop on a curved guideway sector with significant tilt, high wind could lead to a stability problem. This matter was examined only superficially and there is reason to believe from operation of regular railway systems that this can be a major design factor. One could guess it might be critical for the Foster-Miller concept with the small clearance between the sidewall and the vehicle, especially on curves, if not straight guideway runs. Bechtel identified wind as a problem to be dealt with.

2.10.2. Earthquakes

Earthquakes irrespective of whether or not their source is near or far can pose a major problem, not only in the sense of vibration of the guideway system and therefore the operating vehicle, but also from standpoint of rotational motion of the aboveground supports (pillars), differential ground settlement arising from slope instability or liquefaction, and a host of other related affects.

Also, some attention is given to the matter of detecting earthquakes, and the sensing systems that would be needed on high-speed MAGLEV systems, much in the same way that the Japanese designers developed for their high-speed trains.

2.10.3. Debris and Dirt

From an operational point of view debris and dirt, for example, can have a major effect upon the operational characteristics of the system and these have not been addressed in any great depth in any of the reports that we have reviewed. The debris could originate from environmental effects (i.e. wind) or be placed by people (sabotage). Some type of detection system to counter those effects would seem desirable.

2.10.4. Noise and Vibration

Noising arising from operation of these high-speed systems can be a factor, especially in urban areas. It was noted that all four designers (Bechtel, Magneplane, Foster-Miller and Grumman) gave some attention to this matter; Grumman paid particular attention to aero-acoustic noise, as well as aerodynamic studies.

2.10.5. Safety

Safety is mentioned in all four conceptual designs, but receives the most comprehensive attention in the Bechtel and Grumman submissions. Of great concern, of course, is the matter of derailment as it might occur at switches, and more unlikely (but possible) in the event of ground motions arising from unanticipated settlement, slides, or possibly earthquake effects. The safety of passengers and operating personnel, in case of emergencies, is addressed under the Section 2.1 on Route.

2.10.6. Electromagnetic Effects

Electromagnetic effects were singled out by all four design groups as being a major factor, especially as it might

affect passengers, much less those staff and maintenance workers located near the vehicles at stations.

A factor that was not noted by the reviewers of the design submissions is electromagnetic effects in the sense that the maglev guideway system is a 'string'. Strings crossing large sectors of the earth can have magnetic effects induced in them to such an extent that this can be a factor of design concern with regard to the performance of the electrical systems themselves, as well as corrosion of metals in the system. Telluric currents may need study in the next phase of the design.

3. Conceptual Guideway Designs of Four Alternatives

All four of the major design teams paid varying degrees of attention to the design criteria and preliminary design of the guideways. The assessment that follows begins with a short description of each of the four conceptual guideway designs; it suffices to note that the reviewers are aware that in many cases the descriptions and studies must be general a most in light of the uncertainty of the vehicle design, including levitation and motivation.

3.1 Bechtel Corporation and Subcontractors

The Bechtel design is consisted of two parallel eight span continuous prestressed haunched concrete box girders (each supporting a vehicle transit system) shown in Fig.1. The girders, in turn, are supported on a bent with sloped legs, tapered as viewed in elevation, supported in the general case on integral spread footings. The column bents have a spacing of 25m. The girder connection to the adjacent continuous span would be with a simply supported partial interior span that would permit adjustment during construction and thereafter. Bechtel typical guideway structural details are given in Fig.2.

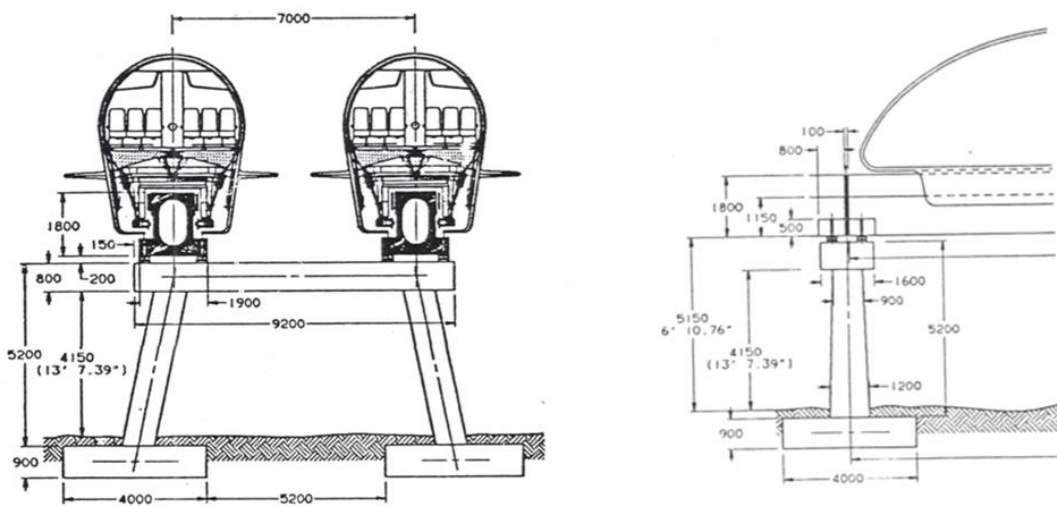


Fig. 1. Bechtel design typical guideway sections.

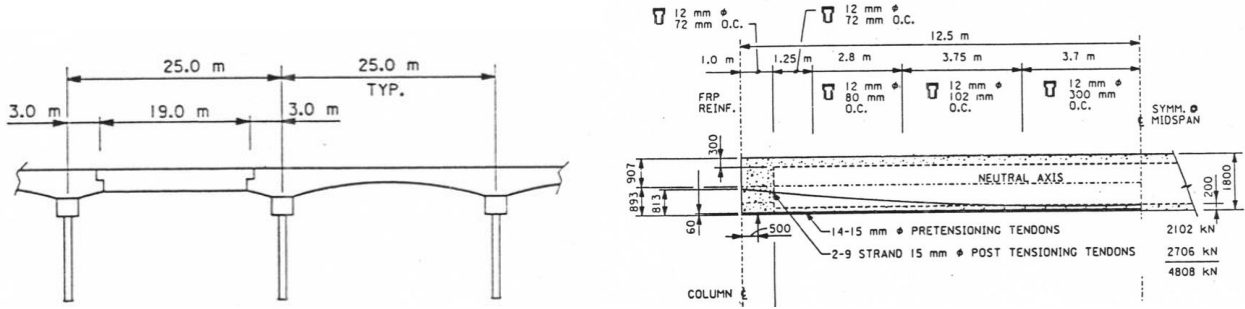


Fig. 2. Bechtel design typical guideway structural details.

The authors note that the bearing surfaces at the top of the bents are large with provision for adjustment, and providing a platform in the event of unexpected deformation, and thereby safety. Moreover, the load path from the beams is directly down through the columns of the bent, providing a stiff, aesthetically pleasing system. These closed box sections have the advantage of being stiff in torsion, and would lead to reduce deflection, the overall effect being a smooth base for the vehicle ride.

The levitation system is based on a ‘flux canceling’ electrodynamic (EDS) system in which superconducting coils on the vehicle interact with a ladder-like structure on the guideway, with the latter providing suspension and some guidance of the vehicle. No information was found that related to clearances above the rail, or at the sides.

3.2 Magneplane and Subcontractors

Several schematics are shown in Fig.3 for the Magneplane guideway system. In general form the longitudinal guideway structure consists of continuous steel truss ‘beams’ of varying form. The ‘two’ guideway systems are supported in turn on a concrete cap girder, and thence

down to earth on two concrete columns to a spread footing or pile foundation. The guideway trusses were noted to be continuous over two spans. The columns spacing along the guideway was just a little over 9 m, meaning that the columns are spaced relatively close along the guideway. In some configurations the single-track system is shown supported on single concrete columns. Magneplane typical guideway structural details are given in Fig.4.

The ‘magway’ consists of aluminum box beams supported in turn by the steel truss members. Concrete beams also were considered, but were ruled out for cost reasons. The unusual and novel feature of this vehicle system is that it essentially is supported on a hexagonal base, permitting it to move, as required to handle curves and other system requirements.

The levitation is noted to be of the EMS (attractive) type, although levitation and propulsion were noted as not having been studied in detail as a part of the conceptual study. The clearance during operation is currently planned to be about 0.15m or 15 cm, the largest of any of the systems.

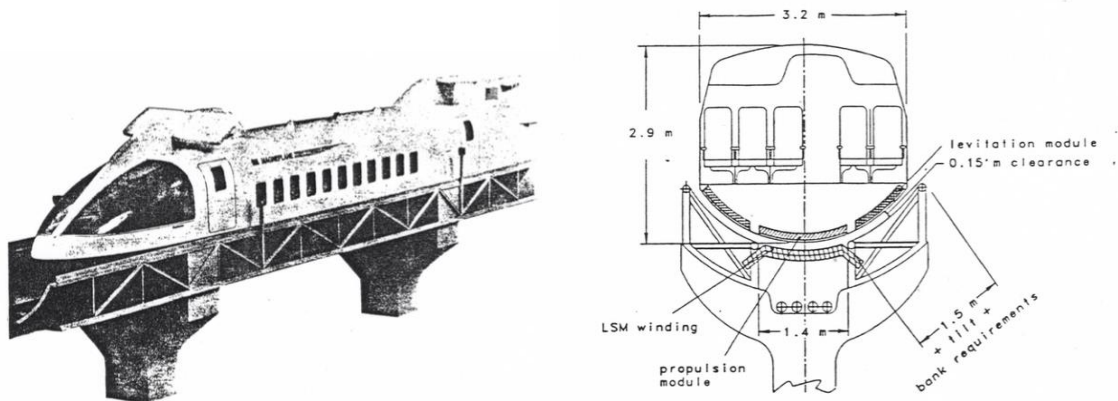


Fig. 3. Magneplane design typical guideway sections.

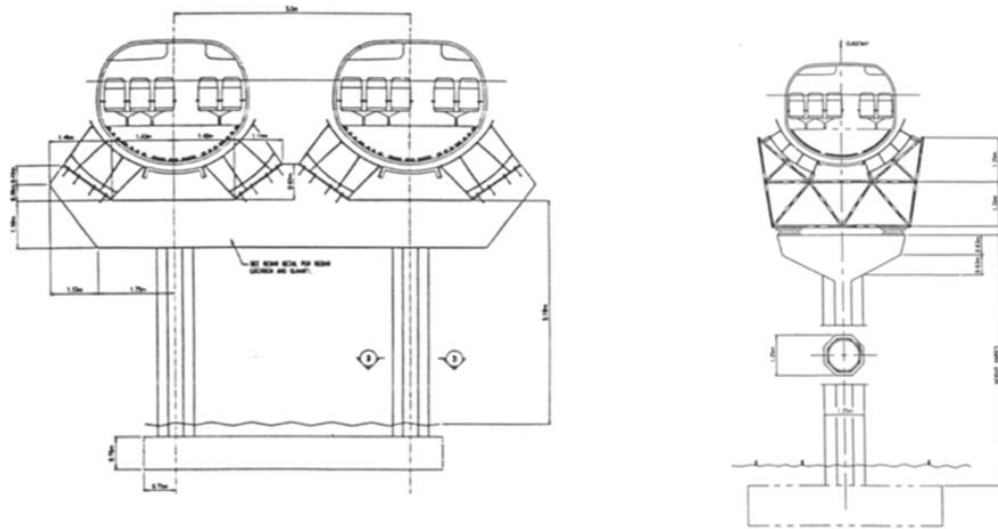


Fig. 4. Magneplane design typical structural design.

3.3 Grumman and Subcontractors

The Grumman guideway system as shown in Fig.4 is envisioned as a twin-track guideway, with a central prestressed box girder (the so-called spine girder concept), simply supported on pedestals, and in turn with the maglev rail supported on cantilever members in turn supported by the central prestressed concrete box girder. The depth of the prestressed concrete central box girder varies, and is dependent on the span length. The column is founded on a rectangular concrete footing that in many cases will be on piles; various types of footing supports were examined.

Computations were made for simply supported spans, of varying lengths of 18m (baseline) up to 49.5m. The loadings, for the most part, from the vehicle are unsymmetrical as can be seen visually in the figures. Grumman typical guideway structural details are given in Fig.6.

The vehicle levitation system is of the EMS type, namely an ‘attraction system’ that helps remove some of the electrical filed from the cabin area. Other advantages claimed are that it leads to a uniform load distribution along the full length of the vehicle, leads to smaller pole pitch, levitation at all speeds, and leads to a wrap around configuration that promotes safety during operation.

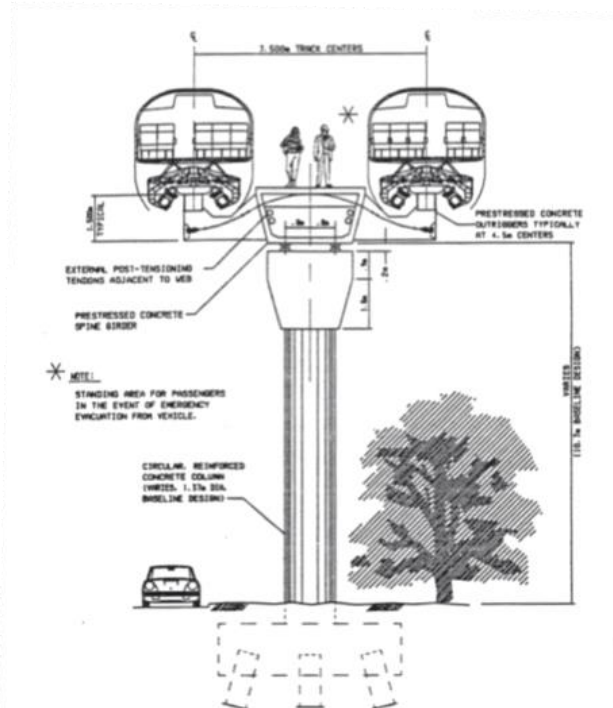


Fig. 5. Grumman design typical guideway sections.

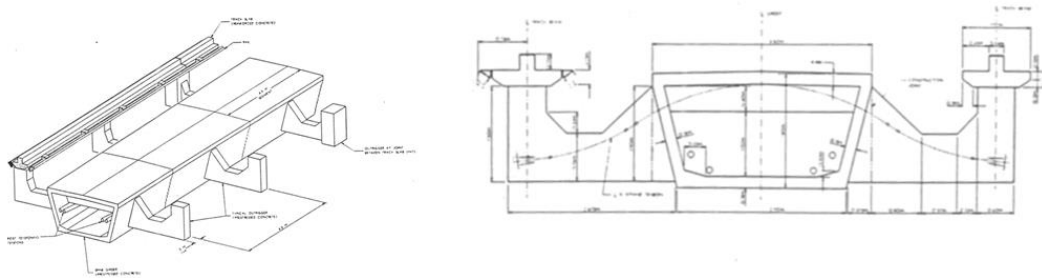


Fig. 6. Grumman design typical guideway structural details.

3.4 Foster-Miller and Subcontractors

As gleaned from the description shown in Fig. 7 and design report [5], the preferred guideway system is one of modular construction and has twin hollow beams connected by structural diaphragms. Foster-Miller typical guideway structural details are given in Fig.8. The designers note the following advantages of their system: (1) Open bottom eliminating problems of ice, snow and debris accumulation; (2) wide 'track gauge' for vehicle stability; (3) sidewalls offering significant protection of vehicles under crosswinds

and gusts and (4) most convenient for sidewall levitation scheme.

The vehicle system is based on the EDS system (repulsive principle); the conceptual design calls for a null-flux sidewall levitation system. The propulsion is by a locally switched advanced linear motor. The gap clearance is reported in one table to be as great as 7.5 cm. The clearances between the vehicle and the levitation walls are quite small (measured in cm), suggesting major problems if there are any distortions in the system, at super elevation/curve geometries, etc.

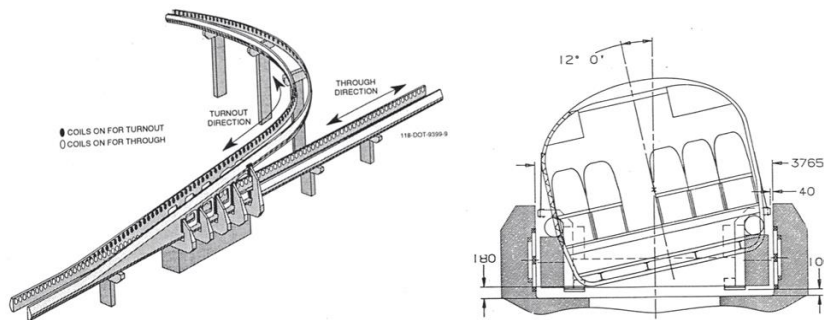


Fig. 7. Foster-Miller design typical guideway sections.

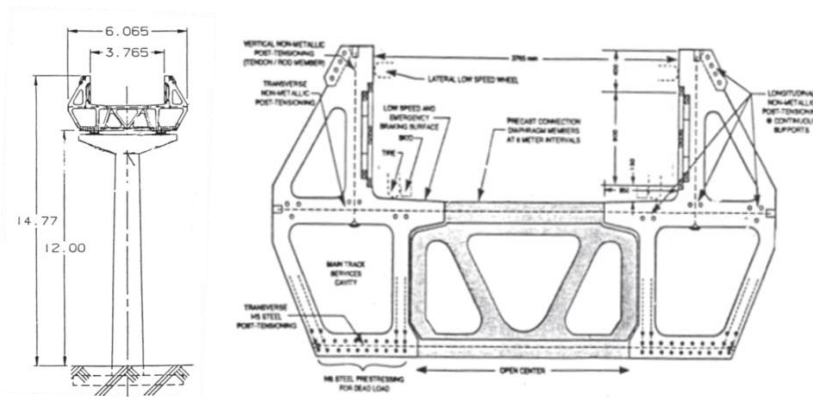


Fig. 8. Foster-Miller design typical guideway structural design.

4. Guideway Structural Design Concepts for MAGLEV

4.1 Loadings

All of the designers provided some degree of attention to the loading criteria to which the guideway should be designed. Grumman and Bechtel probably provided as much information as anyone. With respect to seismic effects, all

mentioned it, but probably Bechtel was most realistic in noting that no transportation system is completely invulnerable from seismic effects. Some indicated code design requirements, which would be the minimum under any circumstances. Bechtel called out a need for sensors to provide warning of seismic activity, and intelligence for being aware of possible alignment problems and disruptions that might be associated with seismic activity. Fatigue

considerations were not singled out as an important problem at this stage. Other considerations that might be considered 'loadings' in a generic sense are discussed under Vehicle-Guideway interaction, below.

Vibrations, magnetic forces, and braking forces were considered in some detail by Bechtel as well as Foster-Miller. Magneplane had a few comments on vibrations and braking forces, as did Grumman.

4.2 Deflection, Camber and Tolerances

In the design of the guideways, attention will be given to the matter of the deflection tolerances and how much camber should be initially built in to take account of vehicle loads and/or creep and thermal affects. Such considerations refer not only vertical effects, in the sense of vertical loads on the guideways, but also to horizontal effects in the sense of straightness of the guideway members, and the control on the guideway system as vehicles traverse bends in the system.

This is an important topic that in the next level of design will need detailed attention both with respect to vehicle/guideway system operation, but particularly to long-term performance and maintenance considerations.

4.3 Construction of the Guideway

Particular notice was made of attention paid to construction considerations. In that regard, Bechtel and Grumman clearly addressed the most fully problems in this topical area, and included attention to connections at all levels, and some attention to foundation conditions in this regard. Foster-Miller comments on construction were much less exhaustive in term of treatment and thought, as compared to the other designers. Magneplane comments were minimal at best.

4.4 Vehicle-Guideway Interaction

All of the designs, in one way or another, address the matter of vehicle-guideway interaction, which is important from the standpoint of the operation of the vehicle and the comfort of the passengers, as well as system safety and ride comfort. The vehicle-guideway interaction problem increasingly complicated as the speed of the vehicle increases, both from the operational/aerodynamic aspect, especially as they relate to the operation of the system. All of the designers gave some degree of attention to guideway imperfections, such as those that might arise from changes of alignment between spans, or 'bumps' associates with debris. Thermal effects were noted to be important, especially in the Magneplane presentation where high thermal gradients were noted in connection with vehicle operation; others had lesser attention, with Grumman, so far as the reviewers could tell, giving little attention to this topic apparently.

External factors that could affect the performance, in addition to debris that might be deposited by humans, would include ice, snow, debris deposited by wind, misalignment arising from seismic activity, and thermal effects.

4.5 Foundation and Pillars

Various designs gave different attention to the foundations for the pillars or columns that support the guideway system. Probably the magneplane group did the most study in this regard, but all of the studies need additional attention to the different forms of foundations that would be required for an elevated system of this type. It was noticed that the conceptual designs thus far have not given much attention to matters of multiple support of the foundation pads (an exception is Magneplane that showed some multiple piles) to preclude long term settlement and/or rotations that might occur under environmental effects, much less settlement and other factors associated with the guideway operation. It can be envisioned that the footings, a large part of the construction cost, can range from slab on grade in some cases, to those supported on drilled caissons, or on piling. The foundations will need to be firm to resist environmental effects arising from earthquakes, wind, flood, etc. Hopefully in view of the large number of such installations, the cost can be reduced to a degree through novel prefabrication techniques. It is our belief, based on our study that the foundation systems for this elevated guideway system will turn out to be somewhat more complicated, as well as more expensive than has been indicated thus far in the studies.

4.6 Guideway and Pedestals

The design of the pedestals or columns varied between the various conceptual designs by reason of the fact that they supported different types of guideway/beam systems. The Bechtel design, as described earlier, uses a canted pair columns that form a frame; the Grumman design employs a single pedestal. The Magneplane and Foster-Miller designs appear to center on double vertical columns, with the caps independent or tied as the case may be. As a result, little can be said about the pedestal designs except to emphasize that these column guideway systems are inverted pendulums in the sense of dynamic effects arising from earthquakes and, thus, will require great attention, not only in terms of the stability of the structural systems, but also their actual design to insure that they can accommodate the lateral forces that arise from vehicle, wind, earthquakes, as well as other unequal and unsymmetrical loadings. In this sense, the Bechtel design is the more stable of those proposed.

In the case of the girders, these ranged in the conceptual design from simple spans (i.e. Grumman) where considerable attention was given to end effects, rotations, creep, settlement, differential settlement, etc., although it was not clear whether or not Grumman had considered twist around the rail, to box girders in some cases, and conceptually continuous girders (i.e. Bechtel). There is a great deal of design and construction trade off that needs to be considered in this area in the sense of construction such systems, as well as handling adjustments with time. Obviously, in the case of simple beam systems, there can be difficulties, as has been experienced with some monorail systems in the United States at the discontinuities that occur at the ends of the girders, as well as the effects of creep and thermal effects (especially in

areas of the country where there is great temperature extremes). Novel designs were put forth, for example, Magneplane employed a hexagonal guideway support system for their vehicles, which included a truss, a linear arrangement that in essence lightens the guideway system, but perhaps leads to other problems. As an example, it was not so clear in the case of the Magneplane design what may happen in the case of ice, snow and rain in the sense of the vehicles; in one sense, it seemed to be attractive from that standpoint, and in another sense it was not so clear that these factors could be handled as easily as suggested. Another important aspect of the design of the girders is that of the continuity and in a sense continuous spans going across a half dozen or so girders would make it possible to have more control over the reliability and ride comfort. On the other hand, the adjustments needed for effects of creep, shrinkage and thermal effects might be more difficult to handle, although this was explored in some degree with prestressing in the case of Bechtel and Grumman. Thus, we see a range of considerations in the possible construction of the guideways.

Another aspect of the design that has needed attention, of course, is that some of the designers have given attention to fiber reinforced plastic (FRP) or glass fiber reinforced plastics (GFRP) as being a reinforcing material to cut down on electromagnetic interference and effects with regard to levitation and propulsion. This is a subject needing additional attention for the studies thus far on FRP have shown good, as well as not-so-good, characteristics with regard to creep, long-term strength, and perhaps thermal behavior.

In terms of general treatment, reinforcing, restressing and anchorage all received some degree of attention, in the most detail by Bechtel, and in lesser detail by Foster-Miller. No significant inclusions were noted by Magneplane and Grumman. This topical area will require great attention in the next design phase, not only in the sense of initial construction, but also in the sense of maintenance adjustments to the system over time to insure adequate system performance. Guideway design requires great additional study in light of the construction costs involved. It may well prove advisable to build short trial sections for pilot use/testing in widely different climates.

4.7 Thermal Effects

Thermal effects need a great deal of additional attention. None of the conceptual designs really addressed that question in any great detail. To their credit Magneplane did describe some schemes for use of aluminum materials to dissipate heat they envisioned being generated with their system. Such effects are not only important in the case of pedestals and girders, especially in the sense of their structural adequacy, but also it has an effect upon the vehicles, vehicle guideway interaction, and possibly guideway expansion problems.

4.8 Air Gap

The vehicle systems investigated thus far call air gaps ranging from as large as a 15 cm levitation gap in the case of Magneplane (but 5 cm was more probable the report

indicated) to 4 cm in the case of Grumman. In any case, whatever the system, whether it be a repulsive or attractive electromagnetic levitation system, the matter of clearances is going to be one of great concern in connection with the design and maintenance of the guideways, and especially operation of the systems. This gap hopefully will provide for differences in deflections and alignments of the guideways, at joints in the guideway, as well as accommodation of debris, ice and snow. Laterally in the case of Foster-Miller, the vehicle appears to have little clearance with the guideway, especially if the vehicle tilts on super elevated curves, or in the wind. Thus, there is a wide range of parameters that must be considered in terms of support of the system.

4.9 System Stability and Rocking Analysis

Attention was given in some of the reports, especially Bechtel, with regard to the vehicle instability that might occur under normal operation or in taking curves. Wind effects also received consideration, especially in the Bechtel design with respect to rocking considerations. That is one kind of analysis that needs more study. At the other extreme, system stability in general, for example the keel effects need to be studied; Magneplane did, for obvious reasons, look into this matter, but the findings would appear questionable. In the Magneplane design, one can envision a rolling/swooping effect as the vehicle traverses the guideway, which could be of concern not only to operation but also to rideability. Also, these stability effects are important with regard to the operational reliability, especially in terms of the gap that must be maintained for satisfactory operation.

4.10 Emergency Stops

Certain of the designs did pay attention to the guideways with regard to the emergency stops. Bechtel concentrated on preferred stop points, or safe stop points, where the vehicles could stop and efficiently handle the passengers.

4.11 Switching

Most of the designs considered switching arrangements for their particular vehicle design, but, at this point in time, it is difficult to envision how these would be handled with the guideways that were proposed and (or the terminals that were envisioned. Since some of the switching will occur at high speed and some at low speed, varying criteria will come into play. This is a very difficult technical aspect of design.

4.12 Stations and Facilities

All conceptual designers mentioned stations and facilities, although Grumman is the only one to spend some limited space on the matter. It is appreciated that these are more 'routine' in the nature, and would be addressed. The reviewers did notice some attention to passengers and public safety, in term of addressing the 'standoff distance' at stations, from the standpoint of avoiding electromagnetic effects.

5. Specific Observations on Guideways

5.1 Magnetic Effects

Among the effects needing more study in the future were magnetic effects (on passengers and operating personnel), vibrations, air gaps, construction tolerances, keel effects, and suspension (especially for emergency conditions). Every report indicated further studies of this topic are needed. Each of the four conceptual designs studied the technical details associated with magnetic effects, on passengers as well as crew and others in the immediate vicinity. Quite different details are noted for each of the designs, as would be expected, each pointing up the advantages of this system.

5.2 Vibration

All four designs looked extensively into vibrations as they affect ride quality and the frequencies of such vibrations. The frequencies will be important factors in assessing the vehicle/guideway interaction, vehicle performance, passenger comfort, and long-term maintenance.

It appeared that although some attention to wind had been given in the conceptual designs, in some instances for the guideway curvatures and tilts envisioned, the vehicles were clearly unstable. Bechtel took pains to address this point.

5.3 Air Gap

This topic was addressed in the earlier Section 4.8.

5.4 Keel Effect

The keel effect, as it affects the stability of the vehicle, is an important factor. The matter is of particular importance to those systems using large clearances, as for Magneplane. Somehow, in the design process, there will need to be some balance between the air gap associated with levitation and stability of the vehicle under all of its operating modes. Considerations will not only focus on a gap to preclude difficulties with debris, ice and other factors already identified, but also the important matter of safety of control of the system at high speed to preclude accidents of various types, including 'running off the guideways' especially for some designs.

6. Maintenance/Repair

Although there was passing mention in the conceptual design reports given to maintenance and repair, little information of that type were presented. Perhaps the most attention to service vehicles and surveillance is that given in the Bechtel [2] and Grumman [4] reports. This is a major topic needing detailed consideration, not only with regard to the vehicles and guideways, but the power system and its reliability, and the viability of the systems under the environmental effects outlined previously. The Bechtel report [2] did give some attention for example, to a service

vehicle concept, which would be needed for the safe and efficient operation of a MAGLEV System.

Numerous questions arise. For example, will corrosion of the guideway electronics be a factor? Will surface deterioration of concrete, as well as reinforcing corrosion be a problem? How will adjustments in alignment be made?

7. Conclusion

High-speed trains constructed on guideway structures for ground transportation system as magnetic-levitation system require the important conceptual structural design parameters. There are variety of design parameters not only design loads, selection of structural section, but also disaster management, engineering planning and design for unexpected loads as well as maintenance and repair of the system. Specific observations on guideways are discussed as loads including seismic loads, vibrations, magnetic forces, breaking forces as well as considering imperfections due to alignment or bumps in case of debris, ice, snow and rain; operational/aerodynamic effects considering vehicle-guideway interaction; deflection, camber and tolerances both in vertical direction and in the horizontal direction, vehicle loads and/or creep, fatigue, and thermal effects must be considered. On the other hand, construction of guideways, route type factor for a specific route including special passes such as tunnels, lakes; foundation systems, problems in tropical areas, structural connections will be considered. To control the system and uncertainties, sensors to provide warning of seismic activity, intelligence for being aware of possible alignment problems, GIS systems are necessary. Vehicle-guideway interaction is another important parameter for the operation of the vehicle, comfort of the passengers, safety and ride comfort. In the design of girders continuity is also important to redistribute the additional unexpected forces and displacements. Other design parameters are air gap, system stability and rocking analysis, emergency stops, switching stations and facilities.

For future studies corrosion of the guideway electronics, deterioration of concrete, corrosion of reinforcement, terror attacks, seismic faults effects, unexpected support settlement, interruption of electromagnetic effects, problems in monitoring and other safety problems will be considered as conceptual design parameters.

Acknowledgements

This work [1] was undertaken in part under USACERL with University of Illinois, with Dr. Can Balkaya and W.J. Hall. We gratefully acknowledge the assistance provided by USACERL and its staff, and particularly the guidance and oversight provided by Mr. Don Plotkin, USACERL.

References

- [1] W.J. Hall and Can Balkaya, 'Final Report on MAGLEV Guideway Design Review, Task-2 Long Term Performance and Seismic Assessment of Maglev Guideways' USACERL, 1993.

- [2] Bechtel Corporation et al, 'Maglev System Concept Definitions' Final Report to US Department of Transportation, Federal Railroad Administration, 1992. (Co-investigators: Hughes; GM Electro-Motive; Draper Laboratory; Massachusetts Institute of Technology).
- [3] Magneplane International Inc., 'System Concept Definition Report for the National Maglev Initiative', 1992. (Co-investigators: Massachusetts Institute of Technology; United Engineers and Constructors; Raytheon Equipment Division; Failure Analysis Associates; Bromwell & Carrier; Beech Aircraft Corporation; Process Systems International).
- [4] Grumman Aerospace Corporation, 'System Concept Definition of a Superconducting Maglev Electromagnetic System' Final Report, 1992. (Co-investigators: Parsons Brinckerhoff; Intermagnetic General Corporation; PSM Technologies; Honeywell; Battelle; Gibbs and Hill; NYSIS).
- [5] Foster-Miller Inc., 'Maglev System Concept Definition Report' Final Report, 1992.
- [6] Don Plotkin and Simon Kim, 'Maglev Guideway Design Issues' Journal of Transportation Engineering, May/June 1997, 189-191.

Optimum Insulation Thickness for the Exterior Walls of Buildings in Turkey Based on Different Materials, Energy Sources and Climate Regions

Cenker Aktemur*[‡], Uğur Atikol*

* Department of Mechanical Engineering, Eastern Mediterranean University, via Mersin 10, Famagusta, N.Cyprus

(cenkeraktemur41@hotmail.com, ugur.atikol@emu.edu.tr)

[‡]Corresponding Author; Cenker Aktemur, Department of Mechanical Engineering, Eastern Mediterranean University, via Mersin 10, Famagusta, N.Cyprus, Tel: +90 538 266 0367

cenkeraktemur_41@hotmail.com

Received: 20.04.2017 Accepted: 21.06.2017

Abstract- Thermal insulation improves the strength and longevity of buildings by reducing energy consumption, and as a related result, improved energy use. The selection of insulation material is governed by important parameters, including the average outdoor air temperature, the thermal conductivity of the buildings and the cost of the insulation material. Increases in the thickness of the insulation material will gradually decrease the energy consumption for heating; however, the insulation thickness has an optimum value that minimises the total investment cost, and determination of this optimum value is critical for economic analysis. In this paper, a life-cycle cost analysis is presented to show the optimum insulation thickness, energy savings over a lifetime of 15 years and payback periods for six different fuels and insulation materials for four cities in Turkey selected from climate regions identified by the Turkish Thermal Insulation Standard (TS 825). Muğla (1st region), Kocaeli (2nd region), Ankara (3rd region) and Ardahan (4th region) were selected for analysis of a sandwich-type wall constructed from the following six insulation materials: extruded polystyrene, expanded polystyrene, glass wool, rock wool, polyisocyanurate and polyurethane. The calculations were also made on the basis of six different fuels, such as motorin, natural gas, propane (LPG), electricity, coal (imported), and fuel-oil No. 4. As a consequence, results demonstrated that the optimum insulation thickness varies between 2.8 cm and 45.1 cm, with energy savings between 16.4 $\text{₺}/\text{m}^2$ and 479 $\text{₺}/\text{m}^2$, and payback periods fluctuating between 0.078 and 0.860 years, depending on the city, the insulation material, and the cost of fuel.

Keywords Energy saving, optimum insulation thickness, payback period, climate region, life-cycle cost.

1. Introduction

Energy is a basic resource needed in all areas of human life, and it is consequently a significant component that influences economic and social development. As an energy source, fossil fuels (fuel oil, natural gas, coal, etc.) are preserving their place as primary energy resources and continue to meet a substantial portion of the world's energy requirements [1].

Statistics presented by the Turkish Ministry of Energy and Natural Resources [2] have indicated that Turkey has the potential for significant energy savings of 30% in the building sector, 20% in the industry sector and 15% in the transportation sector. In the building sector, most of the energy

is consumed as heating energy, and one of the most important methods for reducing heating energy consumption is the use of insulation. The application of thermal insulation to buildings reduces the energy requirements for heating and cooling, thereby conserving fuel.

Many countries have developed new building codes and standards since the 1970s, and these standards have undergone constant renewal due to ever-evolving insulation technology. In Turkey, the TS 825 standard, "Thermal Insulation Rules in Buildings", aims to save energy by reducing the amount of energy consumed in the heating of buildings, as this represents a significant share of the energy consumption in the country.

A substantial 25% of this energy is consumed by the residential sector, and a recent study indicates a savings potential in this sector of between 25 and 45%. In the residential sector, the amount of energy used for heating is twice that used for other sources of consumption (cooking, etc.). Notably, the use of insulation material in the residential sector not only saves energy, but it also reduces the harmful emissions caused by the burning of fossil fuels.

Insulation thickness in buildings is a vital parameter in the design of exterior walls [3], as too low an insulation thickness allows heat to pass from the inside to the outside or from the outside to the inside, resulting in a negative effect on thermal comfort and energy savings. Increasing the insulation thickness in the walls reduces heat loss and the subsequent heating load and fuel cost; however, an increase in insulation thickness results in an increase in insulation investment costs.

The total cost, which is the sum of the costs of the fuel consumption of the building and the insulation, decreases to a certain value and then increases beyond that level [4]. For this reason, it is important that in the optimization of insulation thickness the environment in which the building is located, the type of fuel and the choice of insulation material are all taken into account.

2. A review on the Determination of Optimum Insulation Thickness

The previous studies on the efficient use of energy reported in the literature were generally aimed at determining the optimum insulation thickness and a simple payback period. For example, Dombaycı et al. [5] calculated the optimum insulation thickness for Denizli based on the use of two different insulants and five different fuel types. Similarly, Çomaklı and Yüksel [6] calculated the optimum insulation thickness for the three coldest cities in the fourth DD region of Turkey in accordance with the TS Standard no 825. Bolattürk [7] carried out a comparative analysis to determine the optimum insulation thickness on the outside walls of buildings, whereas Kaynaklı [8] determined the optimum insulation thicknesses for different types of fuel, such as natural gas, coal, fuel oil, propane (LPG) and electricity in a prototype building in Bursa. Kaynaklı and Yamankaradeniz [9] determined the annual fuel costs for the use of natural gas as a fuel with different insulation thicknesses for two different wall types in various climate regions in Turkey.

Gölcü et al. [10] used a life-cycle cost analysis method to calculate the optimum external wall insulation thicknesses, the energy savings and simple payback periods for heating of buildings in the Denizli province of Turkey, based on the use of different energy sources, such as imported coal and fuel oil. Uçar and Balo [11] used a degree-day method and a life-cycle cost analysis method to calculate the optimum insulation thicknesses of the outer walls, the energy savings and simple payback periods for four cities located in four different regions of Turkey (Mersin, Elazığ, Şanlıurfa and Bitlis), five different energy types (coal, natural gas, fuel-oil, LPG and electricity) and three different insulation materials (expanded polystyrene, extruded polystyrene, and rock wool).

Kon and Yüksel [12] conducted a complex three-part study (focused on business and service bureaus, training halls and textile production) in Balıkesir province to determine the optimum insulation thickness and the achievable savings for the exterior walls of buildings. Ozkan and Onan [13], using a new approach, investigated the effects of altering the glazing area percentage of windows, which ranged from 10 to 50%, on the optimum insulation thickness for four regions in Turkey.

Mahlia et al. [14], who analysed the relationship between the thickness of the insulation materials selected for the building walls and the thermal conductivity, found a polynomial function that showed a non-linear relationship between the thermal conductivity and the optimum thickness of the insulation material. This particular study was designed for Malaysia, which is a hot and humid country and does not typically undergo major changes in atmospheric temperature. Kürekçi [15] carried out a similar study to determine the optimum insulation thicknesses required in Turkey's 81 provincial centres, with calculations made based on four different fuels (natural gas, coal, fuel-oil and propane (LPG)) and 5 different insulation materials (extruded polystyrene, expanded polystyrene, glass wool, rock wool and polyurethane).

Ulaş [16] investigated four different heat insulation regions and three different types of fuel for the amount of carbon dioxide released into the atmosphere as a result of the combustion of fuel consumed. The optimum insulation thickness was compared with the insulation thicknesses determined according to TS 825 calculation method. Three different insulation materials (Expanded Polystyrene, Extruded Polystyrene and Glass Wool) and three different fuels (Lignite and Mineral Coal, Natural Gas and Fuel-Oil) were used. The lowest carbon dioxide emissions were found when natural gas is used for Region 1, while the highest carbon dioxide emissions were detected when lignite and coal are used in Region 4.

Hasan [17] calculated the optimum insulation thicknesses for four types of fuel and two insulating materials for Palestine by using the degree-of-day and life cost analysis approach. As a result, he pointed out that the period of payback period for stone wool insulation is between 1.3-2.3 years, for polystyrene insulation is 1-1.7 years. Özel and Pıhtılı [18] calculated the optimum thickness of the insulation applied to the exterior walls for Adana, Elazığ, Erzurum, İstanbul and İzmir considering the heating and cooling degree-day values.

Gürel and Daşdemir [19] calculated the optimum insulation thicknesses and energy savings for heating and cooling loads in Aydın, Edirne, Malatya and Sivas selected from different climatic regions. XPS and EPS were chosen as insulation material in the outer wall. As fuel, natural gas is used for heating and electricity is used for cooling. The results demonstrated that the optimum thickness varies between 0.036 and 0.1 m depending on the insulation material and province selected, the energy savings are between 12.08 ₺ / m² and 58.28 ₺ / m², and payback period vary between 1.5 and 2.52 years.

3. Mathematical Method

3.1 Heating degree-day approach

The base temperature is the temperature at which the generated inner temperature will compensate for the heat loss from the outside. Consequently, the assessment of HDD values depends upon numerous elements including various structural features such as the category of walling, the level of insulation, the presence of air leakage, accessibility of incident sunlight, and so on, as well as the specific climatic circumstances and the personal inclinations of the people using the building. Thus, the number of degree-days is calculated according to the equation (1).

$$HDD = \sum_{j=1}^N (T_b - T_{o,j}) \text{ if } (T_o < T_b) \tag{1}$$

$$HDD = 0 \text{ if } (T_o > T_b) \tag{2}$$

where T_b is base temperature, $T_{o,j}$ is daily mean outside air temperature recorded at a meteorology station, N is the number of days provided that $T_o < T_b$ in a heating season. Therefore, heating degree-day values are calculated as $T_o < T_b$. As it can be seen from equation (2), HDD values only take on positive values.

Turkey is divided into four climate regions for each province according to heating degree-day numbers identified by TS 825 on the map indicated in Fig. 1 below. Region 1 represents the least energy requirement for heating and Region 4 represents the region where energy is needed the most. In this study, the base temperature for heating purpose is assumed as 17.5 °C to calculate heating degree-day values. In the study, insulation analysis was performed for sandwich-type insulated wall-type insulated wall structure using the HDD values of Muğla, Kocaeli, Ankara and Ardahan, which are determined from General of State Meteorology Affairs. Properties and number of heating degree-days of the cities referred to in this study are given in Table 1.

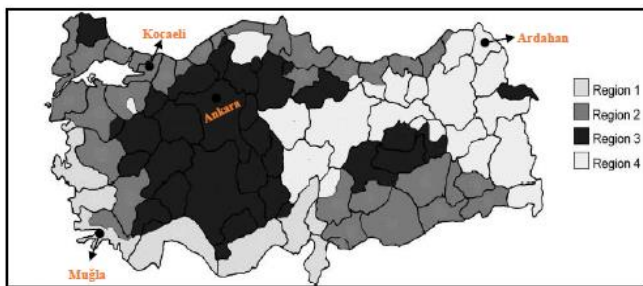


Fig. 1. HDD regions identified by TS 825 in Turkey [21].

The amount of energy required to heat a building, relative to a specific base or reference temperature, is evaluated by the heating degree day (HDD) method.

Table 1. Climate regions and certain data for selected cities

Region	City	Altitude (m)	Longitude (°)	Latitude (°)	HDD (°C-day)
1 st	Muğla	661	28.36 E	37.22 N	1560
2 nd	Kocaeli	465	29.88 E	40.85 N	1762
3 rd	Ankara	896	32.86 E	39.93 N	2425
4 th	Ardahan	1915	42.78 E	41.13 N	4687

3.2 The structure of the external walls

Heat is broadly lost to the building via the exterior walls, windows, floors and ceilings and by ingress of air from the exterior. The majority of heat is lost to buildings through exterior walls constructed of conventional building materials such as perforated bricks, concrete and wood. Hence, the present work took into consideration only heat loss via the external walls in order to evaluate the optimum insulation thickness [22]. The thermal insulation on the outer walls is applied in three ways; internally externally or sandwiched between two walls. Insulation applications are usually carried out by a wall model with a composite structure called a sandwich-type wall. The structure of sandwich-type wall makes up of 3 cm internal plaster, 22 cm horizontal hollow brick, insulation material, 22 cm horizontal hollow brick, and 4 cm external plaster. This structure is used in calculations for analyzed cities. In this case study, a sandwich-type insulated wall depicted in Fig. 2 is examined considering six different insulation materials, namely Extruded polystyrene (XPS), Expanded polystyrene (EPS), Glass wool (GW), Rock wool (RW), Polyisocyanurate (PIR), and Polyurethane (PUR) are pointed out in Table 2 with their thermal conductivities and costs.

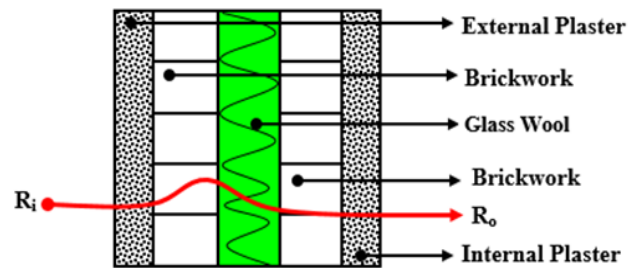


Fig. 2. A cross-view of the sandwich-type insulated wall structure.

Table 2. Parameters of the insulation wall [23]

Insulation material	$k_{ins.}$ (W/mK)	$C_{ins.}$ (₺/m ³)
Extruded polystyrene (XPS)	0.031	300
Expanded polystyrene (EPS)	0.039	200
Glass wool (GW)	0.040	100
Rock wool (RW)	0.040	145
Polyurethane (PUR)	0.024	450
Polyisocyanurate (PIR)	0.023	400

3.3 Heating load for external walls

The transfer of heat into and out of the building, via the walls, involves the processes of radiation, conduction and convection. Solar radiation can be directly absorbed at the outer surface of the walls to produce heat which is then transferred through the bulk of the wall. Further heat can be transferred by convective movements of the atmosphere in contact with both exterior and interior wall surfaces. The amount of heat lost per unit surface area of external wall is obtained from the equation (3) [24].

$$Q = U \times (T_i - T_o) \tag{3}$$

where U is the total heat transfer coefficient of the wall, T_i is the indoor air temperature and T_o is the outdoor air temperature.

The overall heat transfer coefficient of the outside wall (U) that includes a layer of insulation is given by equation (4) [23].

$$U = \frac{1}{R_i + R_w + \frac{x_{ins}}{k_{ins}} + R_o} \tag{4}$$

where R_i and R_o are the heat transfer coefficients of the inside and outside environment respectively, R_w is the thermal resistance of the wall without insulation, x and k are the thickness and thermal conductivity coefficient of the insulation material, respectively. The values of $R_i = 0.13$ W/m²K and $R_o = 0.04$ m²K/W are used for heat transfer coefficients on the inside and outside of the building.

Total resistance of the non-insulated wall layer $R_{w,t}$ is determined by help of the equation (5) below and a brief summary of physical and thermal properties of building construction materials is presented in Table 3 below.

$$R_{w,t} = R_i + R_w + R_o \tag{5}$$

Table 3. Physical and thermal properties of building construction materials of the external wall

Wall structure	Thickness (m)	k (W/mK)	R (m ² K/W)
Internal plaster	0.03	0.87	0.034
Hollow brick	0.22	0.84	0.262
Insulation	See Table 2 for further information		
Hollow brick	0.22	0.84	0.262
External plaster	0.04	0.87	0.046
R_i			0.13
R_o			0.04
$R_{w,t}$			0.774

then, total heat transfer coefficient U is expressed as in the following equation (6).

$$U = \frac{1}{R_{w,t} + \frac{x_{ins.}}{k_{ins.}}} \tag{6}$$

Using the HDD concept, annual heat loss for a unit surface area can be found through the following equation (7) [25].

$$q_{year} = 86400 \times HDD \times U \tag{7}$$

The annual amount of energy required for heating by the heat loss from the unit surface of the outer wall is obtained by

dividing the annual heat loss by the efficiency (η) of the combustion system.

$$E = \frac{q_{year}}{\eta} \tag{8}$$

Equation (7) is substituted into equation (8), then the amount of annual heating energy requirement can be written the following equation (9) [11].

$$E_H = \frac{86400 \times HDD}{\left(R_{w,t} + \frac{x_{ins.}}{k_{ins.}}\right) \times \eta} \tag{9}$$

LHV, efficiencies and prices of various heating systems are indicated in Table 4 below.

Table 4. Fuel costs (C_f) and lower heating values (LHV) of heating systems and efficiencies of fuel (η) [26]

Fuel type	LHV	η (%)	Fuel cost (cf)
Coal (imported)	29.295x10 ⁶ J/kg	66	0.94 ₺/kg
Natural gas	34.526x10 ⁶ J/m ³	90	1.08 ₺/m ³
Propane (LPG)	46.453x10 ⁶ J/kg	88	6.8 ₺/kg
Fuel-oil no:4	40.594x10 ⁶ J/kg	80	2.77 ₺/kg
Motorin	42.636x10 ⁶ J/kg	83	5.49 ₺/kg
Electricity	3.599x10 ⁶ J/kWh	99	0.42 ₺/kWh

3.4 Annual energy cost and calculation of the optimum insulation thickness

The annual fuel cost is obtained by multiplying the amount of fuel to be used per year by the unit price of the fuel. The annual cost of fuel for unit surface area, which is the unit price of the fuel, can be calculated the following equation (11).

$$C_H = m_f \cdot C_f \quad (11)$$

Equation (11) can be rewritten as equation (12):

$$C_H = \frac{86400 \times HDD \times C_f \times PWF}{\left(R_{w,t} + \frac{x_{ins.}}{k_{ins.}}\right) \times \eta \times LHV} \quad (12)$$

where PWF is present value and C_f is the fuel cost in ₺/kg, ₺/m³ or ₺/kWh depending on the fuel type, which can be taken from Table 4 above.

Expected lifetime (LT) and the PWF must be evaluated together while calculating the total heating cost. The PWF value depends on the actual interest rate (r) and time. The interest rate adjusted for inflation rate (i^*) is given by the following equations (13) and (14) [21, 27].

$$i^* = \frac{i - g}{i + g}, \quad \text{for } (i > g) \quad (13)$$

$$i^* = \frac{i + g}{i - g}, \quad \text{for } (i < g) \quad (14)$$

where g is the inflation rate. In this case, PWF is determined by aid of the equation (15):

$$PWF = \frac{(1 + i^*)^{LT} - 1}{i^* (1 + i^*)^{LT}} \quad (15)$$

where LT is the expected lifetime, which is taken to be 15 years. If $i=g$, then

$$PWF = \frac{LT}{1 + i} \quad (16)$$

Lifetime, interest and inflation rate values employed in calculating the PWF are summarized in Table 5.

Table 5. Parameters used in the calculations

Interest rate (i)	9 %
Inflation rate (g)	8.53 %
Lifetime (LT)	15-years
Present worth factor (PWF)	8.58

Since the cost of insulation will increase in proportion to the unit thickness of the insulation material, the cost of insulation is given by the following equation (17).

$$C_{ins} = C_y \cdot x_{ins} \quad (17)$$

The total cost of heating the insulated building in Turkish Lira is given by the equation (18) below.

$$C_{t,H} = C_f \cdot PWF + C_{t,ins} \quad (18)$$

Equation (12) is substituted into equation (18) and then the total heating cost can be written as indicated in the following equation (19).

$$C_{t,H} = \frac{86400 \times HDD \times C_f \times PWF}{\left(R_{w,t} + \frac{x_{ins.}}{k_{ins.}}\right) \times \eta \times LHV} + C_y \cdot x_{ins} \quad (19)$$

Optimum insulation thickness minimizing the total heating cost is calculated with the equation (20) below [6, 7, 10, 11, 27].

$$X_{opt,H} = 293.94 \times \left(\frac{HDD \times C_f \times PWF \times k_{ins}}{LHV \times C_y \times \eta} \right)^{\frac{1}{2}} - k_{ins} \times R_{w,t} \quad (20)$$

As shown by equation (20) above, optimum insulation thickness varies depending on the properties of the wall, insulation material, unit price of fuel, PWF, inflation rate, the fuel type, and the total number of heating degrees-days.

3.5 Simple payback period

In situations where interest rates vary, it is important to consider the period of payback as it is not possible to estimate the long-term interest rate. Interest rates can be estimated to be sensitive for up to 1-2 years. The simple payback period (SPP) is not a method of measuring the economic viability of an investment, but is a method that calculates how many years' incomes will meet expenses. The C_H in the formula represents pre-insulation heating energy costs. Annual total net saving amount for buildings heated is calculated with equation (21) and SPP_H is calculated with equation (22) [21].

$$A_{year,H} = C_H - C_{t,H} \quad (21)$$

$$SPP_H = \frac{C_{ins.}}{A_{year,H}} \quad (22)$$

SPP_H is only meaningful for short periods (typically less than one year) as it does not take into account the time value of money.

4. Results and Discussions

As a widely-used approach for facilitating normalization in the context of energy consumption, the present research employed the HDD technique to determine the optimum insulation thickness for application to the outer walls. Drawing on a sample of four Turkish cities, each situated in a contrasting area of the country characterized by varying climatic conditions, optimum insulation thickness was identified for six categories of fuel and insulation resources. In turn, it was possible for the researcher to determine optimum insulation thickness, energy consumption, and payback period after the insulation materials had been applied to the exterior walls.

Ultimately, insulation and fuel expenses were identified as the central dimensions which impact the overall yearly expense associated with insulating a building, and it should be noted that the loss or gain of thermal energy is lowered for a building that has been insulated. Furthermore, the degree to which the applied insulation is thick is directly and proportionally correlated with the level of heat loss or gain, thereby meaning that overall expense falls in conjunction with a decrease in the thermal energy requirement to heat the unit area. Nevertheless, the fact should not be overlooked that the expense required to apply insulation increases at an almost exponential rate when the thickness of the insulation rises. Subsequently, owing to the elevated insulation expense, overall expense increases significantly once a notable threshold – namely, the optimum insulation thickness figure – has been exceeded. If insulation can be applied at the optimum insulation thickness, the overall cost is minimized to the greatest possible degree. The fuel cost, the insulation cost and the total heating cost relationship with the change of the thickness of the insulation material for selected cities over the 15-year lifetime are shown in the following Fig. 3. As can be seen from Fig. 3, the insulation cost increases linearly while the fuel cost decreases with increasing insulation thickness.

The total cost shows a similar tendency to change depending on the insulation thickness, but the total cost for Ardahan is much higher than for the other cities for all six insulation materials. The total cost of the sum of the cost of fuel and insulation is reduced by a certain value and then increased after this level. In the equation given in (19), the annual heating cost for the non-insulated wall was calculated by taking $x = 0$. Then, in the same equation, total insulation cost was found for the insulated wall by determining the insulation thickness. The heating cost obtained for non-insulated wall of the building is subtracted from the heating cost obtained for the insulated building, and then the annual saving is calculated.

Energy savings are directly proportional to the climatic conditions of the region, and the energy savings for sandwich-type wall. Fig. 4 shows the comparison of energy savings of all insulation materials examined for four cities in case heating requirement is only supplied by Propane (LPG) as an energy source. The optimum insulation thickness is achieved when the savings start to drop as the thickness of insulation material is increased.

The energy saving value becomes maximum at the optimum insulation thickness point. For example, in Ankara, the energy savings is nearly 198.3 ₺/m² at a certain thickness for Polyurethane (PUR), whilst the energy savings for Polyisocyanurate (PIR) is about 288.5 ₺/m². The energy savings in Kocaeli reaches maximum value which is roughly 192 ₺/m² for Polyurethane (PUR) at the optimum insulation thickness. As can be seen from Fig. 4, annual savings for EPS remain the same after a certain insulation thickness (about 0.18 m).

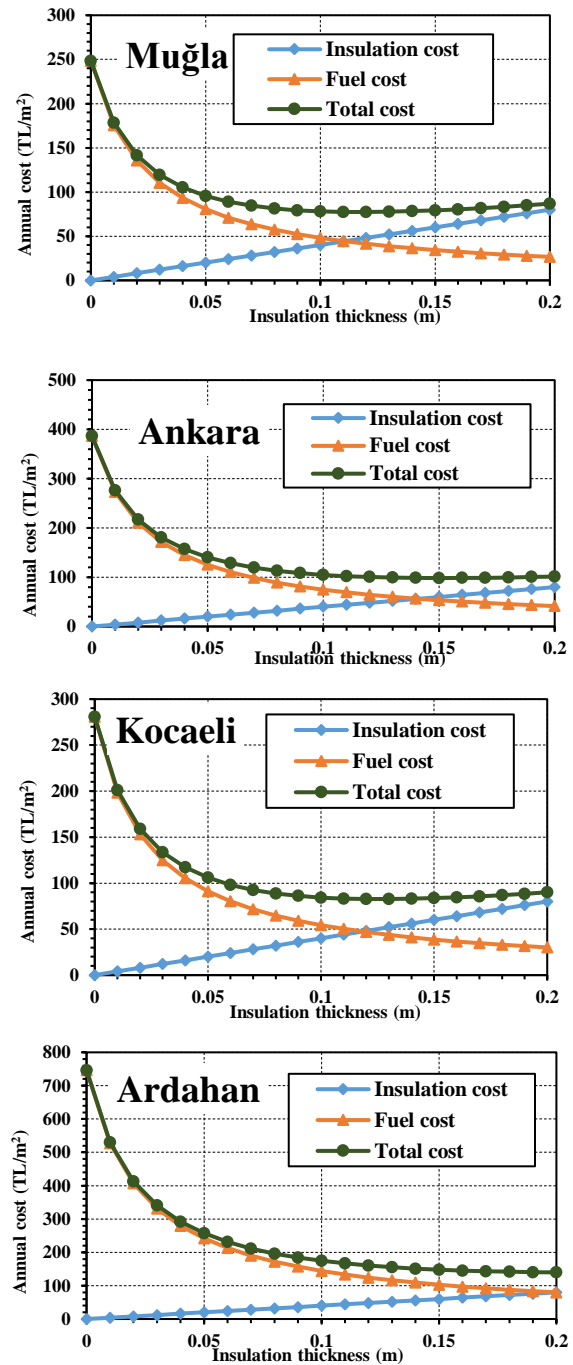


Fig. 3. Effect of insulation thickness of Polyurethane (PUR) on the total cost in case heating energy requirement is only using Propane (LPG) in selected cities.

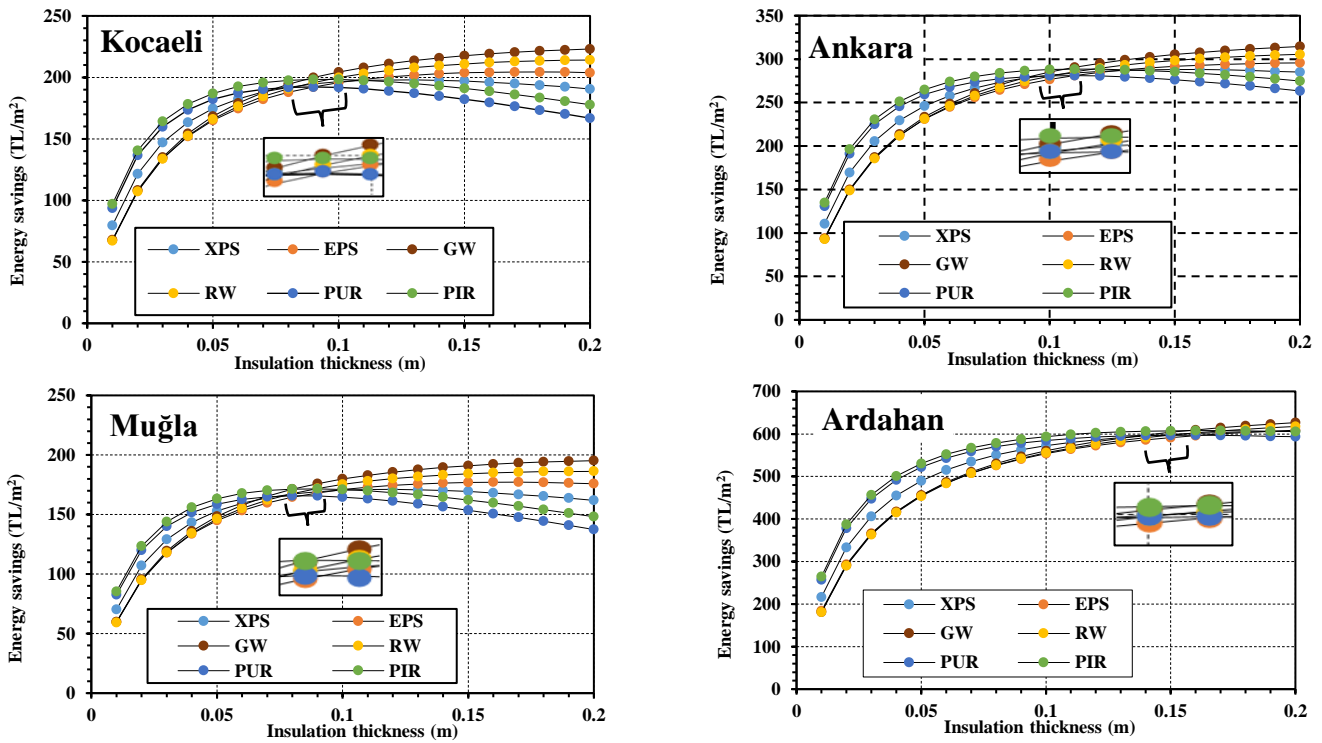


Fig. 4. Comparison of energy savings of all insulation materials for four cities in case heating requirement is only supplied by Propane (LPG) in selected cities.

Optimum insulation thickness is the value that makes the total cost minimum. The optimum insulation thicknesses, energy savings and payback periods for various fuels were calculated for Muğla, Kocaeli, Ankara, and Ardahan selected from four heating degree-day regions, which are given in Tables 6-9. To summarize Tables 6-9, while energy savings are obtained with 117.7 ₺/m² for RW at the optimum insulation thickness (about 24.8 cm) in case of using Propane (LPG) as an energy source in Muğla, energy savings are achieved with 479 ₺/m² for RW at the optimum insulation thickness (about 45 cm) in case of using propane (LPG) as an energy source in Ardahan. Whereas it is determined that the highest energy savings were achieved using Propane (LPG) for all insulation material types, it is detected that the lowest energy savings were attained using natural gas for all insulation material types. Fig. 5 presents optimum insulation

thickness versus various heating systems for different insulation materials in cities of Muğla, Kocaeli, Ankara, and Ardahan.

The variation at the optimum insulation thicknesses determined by HDDs for natural gas and various insulation materials is shown in Fig. 6 below. As the number of HDDs increases, the optimum insulation thickness enhances in parallel and it is clearly seen that glass wool (GW) is significantly higher than the rest insulation materials due to its high thermal conductivity. It is also seen that the optimum insulation thickness is higher in the cases where the HDD value is large, that is, in colder climates. When using EPS as an insulation material, the optimum insulation thickness decreases compared to RW and GW.

Table 6. Optimum insulation thickness, energy savings and payback periods of Muğla for various fuels

Fuel type	Muğla					
	Insulation material type					
	XPS	EPS	PUR	PIR	RW	GW
<i>Optimum insulation thickness (m)</i>						
Natural gas	0,041	0,060	0,028	0,031	0,097	0,076
LPG (propan)	0,118	0,165	0,083	0,088	0,248	0,201
Motorin	0,113	0,158	0,080	0,084	0,238	0,193
Electricity	0,096	0,134	0,067	0,071	0,204	0,164
Fuel-oil no.4	0,078	0,110	0,055	0,058	0,169	0,135
Coal (imported)	0,053	0,076	0,037	0,040	0,120	0,095
<i>Energy savings (TL/m²)</i>						
Natural gas	16,828	17,391	16,399	16,861	19,774	18,426
LPG (propan)	106,470	109,070	104,161	106,633	117,731	113,151
Motorin	98,302	100,774	96,111	98,457	109,039	104,663
Electricity	71,591	73,600	69,829	71,717	80,434	76,795
Fuel-oil no.4	49,007	50,544	47,679	49,102	55,926	53,035
Coal (imported)	25,095	25,973	24,375	25,148	29,325	27,479
<i>Payback period (years)</i>						
Natural gas	0,810	0,748	0,860	0,806	0,770	0,446
LPG (propan)	0,357	0,324	0,388	0,355	0,326	0,190
Motorin	0,371	0,337	0,403	0,369	0,339	0,197
Electricity	0,432	0,392	0,469	0,429	0,394	0,230
Fuel-oil no.4	0,516	0,468	0,559	0,513	0,470	0,274
Coal (imported)	0,693	0,633	0,745	0,689	0,641	0,373

Table 7. Optimum insulation thickness, energy savings and payback periods of Kocaeli for various fuels

Fuel type	Kocaeli					
	Insulation material type					
	XPS	EPS	PUR	PIR	RW	GW
<i>Optimum insulation thickness (m)</i>						
Natural gas	0,045	0,065	0,031	0,034	0,105	0,082
LPG (propan)	0,127	0,177	0,090	0,095	0,265	0,215
Motorin	0,122	0,170	0,086	0,091	0,255	0,207
Electricity	0,103	0,144	0,073	0,077	0,218	0,176
Fuel-oil no.4	0,084	0,118	0,059	0,063	0,181	0,146
Coal (imported)	0,058	0,082	0,040	0,043	0,130	0,103
<i>Energy savings (TL/m²)</i>						
Natural gas	17,126	20,060	14,512	17,310	29,772	24,647
LPG (propan)	181,205	189,021	174,090	181,703	213,809	200,920
Motorin	165,952	173,459	159,121	166,429	197,296	184,897
Electricity	116,309	122,702	110,506	116,715	143,097	132,471
Fuel-oil no.4	74,754	80,016	69,993	75,088	96,920	88,091
Coal (imported)	31,597	35,281	28,290	31,829	47,313	40,994
<i>Payback period (years)</i>						
Natural gas	0,796	0,649	0,972	0,785	0,511	0,333
LPG (propan)	0,210	0,187	0,232	0,208	0,180	0,107
Motorin	0,220	0,196	0,244	0,218	0,187	0,112
Electricity	0,266	0,235	0,296	0,264	0,221	0,133
Fuel-oil no.4	0,338	0,296	0,381	0,335	0,271	0,165
Coal (imported)	0,550	0,466	0,642	0,544	0,397	0,250

Table 8. Optimum insulation thickness, energy savings and payback periods of Ankara for various fuels

Fuel type	Ankara					
	Insulation material type					
	XPS	EPS	PUR	PIR	RW	GW
Optimum insulation thickness (m)						
Natural gas	0,057	0,081	0,040	0,043	0,128	0,102
LPG (propan)	0,153	0,212	0,108	0,114	0,316	0,257
Motorin	0,147	0,204	0,104	0,110	0,304	0,248
Electricity	0,125	0,174	0,088	0,093	0,261	0,212
Fuel-oil no.4	0,103	0,144	0,073	0,077	0,218	0,176
Coal (imported)	0,072	0,102	0,050	0,054	0,157	0,126
Energy savings (TL/m2)						
Natural gas	39,709	42,607	37,126	39,891	52,202	47,139
LPG (propan)	288,078	295,797	281,051	288,570	320,278	307,549
Motorin	265,662	273,076	258,915	266,133	296,617	284,372
Electricity	192,192	198,506	186,460	192,593	218,649	208,154
Fuel-oil no.4	129,778	134,976	125,075	130,108	151,671	142,951
Coal (imported)	63,094	66,734	59,828	63,324	78,618	72,376
Payback period (years)						
Natural gas	0,433	0,382	0,483	0,429	0,356	0,215
LPG (propan)	0,159	0,144	0,174	0,158	0,143	0,084
Motorin	0,166	0,150	0,181	0,165	0,149	0,087
Electricity	0,195	0,176	0,213	0,194	0,173	0,102
Fuel-oil no.4	0,238	0,213	0,261	0,236	0,208	0,123
Coal (imported)	0,342	0,304	0,379	0,340	0,290	0,173

Table 9. Optimum insulation thickness, energy savings and payback periods of Ardahan for various fuels

Fuel type	Ardahan					
	Insulation material type					
	XPS	EPS	PUR	PIR	RW	GW
Optimum insulation thickness (m)						
Natural gas	0,089	0,124	0,062	0,066	0,190	0,153
LPG (propan)	0,221	0,307	0,158	0,165	0,451	0,370
Motorin	0,213	0,295	0,152	0,159	0,435	0,356
Electricity	0,183	0,254	0,130	0,136	0,375	0,306
Fuel-oil no.4	0,152	0,211	0,108	0,113	0,315	0,256
Coal (imported)	0,109	0,152	0,077	0,081	0,230	0,186
Energy savings (TL/m2)						
Natural gas	88,02	88,98	87,25	88,07	92,82	90,69
LPG (propan)	462,30	466,18	458,83	462,55	478,95	472,23
Motorin	429,66	433,36	426,36	429,89	445,56	439,13
Electricity	321,78	324,82	319,08	321,97	335,00	329,61
Fuel-oil no.4	228,54	230,91	226,47	228,69	239,04	234,70
Coal (imported)	125,74	127,17	124,55	125,83	132,41	129,56
Payback period (years)						
Natural gas	0,302	0,280	0,322	0,301	0,297	0,168
LPG (propan)	0,144	0,132	0,155	0,143	0,137	0,078
Motorin	0,149	0,136	0,160	0,148	0,141	0,081
Electricity	0,170	0,156	0,183	0,169	0,162	0,093
Fuel-oil no.4	0,199	0,183	0,214	0,198	0,191	0,109
Coal (imported)	0,260	0,240	0,278	0,259	0,252	0,144

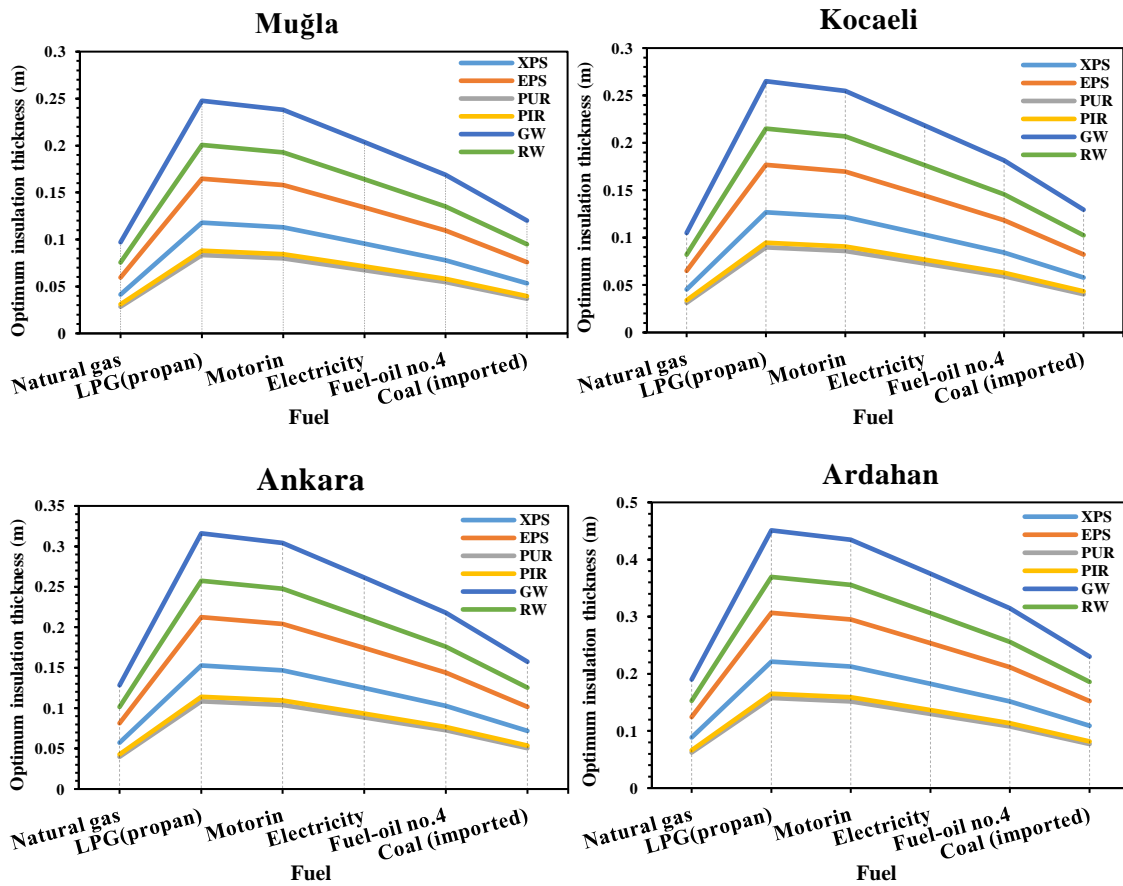


Fig. 5. Optimum insulation thickness versus various heating systems for different insulation materials in cities of Muğla, Kocaeli, Ankara, and Ardahan.

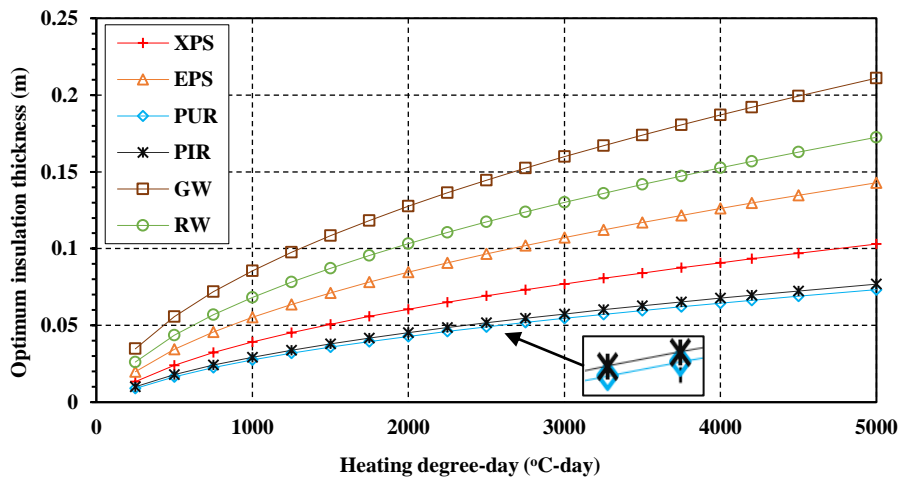


Fig. 6. Alteration of optimum insulation thickness depending on HDDs for different insulation materials in case of utilizing natural gas as an energy source.

5. Conclusions

Thermal insulation is based on two main issues: energy use and the environment. Energy use is a strategic, macro concept in all countries. For example, Turkey is not rich in terms of energy sources, with 60% of its energy requirements being imported from other countries. This is enhancing at an annual rate of 4.4% [6]. Reductions in heating needs can be achieved by minimizing heat losses, so the outer walls of buildings must

be insulated with appropriate insulation materials. These materials are indispensable in the construction of energy efficient buildings; however, achieving the full energy savings potential requires the determination of a solution that optimizes insulation thickness, insulation costs and energy savings.

In this study, insulation material was examined to detect its optimum thickness, as well as its energy savings over a period of 15 years; this includes payback periods in the cities

selected from four different climate regions in Turkey. While calculations were made, six types of energy fuel and insulation materials were considered for sandwich-type wall structure.

The results verify that the optimum insulation thicknesses ranges from 4.1–22.1 cm for XPS, 6–30.7 cm for EPS, 2.8–15.8 cm for PUR, 3.1–16.5 cm for PIR, 9.7–45.1 cm for RW and 7.6–37 cm for GW. The amount of energy savings ranged from 16.8–462.3 $\text{₺}/\text{m}^2$ for XPS, 17.4–466.2 $\text{₺}/\text{m}^2$ for EPS, 16.4–458.8 $\text{₺}/\text{m}^2$ for PUR, 16.9–462.6 $\text{₺}/\text{m}^2$ for PIR, 19.8–479 $\text{₺}/\text{m}^2$ for RW and 18.4–472.2 $\text{₺}/\text{m}^2$ for GW. The payback periods ranged from 0.078– 0.860 years. Based on these data, the greatest energy savings for the four cities is achieved using LPG. Furthermore, the insulation optimum thickness on the exterior walls of the building varies according to the number of heating degree-days and the insulation material used. The increase in fuel costs clearly demonstrates the importance of insulation in residential buildings. Insulation is also necessary for a greater sensitivity to environmental issues, in order to reduce the amount of energy used for heating purposes and the consequent emissions of flue gases into the environment.

References

- [1] A. Aytac & U.T. Aksoy, "Enerji Tasarrufu iç ve Dış Duvarlarda Optimum Yalıtım Kalınlığı ve Isıtma Maliyeti ilişkisi", *J. Gazi Univ. Fac. Eng. Archit.*, vol. 21, pp. 753–758, 2006.
- [2] T. Keskin, "Enerji Verimliliği Kanunu ve Uygulama Süreci", *Mühendis ve Makina*, vol. 569, pp. 106–112, 2007.
- [3] N. Evcil, "Isı İzolasyonu ve Dış Duvarların Enerji Etkin Yenilenmesi", Yüksek Lisans Tezi, İstanbul Teknik Üniversitesi Fen Bilimleri Enstitüsü, İstanbul, 2000.
- [4] İzocam Tic. San. A.Ş., *Isı-Teknik-Ses-Yangın Yalıtımı*, İzocam Ticaret ve Sanayi A.Ş. Yayınları, İstanbul, 2002.
- [5] A. Dombaycı, M. Gölcü & Y. Pancar, "Optimization of insulation thickness for external walls using different energy-sources", *Applied Energy*, vol. 83, pp. 921–928, 2006.
- [6] K. Çomaklı & B. Yüksel, "Optimum insulation thickness of external walls for energy saving", *Applied Thermal Engineering*, vol. 23, pp. 473–479, 2003.
- [7] A. Bolattürk, "Optimum insulation thickness for building walls with respect to cooling and heating degree-hours in the warmest region of Turkey", *Building and Environment*, vol. 43, pp. 1055–1064, 2008.
- [8] O. Kaynaklı, "A study on residential heating energy requirement and optimum insulation thickness", *Renewable Energy*, vol. 33, pp. 1164–1172, 2008.
- [9] O. Kaynaklı & R. Yamankaradeniz, "Isıtma Süreci ve Optimum Yalıtım Kalınlığı Hesabı", VIII. Ulusal Tesisat Mühendisliği Kongresi, pp. 187–195, 2007.
- [10] M. Gölcü, A. Dombaycı & S. Abalı, "Denizli için Optimum Yalıtım Kalınlığının Enerji Tasarrufuna Etkisi ve Sonuçları", *Gazi Üniversitesi Müh. Mim. Fak.Dergisi*, vol. 21, pp. 639–644, 2006.
- [11] A. Uçar & F. Balo, "Determination of the energy savings and the optimum insulation thickness in the four different insulated exterior walls", *Renewable Energy*, vol. 35, pp. 88–94, 2010.
- [12] O. Kon & B. Yüksel, "Konut Dışı Kompleks Yapılar için Optimum Yalıtım Kalınlığı", 18. Ulusal Isı Bilimi ve Tekniği Kongresi, ULIBTK'11, Zonguldak, pp. 604–610, (07–10 Eylül 2011).
- [13] D. B. Özkan & C. Onan, "Optimization of insulation thickness for different glazing areas in buildings for various climatic regions in Turkey", *Applied Energy*, vol. 88, pp. 1331–1342, 2011.
- [14] T.M.I. Mahlia, B. N. Taufiq & H. H. Masjuki, "Correlation between thermal conductivity and the thickness of selected insulation materials for building Wall", *Energy and Buildings*, vol. 39, pp. 182–187, 2007.
- [15] N. A. Kürekçi, "Determination of optimum insulation thickness for building walls by using heating and cooling degree-day values of all Turkey's provincial centers", *Energy and Buildings*, vol. 118, pp. 197–213, 2016.
- [16] A. Ulaş, "Binalarda TS 825 Hesap Yöntemine Göre Isı Kaybı, Yakıt Tüketimi, Karbondioksit Emisyonu Hesabı ve Maliyet Analizi", Gazi Üniversitesi Fen Bilimleri Enstitüsü, Yüksek Lisans Tezi, Ankara, 2010.
- [17] A. Hasan, "Optimizing Insulation Thickness for Buildings Using Life Cycle Cost", *Applied Energy*, vol. 63, pp. 115–124, 1999.
- [18] M. Ozel & K. Pihtili, "Determination of optimum insulation thickness by using heating and cooling degree-day values", *J. Eng. Nat. Sci.*, vol. 26, pp. 191–197, 2008.
- [19] A. Gürel & A. Daşdemir, "Türkiye'nin Dört Farklı İklim Bölgesinde Isıtma ve Soğutma Yükleri İçin Optimum Yalıtım Kalınlıklarının Belirlenmesi", *Erciyes Üniversitesi Fen Bilimleri Enstitüsü Dergisi*, vol. 27, pp. 346–352, 2011.
- [20] H. Sarak & A. Satman, "The degree-day method to estimate the residential heating natural gas consumption in Turkey: a case study", *Energy*, vol. 28, pp. 929–939, 2003.
- [21] N. Sisman, E. Kahya, N. Aras & H. Aras, "Determination of optimum insulation thicknesses of the external walls and roof (ceiling) for Turkey's different degree-day regions", *Energy Policy*, vol. 35, pp. 5151–5155, 2007.
- [22] A. E. Gürel & A. Daşdemir, "Türkiye'nin dört farklı iklim bölgesinde ısıtma ve soğutma yükleri için optimum yalıtım kalınlıklarının belirlenmesi", *Erciyes Üniversitesi Fen Bilimleri Enstitüsü Dergisi*, vol. 27, pp. 346–352, 2016.
- [23] N. A. Kurekci, "Determination of optimum insulation thickness for building walls by using heating and cooling degree-day values of all Turkey's provincial centers", *Energy and Buildings*, vol. 118, pp. 197–213, 2016.
- [24] TSE (Turkish Standards Institution). TS 825: Thermal Insulation in Buildings; 1998.
- [25] N. Daouas, Z. Hassen & H. B. Aissia, "Analytical period solution for the study of thermal performance and optimum insulation thickness of building walls in Tunisia", *Appl Thermal Eng.*, vol. 30, pp. 319–326, 2010.
- [26] M. Tolun, "Farklı derece-gün bölgeleri için yalıtım probleminin incelenmesi", PhD Thesis. Enerji Enstitüsü, 2017.
- [27] A. Aytac & U. T. Aksoy, "Enerji Tasarrufu İçin Dış Duvarlarda Optimum Yalıtım Kalınlığı ve Isıtma Maliyeti ilişkisi", *Gazi Üniversitesi Mühendislik Mimarlık Fakültesi Dergisi*, vol. 21, pp. 753–758, 2006.

Prominence of Hadfield Steel in Mining and Minerals Industries: A Review

Chijioke Okechukwu^{*,***†}, Olurotimi Akintunde Dahunsi^{*}, Peter Kayode Oke^{*}, Isiaka Oluwole Oladele^{**}, Mohammed Dauda^{***}

^{*}Department of Mechanical Engineering, Federal University of Technology, P. M. B. 704, Akure, Ondo State, Nigeria.

^{**}Department of Metallurgical and Materials Engineering, Federal University of Technology, P. M. B. 704, Akure, Ondo State, Nigeria.

^{***}Advanced Manufacturing Technology Programme, P. M. B. 1174, Jalingo, Taraba State, Nigeria
(okerex2002@yahoo.com, oadahunsi@futa.edu.ng, okekayode2002@gmail.com, wolesuccess2000@yahoo.com, mds matt@gmail.com)

[†]Corresponding Author. E-mail Address: okerex2002@yahoo.com; Telephone: +2347031514470

Post Address 1: Department of Mechanical Engineering, Federal University of Technology, P. M. B. 704, Akure, Ondo State, Nigeria.

Postal Address 2: Advanced Manufacturing Technology Programme, P. M. B. 1174, Jalingo, Taraba State, Nigeria

Received: 20.03.2017 Accepted: 21.06.2017

Abstract – High manganese austenitic steel, popularly called “Hadfield steel” has dominated and played significant role in wear applications, especially in the mines and minerals industries since its invention over a century ago. A review on the researches on this steel revealed that its prominence in these fields is mainly due to its good combination of impact and abrasion wear resistance arising from its high toughness and high hardness respectively. Its strain hardening ability under impact loading is evidenced by increase in hardness as the material work hardens; this lowers the amount of wear in service. The work hardening property of the steel has been linked to governing mechanisms such as dislocation, deformation twinning, and dynamic strain ageing; also, it is enhanced by increase in carbon, ageing temperature and reduction in manganese content. Carbide precipitation along the grain boundaries and within the grains is the major cause of embrittlement of the steel. These carbides together with voids and porosities during casting solidification, improper heat treatment, overheating during welding, use of unsorted scrap metal and wrong wear application have been identified as the causes of premature failure in service. Difficulties encountered during machining of the steel have been overcome through hot machining. Hardfacing method has been proposed as a means of substituting the steel in wear applications, as alternative wear materials such as white cast iron and austempered ductile iron lack the combination of impact and abrasion resistance being offered by the Hadfield steel.

Keywords – Hadfield steel, wear, dominance, mining, minerals, machineries

1. Introduction

Mining and minerals processing activities involve subjection of components of machineries to severe wear. The dominant wear modes in these stone and ore handling facilities being abrasion and impact; while abrasive wear requires components with high surface hardness, impact wear calls for component that are internally tough. Producing wear resistant components that combine these properties has been a major concern of researches in this sector. The Hadfield steel, a high manganese austenitic steel has been the dominant material used in the minerals industries since its

invention by Sir Robert Hadfield in 1882 and patented in Britain in 1883 and in the United States in 1884 with patents 303150 and 305151 [1-4].

Unique properties of Hadfield steel include: high hardness, high toughness, and high strain hardening or work hardening capacity with reasonable ductility [5-9]. According to Fadhila *et al.* and other works [5-13], these peculiar properties have paved way for its applications in sectors such as mining, where it is used in grinding mill liners, crusher jaws, impact hammers, cone crusher mantles and concave; transportation, which includes railroad crossings and frogs; military, where it is used in bullet-proof

helmets and naval vessels; agricultural and earthmoving equipment, such as crawler treads for tractors, track links in heavy excavators and dredge buckets. Limooei and Hosseini [14] noted that the steel is a non-magnetic alloy, which makes it relevant in applications where magnetic effect is avoided.

Notwithstanding the attestation of good performance in wear applications given to high manganese austenitic steel, it has some shortcomings during its processing, utilization and repairs. More so, its dominance as a wear material for over a century needs to be whittled. The objects of this paper are to unveil the root cause of the prominence of the steel as a wear component in the mining and mineral processing industries, challenges encountered in processing and service, and provide alternative ways of replacing or substituting the material.

2. Composition and Heat Treatment of Austenitic Manganese Steel

The ASTM A28 stipulates the composition of the austenitic manganese steel as 1.0 – 1.4 %C, 10 – 14 %Mn, and the balance Fe [7,15-17]. Achieving manganese to carbon ratio of 10 is of great importance. The ratio of Mn to C being < 10 and phosphorus > 0.05 in the composition of the steel is believed to be catastrophic [2]. Owen and Grujicic [18] stated that the manganese steel with a nominal composition Fe- 12 %Mn, 1.2 %C is a stable single phase austenitic alloy and is usually annealed prior to use within temperature range of 1000 – 1100°C, and quenched to retain all the carbon in supersaturated solid solution. Balogun *et al.* [1] cautioned that high pouring temperature above 1450 °C should be avoided as segregation of alloying elements occurs above this melting temperature.

Dissolution of carbides is achieved by heat treatment. Usually, a fully austenitic structure, carbide free and homogeneous solid solution having C and Mn in the right proportion is desired. Homogeneity can be achieved by ensuring that as-cast structure is free from segregation, inclusions and pre-existing cracks; additionally, slow solidification or quenching should be avoided as it leads to carbide precipitation, alloy segregation, dendritic structure and grain growth, which adversely affect the ductility and strength of the Hadfield steel [4]. Olawale *et al.* [19] posited that embrittling carbides present in as-cast structure are removed by solution treatment and quenching.

Austenite can be obtained at 1050 °C after holding for 2 hours and water quenching [6]. Likewise, Balogun *et al* [1] recommended an austenitizing temperature of 1050 °C for 4 hours and soaking time of 5 minutes during quenching in water. Additionally, the usual practice in local foundries where the melt is superheated above 1500 °C to enhance fluidity of the melt and ease slag removal should be avoided as it is counter-productive, due to excessive slag formation resulting from the reaction of manganese with the refractory lining, which leads to erosion of the furnace lining and subsequently furnace leakage and lifespan reduction. Figures 1 and 2 explain the effect of heat treatment on carbides.

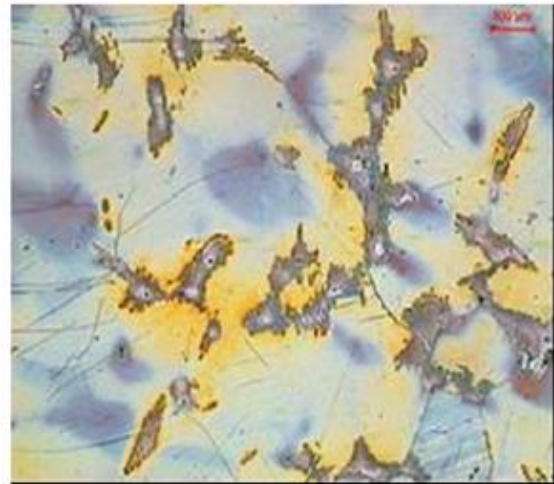


Fig. 1. Microstructure showing carbides in cast high manganese steel before heat treatment [21].

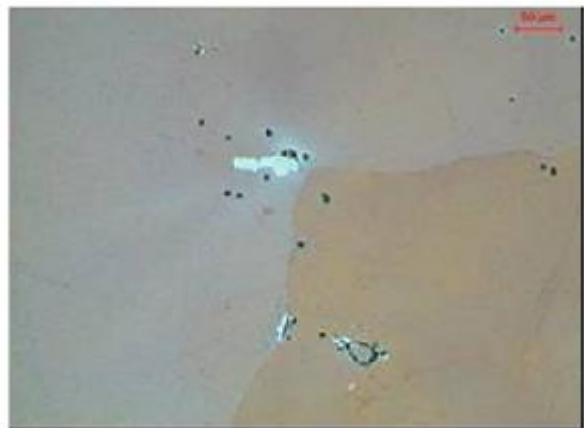


Fig. 2. Carbides in the microstructure of high manganese steel after 5 hours of heat treatment at 1050°C and quenching in water [21].

3. Properties and Alloy Modifications of Hadfield Steel

Hadfield steel exhibits remarkable plastic flow behaviour which is indicated by strain hardening without necking to high levels of strength and strain. This behaviour is valued for severe service applications regardless of its low yield stress [21]. A typical example of this behaviour has been illustrated by Harzallah *et al.* [22] with a rail crossing designated X120Mn12, having composition 1.138 %C, 0.46 %Si, 12.89 %Mn, 0.0033 %P, 0.008 %S and 0.18 %Cr, and mechanical properties as follow: yield strength – 400 MPa, ultimate tensile strength – 1000 MPa, and hardness – 220 HV; with an applied load of 700 N and rolling speed of 275 RPM, the alloy showed the highest surface hardness of 1000 HV after 150,000 cycles, implying four times its initial hardness.

Another railway crossing with composition 1.2 %C, 12.4 %Mn, 0.60 %Si, 0.016 %S, 0.022 %P and the balance Fe,

which was subjected to about 160 million tonne transportation load with a combination of repeated rolling compression and impact forces from train wheels was solution treated and water quenched with the resulting mechanical properties as follow: percentage elongation – 35.8 %, percentage reduction in area – 22.9 %, ultimate tensile strength – 840 MPa, impact toughness – 320 J/cm², and hardness – 225 HV; the average hardness of the deformed steel ranges from 520 to 580 HV [23].

The high toughness of the Hadfield steel results from high strain hardening capacity which enhances stable plastic deformation, thereby avoiding shear localization and loss of load-bearing capacity [24]. Canadinc *et al.* [25] disclosed that the strain hardening response of a manganese steel of composition 13.93 %Mn, 1.3 %C and alloyed with 2.5 %Al was governed by high density dislocation walls that interact with glide dislocations at room temperature. According to Jingpei *et al.* [26], work hardening ability of the austenitic manganese steel increases with carbon and ageing temperature but decreases with increase in manganese; it is enhanced by dispersed secondary particles and dislocation. Reduction in the manganese content results in low austenite stability, which leads to strain-induced martensite transformation and increase in the work hardening ability of the steel.

The work hardening characteristics of the high manganese steel has been attributed to deformation twinning over a wide temperature and strain range, which can combine with any unique ageing effects [27]. Owen and Grujicic [18] apportioned the work hardening behaviour of the steel to dynamic strain ageing, which they described as a direct result of the increase in the number of Mn-C pair produced by the ageing process, and twinning, which adds to the hardening when it occurs.

Additionally, Hai-lun *et al.* [6] observed that the work hardening ability of Hadfield steel castings does not manifest fully when subjected to non-severe impact service conditions. Karaman *et al.* [28] concluded that twinning is the main deformation mechanism in the steel. Also, Mahlami and Pan [17] summarized that work hardening behaviour is responsible for the rapid surface hardening and arises due to dislocation interactions, slips, twins and stacking fault that occur at high impact or compressive loads. Qian *et al.* [23] disclosed that large non-uniformity of hardness distribution in deformed Hadfield steel arises from the underlying non-homogeneous substructure with higher hardness in multiple twin regions and lower hardness in regions where dislocation prevails; hence, hardness value decreases slightly with increasing depth due to larger deformation at locations closer

to component surface which generates increasing work hardening compared to inner locations.

A comparative study of the hardness of as-cast Mn13-steel and explosion depth hardened M13EDH-steel showed the hardness of M13EDH was higher than the as-cast steel having recorded a hardness of 315 HV. However, strain hardening was low in Mn13EDH [30]. Zhang *et al.* [30] showed that a Hadfield steel sample with composition 13 %Mn, 1.2 %C, solidified under a pressure of 6 GPa gave rise to refined grain size $\sim 7.5 \pm 2.5\mu\text{m}$ as against $\sim 160 \pm 45\mu\text{m}$ recorded under pressure when subjected to metallographic examination, x-ray diffraction revealed that M₂₃C₆ carbide was obtained in the steel solidified under 6 GPa, while M₃C was obtained by solidification under normal pressure.

Hadfield steel alloyed with Al and Si and microalloyed with Nb and Ti and subjected to thermomechanical treatment resulted in fine grained structure with the expectation of increase in mechanical properties during subsequent cold plastic deformations [31]. This expectation will be right if the steel obeys Hall-Petch relation which Chinella [21] reported that alloys which obey this relation have increased yield stress and hardness with decrease in their grain size.

Wear resistance of the manganese steel has been raised up to 40 % by addition of titanium and grain refinement [14]. The yield strength, hardening rate and ultimate strength of the steel weld region have been increased by a combination of nitrogen alloying and microstructural refinement [7]. To attain optimal tensile strength, 12 to 13%Mn should be used. Manganese acts as an austenite stabilizer and delays isothermal transformation to bainite. Carbon content below 1 % leads to a decrease in the yield strength. The optimal carbon content has been found to be between 1 and 1.2 %. Above 1.2 %C, yield strength is unaffected; however, > 1.4 %C should not be used as this results in the segregation of carbon to the grain boundaries as carbides, which affects the strength and ductility adversely. Silicon acts as a deoxidizer when present, while chromium increases yield strength and decreases ductility [32].

Also, Balogun *et al.* [1] posited that the presence of chromium in purely austenitic Hadfield steel results in the appearance of cracks arising from elevated internal stresses associated with the liberation of carbides which segregates at grain boundary; however, uniformly dispersed chromium carbides in the base of the austenitic grains provides higher resistance to impact abrasion resistance. Hamada *et al.* [33] stated that strengthening of the steel by addition of manganese offers opportunities for refinement of structure by dynamic recrystallization; similarly, Dobrzański *et al.* [34] reported that dynamic recrystallization occurred in high manganese steel containing 3%Al and 3%Si.

4. Weldability and Failure of the Hadfield Steel

Carbide precipitation is a major challenge encountered during welding of austenitic manganese steel. This is avoided by keeping the temperature of the steel below 300 °C; arc welding, which involves short period of heating has been suggested as a suitable method for this purpose. Work hardening characteristics and plastic deformation of weld overlay have been exhibited by electrode containing molybdenum than electrodes with nickel-chromium and chromium electrodes [11]. Hence, early failure may be prevented by avoiding overheating of the material. High carbon content in the steel makes it difficult to process due to carbide precipitation which results in poor weldability [35].

According to Olawale *et al.* [19], inadequate quenching operations during manufacturing process of the steel leads to the formation of carbide precipitates which embrittle the steel, reduce its ability to withstand shock and create non-uniform plastic flow as the material strain hardens. Also, Curiel-Reyna *et al.* [36] noted that microhardness differences resulted from carbide precipitation arising from post cooling process. High brittleness at the heat affected zone of a welded Hadfield steel originated from the presence of discontinuities or defects as voids, micro-voids, carbides and micro-cracks at the grain boundaries. Figures 3 and 4 show the microstructure of a sound crusher jaw and a failed defective crusher jaw with carbides along the grain boundary and within the grains, respectively.

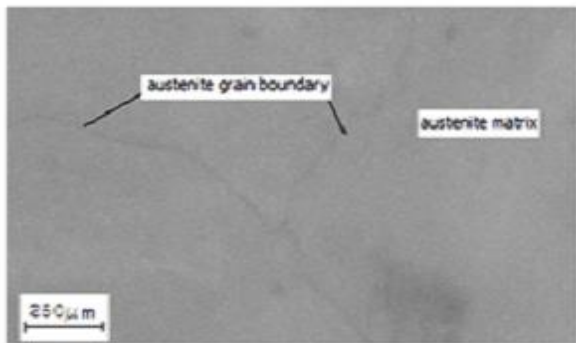


Fig. 3. Optical micrograph of sample of sound crusher jaw showing austenite grain boundaries in austenite matrix [20].

More so, Chojecki and Telejko [20] unveiled the reason for crack formation in service as micro-porosities formed during casting solidification and propagation of the micro-cracks during service conditions involving dynamic stresses. Additionally, castings of wall thickness greater than 60 mm are treated for about 5 hours in foundry practice; this reduces the quantity of carbides to less than 0.8 % and their dimensions to less than 30μm, while secondary carbides are possible nuclei of brittle fracture.

Furthermore, Bhero *et al.* [4] identified major causes of poor field performance of Hadfield steel as: random use of unsorted scrap, improper casting procedures, faulty heat treatment and inappropriate use of product. Slack quenching or warm roll reheating may initiate grain boundary carbide precipitation in high carbon content Hadfield steel, resulting in the introduction of grain boundary void nucleation softening mechanism, leading to plastic instability, low strain and strength [21].

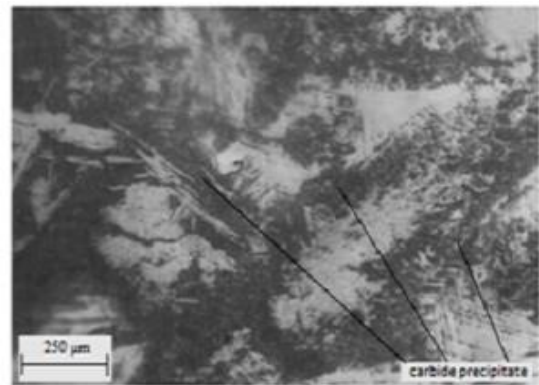


Fig. 4. Optical micrograph of sample of failed crusher jaw showing microstructure of large carbides at the grain boundaries and in the grains of austenite matrix [20].

5. Machinability of Hadfield Steel

Machinability of austenitic manganese steel has been reported to be very low; this has been attributed to its high hardness, strain hardening behaviour, strength, toughness, wear resistance and low thermal conductivity [37,38]. Hadfield steel containing dispersed Ti(CN) has higher wear resistance but severely reduced machinability [37]; consequently, the high manganese steels are referred to as difficult-to-cut materials [39]. Armstrong *et al.* [40] posited that the steel has metastable austenite at room temperature, which transforms to stable martensite during machining. Cebon *et al.* [41] noted that the steel hardens substantially during machining and causes wear of the cutting tool; the degradation of the tool can be linked to the strain hardening while being worked on and the structure of the material after heat treatment.

Strong abrasion and notch wear have been observed when turning Hadfield steel [37]; more so, increase in micro-hardness was recorded from cutting and machining the material [22]. Rapid tool wear occurs as well as built-up edge on cutting tool tip [42]. Increasing the feed rate or cutting speed leads to an increment in the level of hardening [41]; these machining difficulties led to the search for a better way of machining the material. Armstrong *et al.* [40] noted that it was impracticable to machine Hadfield steel at room temperature; however, the material was easily machined at higher temperature and martensite transformation did not

occur; hence, they concluded that hot machining improved the machining property of the material.

According to Çakir [43], hot machining has been established as the solution to the machining challenges of Hadfield steel. This process offers high tool life, better surface finish and higher material removal rates. Potter [44] recommended that the material should be heated to a temperature between 300° C and 420° C, while being machined. Pal and Basu [45] recorded tool lives of 1 min at room temperature, 5 – 6 mins at 400° C, 7 – 8 mins at 500° C and 10 mins at 650° C. The work piece is heated before or during machining around the area being machined. Heating methods that have been used include: plasma arc, electric current, flame, induction, laser and arc heating. Also, hot machining leads to reduced cutting forces and lowers machining costs [46]. Kopac [38] reported that increase in the temperature of the material results in reduction in hardness and the material will likely lose its hardness and related properties after 500° C. Figure 5 shows a diagram of Hadfield steel workpiece undergoing hot machining.

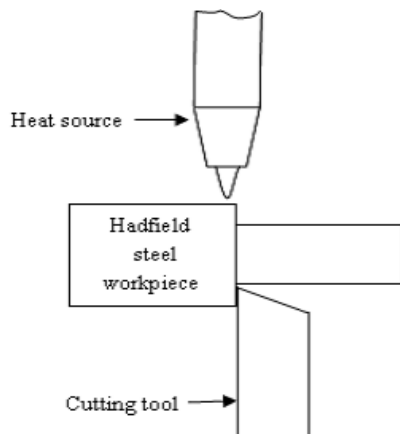


Fig. 5. Hot machining of Hadfield steel.

Uncoated Al_2O_3/TiC mixed with ceramics which composed of 70% of Al_2O_3 and 30% of TiC has been used a cutting tool for the material [47]. Coated $TiAlN$ tools produced by physical vapour deposition method showed lowest surface roughness and cutting forces when compared with $TiCN/Al_2O_3/TiN$ and $TiAlN/AlCrO$ coated by chemical vapour deposition and physical vapour deposition, respectively [39]. While carbide cutting tools have been found to provide better tool life and surface finish than high speed steel tools, cubic boron nitrate tools were more useful as they offer the highest cutting speed of about 200 m/min. Moderate feed rate has been recommended, as lower feed rates would cause higher strain hardening due to longer contact between the cutting tool and workpiece.

Additionally, the depth of cut must be higher than the work-hardened thickness, to prevent higher tool wear [43].

6. Alternative Wear Materials to Hadfield Steel

Low alloy wear resistant steels and high chromium white cast iron are alternative wear materials to Hadfield steel. However, their applications are by either complex manufacturing process or too low toughness [10]. Austempered ductile iron (ADI) has been suggested by Skoczylas *et al.* [48] as a substitute to Hadfield steel due to its excellent combination of strength, ductility and toughness in addition to low weight loss when subjected to abrasive wear test. The authors did not take into cognizance the increase in hardness of the Hadfield steel as it workhardens under impact loading. Modern trend in wear applications is that parts are being hardfaced based on the wear mechanisms and service conditions, which determine the selection of the hardfacing alloy, substrate material and welding method.

7. Conclusions

Findings of different researchers on Hadfield steel regarding its composition requirements, unique combination of mechanical properties, special care and shortcomings are summarized as follow:

The optimal manganese to carbon ratio in the austenitic manganese steel is 10, with carbon ranging from 1 to 1.2 % and manganese content between 12 and 13 %, in order to attain optimal tensile strength. Carbon content greater than 1.4 % leads to segregation of carbides, which results in the embrittlement of the steel.

Wear resistance of the steel can be increased by addition of alloying elements such as titanium or chromium. Explosive depth hardening has been used to increase its hardness prior to use, while appreciable grain refinement has been achieved through solidification under pressure. Dynamic recrystallization in the steel has been associated with the presence of manganese, aluminium and silicon.

High strain hardening ability of the steel favours toughness, while dispersed carbides in the microstructure favours hardness. Work hardening is enhanced by increase in carbon, ageing temperature, dispersed secondary particles and dislocation. It has been associated with mechanisms such as deformation twinning and dynamic strain ageing. The rate of work hardening in as-cast structure is greater than that of a previously hardened bulk material. However, the latter has the advantage of high hardness before use which translates to less wear damage of the latter than the wear in the former. This explains why the steel performs best when subjected to impact and abrasive loading conditions.

Precipitation of carbides at the grain boundaries arises from improper heat treatment procedures such as holding at inadequate austenitizing temperature for a short period and slack quenching. Usually, the carbide precipitates in the microstructure are dissolved by solution treatment at an austenitizing temperature of 1050 °C, at holding time from about 3 hours and above, depending on the amount of carbide present, while quenching in water is carried out at very fast rates to ensure austenitic microstructure. These carbide precipitates embrittle the steel and results in poor weldability.

Difficulties experienced during machining of Hadfield steel arise due its high hardness, strain hardening behaviour, toughness, wear rate and low thermal conductivity. The challenges encountered during machining include: rapid tool wear, hardening of workpiece, built-up edge on cutting tool tip, strong abrasion and notch wear. These have been overcome through the use of hot machining technique, which lowers the cutting forces and machining costs, increases the tool life, offers better surface finish and material removal. Coated carbide tools are more effective in machining the material than high speed steel; however, moderate feed rate should be used, while the depth of cut should be higher than the work-hardened thickness to prevent strain hardening and higher tool wear, respectively.

Alternative wear materials such as white cast iron and austempered ductile iron lack good combination of hardness and toughness to replace Hadfield steel in wear applications; hence, its prominence in the mining and minerals processing industries. Development of economical hardfaced wear components with good combination of hardness and toughness is being proposed as a means of substituting the Hadfield steel in ores and stones processing involving impact and abrasive wears.

References

- [1] Balogun S. A., Esezobor D. E. and Agunsoye J. O., Effect of melting temperature on wear characteristics of austenitic manganese steel, *Journal of Minerals & Materials Characteristics & Engineering*, Vol. 7, pp. 277 – 289, 2008.
- [2] Allahkaram S. R., Causes of catastrophic failure of high Mn steel utilized as crusher overlaying shields, *IJE Transactions B: Applications*, Vol. 21, pp. 55 – 64, 2008.
- [3] Haakonsen F., *Optimizing of Strømhard austenitic manganese steel*, Doctoral Thesis submitted to the Department of Materials Science and Engineering, Norwegian University of Science and Technology, Trondheim, 2009.
- [4] Bhero S. W., Nyembe B. and Lentsoana K., “Common causes of premature failure of Hadfield steel crushers and hammers used in the mining industry”, *International Conference on Mining, Mineral Processing and Metallurgical Engineering, ICMME*, Johannesburg, South Africa, pp. 174 -176, 2013.
- [5] Fadhila R., Jaharah A. G., Omar M. Z., Haron C. H. C., Ghazali M. J., et al., Austenite formation of steel – 3401 subjected to rapid cooling process, *International Journal of Mechanical and Materials Engineering (IJMME)*, Vol. 2, pp. 150 – 153, 2007.
- [6] Hai-lun Y., Jing-pei X, Ai-qin W., Wen-yan W. and Cheng, W., Plastic deformation wear in modified medium manganese steel, *China Foundry*, Vol. 4, pp. 194 – 197, 2007.
- [7] Efstathiou C. and Sehitoglu H., Strengthening Hadfield steel welds by nitrogen alloying, *Materials Science and Engineering A*, Vol. 11, pp. 1 – 6, 2009.
- [8] Efstathiou, C. and Sehitoglu, H., Strain hardening and heterogeneous deformation during twinning in Hadfield steel, *Acta Materialia*, Vol. 58, pp. 1479 – 1488, 2010.
- [9] Hosseini S. and Limoei M. B., Optimization of heat treatment to obtain desired mechanical properties of high carbon Hadfield steels, *World Applied Sciences Journal*, Vol. 15, pp. 1421 – 1424, 2011.
- [10] Qichuan J., Zhenming H. and Yanping C. Influence of carbides and strain-induced martensite on wear resistance of austenitic medium manganese steels, *Chin. J. Met. Sci. Technol.*, Vol. 5, pp. 268 – 272, 1989.
- [11] Mendez J., Ghosh M., Mackay W. B. F., Smith T. J. N., and Smith R. W., Weldability of austenitic manganese steel, *Journal of Materials Processing Technology*, pp. 596 – 602, 2004.
- [12] Xiaodong D., Guodong S., Yifei W., Jianfeng W. and Haoyu y., Abrasion behaviour of high manganese steel under low impact energy and corrosive conditions, *Advances in Tribology*, doi: 10.1155/2009/685648, pp. 1 – 5, 2009.
- [13] Havliček P. and Bušová K., Experience with explosive hardening of railway frogs from Hadfield steel, *Metal*, Vol. 23, 2012.
- [14] Limoei M. B. and Hosseini S., Optimization of properties and structure with addition of titanium in Hadfield steels, *Metal*, Vol. 5, pp. 23 – 25, 2012.
- [15] Subhi A. D. and Abdulrazaq O. A., Phase transformations of Hadfield manganese steels. *Eng. & Technology*, Vol. 25, pp 808 – 814, 2007.
- [16] Safarian J. and Kolbeinsen L., Purity requirements for Mn-alloys for producing high manganese TRIP and TWIP steels, *The Thirteenth International Ferrous Congress*, Almaty, Kazakhstan, pp. 175 – 184, 2013.
- [17] Mahlami C. S. and Pan X., An overview on high manganese steel casting, *71st World Foundry Congress*, Palacio Euskalduna, Bilbao. 19 – 21 May, 2014.
- [18] Owen W. S. and Grujicic, M., Strain aging of austenitic Hadfield manganese steel, *Acta Materialia*, Vol. 47, pp. 111 – 126, 1999.
- [19] Olawale J. O., Ibitoye S. A. and Shittu M. D., Work hardening behaviour and microstructural analysis of failed austenitic manganese steel crusher jaws, *Materials Research*, Vol. 16, pp. 1274 – 1281, 2013.
- [20] Chojecki A. and Telejko I., Cracks in high-manganese cast steel, *Archives of Foundry Engineering*, Vol. 9, pp. 17 – 22, 2009.

- [21] Chinella J. F., Processing and characterization of high strength, high ductility Hadfield steel, *Unclassified Report submitted to U. S. Army Materials Technology Laboratory, Watertown, Massachusetts*, 1990.
- [22] Harzallah R., Mouftiez A., Felder E., Hariri S. and Maujean J. -P., Rolling contact fatigue of Hadfield steel X120Mn12, *Wear*, Vol. 269, pp. 647 – 654, 2010.
- [23] Qian L., Feng X. and Zhang F. Deformed microstructure and hardness of Hadfield high manganese steel, *Materials Transactions*, Vol. 52, pp. 1623 – 1628, 2011.
- [24] Rittel D. and Roman I., Tensile fracture of coarse-grained cast austenitic manganese steels. *Metallurgical Transactions A*, Vol. 19A, pp. 2269 – 2277, 1988.
- [25] Canadinc D., Sehitoglu H., Maier H. J., Niklasch D. and Chumlyakov Y. I., Orientation evolution in Hadfield steel single crystals under combined slip and twinning, *International Journals of Solids and Structures*, Vol. 44, pp. 34 – 50, 2007.
- [26] Jingpei X., Qichuan j., Zhenming H., Quanshun L. and Sommer K., Mechanism of work-hardening for austenitic manganese steel under non-severe impact loading conditions, *Chin. J. Met. Sci. Technol.*, Vol. 8, pp 406 – 410, 1992.
- [27] Tsakiris V. and Edmonds D. V., Martensite and deformation twinning in austenitic steels, *Materials Science and Engineering A*, pp. 430 – 436, 1999.
- [28] Karaman I., Sehitoglu H., Beaudoin A. J., Chumlyakov Y. I., Maier H. J. *et al.*, Modeling the deformation behaviour of Hadfield steel single and polycrystals due to twinning and slip, *Acta Materialia*, Vol. 48, pp. 2031 – 2047, 2000.
- [29] Norberg L., *Fatigue properties of austenitic Mn-steel in explosion depth hardened condition*, A Master Thesis submitted to the Department of Materials and Manufacturing Technology, Chalmers University of Technology, Gothenburg, Sweden, 2010.
- [30] Zhang Y., Li Y., Han B., Zhang F. and Qian L., Microstructural characteristics of Hadfield steel solidified under high pressure. *High Pressure Research: An International Journal*, Vol. 3, pp. 634 – 639, 2011.
- [31] Grajcar A. and Borek W., Thermo-mechanical processing of high-manganese austenitic TWIP-type steels, *Archives of Civil and Mechanical Engineering*, Vol. VIII, pp. 29 – 38, 2008.
- [32] Subramanyam D. K., Swansieger A. E. and Avery H. S., Austenitic manganese steels, 10th Ed., Vol. 1, ASM Metal Handbook, American Society of Metals, pp. 822 – 840, 1990.
- [33] Hamada A. S., Karjalainen L. P. and Somani M. C., The influence of aluminium on hot deformation behaviour and tensile properties of high-Mn TWIP steels, *Materials Science and Engineering A*, Vol. 467, pp. 114 – 124, 2007.
- [34] Dobrzański L. A., Grajcar A. and Borek W., Microstructure evolution and phase composition of high-manganese austenitic steels, *Journal of Achievements in Materials and Manufacturing Engineering*, Vol. 31, pp. 218 – 225., 2008.
- [35] Scott C., Guelton N., Allain S. and Faral M., The development of a new Fe-Mn-C austenitic steel for automotive applications, *Materials Science and Technology Conference*, Pittsburgh, PA, pp. 127 – 138, 25 – 28 September 2005.
- [36] Curiel-Reyna E., Rojas-Rodriguez I., Terán J., Del-Real A., Lara-Guevar A., *et al.*, Postcooling treatment impact on mechanical properties of welded Hadfield steel pieces. *Journal of Emerging Trends in Engineering and Applied Science*, Vol. 5, pp. 105 – 110, 2014.
- [37] Kuljanic, E., Sortino, M., Totis, G. and Prospero, F., Evaluation of commercial tools for machining special alloy Hadfield steel, Retrieved on May 27, 2017, from www.mech-ing.com/journal/Archive/2012/7/MTM/156_Sortino, pp 96 – 99.
- [38] Kopac, J., Hardening phenomena of Mn-austenite steels in the cutting process, *Journal of Materials Processing Technology*, Vol. 109, pp. 96 – 104, 2001.
- [39] Kivak, T., Uzun, G. and Ekici, E., An experimental and statistical evaluation of cutting parameters on the machinability of Hadfield steel, *Gazi University Journal of Science*, Vol. 29, pp. 9 – 17, 2016.
- [40] Armstrong, E., Cosler, A. S., and Katz, E. F., Machining of heated metals, *Trans. Of the ASME*, Vol. 73, pp. 35 – 43, 1951.
- [41] Cebon, M., Kosel, F. and Kopac, J., Effect of cutting on the surface hardness and residual stresses for 12Mn austenitic steel, *Journal of Achievements in Materials and Manufacturing Engineering*, Vol. 55, pp. 80 – 89, 2012.
- [42] Dolinsek, S., Work-hardening in the drilling of austenitic stainless steel, *Journal of Materials Processing Technology*, Vol. 133, pp. 63 – 70, 2003.
- [43] Çakir, O., Machining of Hadfield steel: an overview, *2nd International Conference on Advances in Mechanical Engineering (ICAME2016)*, Proceeding Book, pp. 227 – 232, Yildiz Technical University, Istanbul, Turkey, 11 – 13 May, 2016.
- [44] Potter, W. S., Method of machining manganese steel, United States Patent No. 1,018,001, 1912
- [45] Pal, D. K. and Basu, S. K., Hot machining of austenitic manganese steel by shaping, *International Journal of Machine Tool Design and Research*, Vol. 11, pp. 45 – 61, 1971.
- [46] Çakir, O. and Altan, E., Hot Machining of high manganese steel: a review. *12th International Research/Expert Conference “Trends in the Development of Machinery and Associated Technology” TMT*, Istanbul, Turkey, 26 – 30 August, 2008.

- [47] Horng, J. – T., Liu, N. – M., and Chiang, K. – T., Investigating the machinability evaluation of Hadfield steel in hard turning with Al₂O₃/TiC mixed ceramic tool based on the response surface methodology, *Journal of Materials Processing Technology*, Vol. 208, pp. 532 – 541, 2008.
- [48] Skoczylas P., Krzyńska A. and Kacorowski M., The comparative studies of ADI versus Hadfield cast steel wear resistance, *Archives of Foundry Engineering*, Vol. 11, pp. 123 – 126, 2011.

INTERNATIONAL JOURNAL OF ENGINEERING TECHNOLOGIES-IJET

Guide for Authors

The **International Journal of Engineering Technologies (IJET)** seeks to promote and disseminate knowledge of the various topics of engineering technologies. The journal aims to present to the international community important results of work in the fields of engineering such as imagining, researching, planning, creating, testing, improving, implementing, using and asking. The journal also aims to help researchers, scientists, manufacturers, institutions, world agencies, societies, etc. to keep up with new developments in theory and applications and to provide alternative engineering solutions to current.

The *International Journal of Engineering Technologies* is a quarterly published journal and operates an online submission and peer review system allowing authors to submit articles online and track their progress via its web interface. The journal aims for a publication speed of **60 days** from submission until final publication.

The coverage of IJET includes the following engineering areas, but not limited to:

All filed of engineering such as;

Chemical engineering

- Biomolecular engineering
- Materials engineering
- Molecular engineering
- Process engineering

Civil engineering

- Environmental engineering
- Geotechnical engineering
- Structural engineering
- Transport engineering
- Water resources engineering

Electrical engineering

- Computer engineering
- Electronic engineering
- Optical engineering
- Power engineering

Mechanical engineering

- Acoustical engineering
- Manufacturing engineering
- Thermal engineering
- Vehicle engineering

Systems (interdisciplinary) engineering

- Aerospace engineering
- Agricultural engineering
- Applied engineering
- Biological engineering
- Building services engineering
- Energy engineering
- Railway engineering
- Industrial engineering
- Mechatronics
- Military engineering
- Nano engineering
- Nuclear engineering
- Petroleum engineering

Types of Articles submitted should be original research papers, not previously published, in one of the following categories,

- Applicational and design studies.
- Technology development,
- Comparative case studies.
- Reviews of special topics.
- Reviews of work in progress and facilities development.
- Survey articles.
- Guest editorials for special issues.

Editor-in-Chief and Associate Editors

Editor-in-Chief:

Prof. Dr. Mustafa BAYRAM

Associate Editors:

Prof. Dr. A. Burak POLAT

Assoc. Prof. Dr. Baris SEVIM

Asst. Prof. Dr. Ahmet AKTAS

Asst. Prof. Dr. Yalcin CEKIC

Asst. Prof. Dr. Ali ETEMADI

Ethic Responsibilities

The publication of an article in peer-reviewed “*International Journal of Engineering Technologies*” is an essential building block in the development of a coherent and respected network of knowledge. It is a direct reflection of the quality of the work. Peer-reviewed articles support and embody the scientific method. It is therefore important to agree upon standards of expected ethical behavior for all parties involved in the act of publishing: the author, the journal editor, the peer reviewer, the publisher and the society of society-owned or sponsored journals.

All authors are requested to disclose any actual or potential conflict of interest including any financial, personal or other relationships with other people or organizations within three years of beginning the submitted work that could inappropriately influence, or be perceived to influence, their work.

Submission of an article implies that the work described has not been published previously that it is not under consideration for publication elsewhere. The submission should be approved by all authors and tacitly or explicitly by the responsible authorities where the work was carried out, and that, if accepted, it will not be published elsewhere in the same form, in English or in any other language, including electronically without the written consent of the copyright-holder.

Upon acceptance of an article, authors will be asked to complete a “Copyright Form”. Acceptance of the agreement will ensure the widest possible dissemination of information. An e-mail will be sent to the corresponding author confirming receipt of the manuscript together with a “Copyright Form” form or a link to the online version of this agreement.

Author Rights

As a journal author, you retain rights for a large number of author uses, including use by your employing institute or company. These rights are retained and permitted without the need to obtain specific permission from *IJET*. These include:

- ❖ The right to make copies (print or electronic) of the journal article for your own personal use, including for your own classroom teaching use;
- ❖ The right to make copies and distribute copies (including via e-mail) of the journal article to research colleagues, for personal use by such colleagues for scholarly purposes;
- ❖ The right to post a pre-print version of the journal article on internet web sites including electronic pre-print servers, and to retain indefinitely such version on such servers or sites for scholarly purposes
- ❖ the right to post a revised personal version of the text of the final journal article on your personal or institutional web site or server for scholarly purposes
- ❖ The right to use the journal article or any part thereof in a printed compilation of your works, such as collected writings or lecture notes.

Article Style

Authors must strictly follow the guide for authors, or their articles may be rejected without review. Editors reserve the right to adjust the style to certain standards of uniformity. Follow Title, Authors, Affiliations, Abstract, Keywords, Introduction, Materials and Methods, Theory/Calculation, Conclusions, Acknowledgements, References order when typing articles. The corresponding author should be identified with an asterisk and footnote. Collate acknowledgements in a separate section at the end of the article and do not include them on the title page, as a footnote to the title or otherwise.

Abstract and Keywords:

Enter an abstract of up to 250 words for all articles. This is a concise summary of the whole paper, not just the conclusions, and is understandable without reference to the rest of the paper. It should contain no citation to other published work. Include up to six keywords that describe your paper for indexing purposes.

Abbreviations and Acronyms:

Define abbreviations and acronyms the first time they are used in the text, even if they have been defined in the abstract. Abbreviations such as IEEE, SI, MKS, CGS, sc, dc, and rms do not have to be defined. Do not use abbreviations in the title unless they are unavoidable.

Text Layout for Peer Review:

Use single column layout, double spacing and wide (3 cm) margins on white paper at the peer review stage. Ensure that each new paragraph is clearly indicated. Present tables and figure legends in the text where they are related and cited. Number all pages consecutively; use 12 pt font size and standard fonts; Times New Roman, Helvetica, or Courier is preferred.

Research Papers should not exceed 12 printed pages in two-column publishing format, including figures and tables.

Technical Notes and Letters should not exceed 2,000 words.

Reviews should not exceed 20 printed pages in two-column publishing format, including figures and tables.

Equations:

Number equations consecutively with equation numbers in parentheses flush with the right margin, as in (1). To make equations more compact, you may use the solidus (/), the exp function, or appropriate exponents. Italicize Roman symbols for quantities and variables, but not Greek symbols. Use an dash (–) rather than a hyphen for a minus sign. Use parentheses to avoid ambiguities in denominators. Punctuate equations with commas or periods when they are part of a sentence, as in

$$C = a + b \tag{1}$$

Symbols in your equation should be defined before the equation appears or immediately following. Use “Eq. (1)” or “equation (1),” while citing.

Figures and Tables:

All illustrations must be supplied at the correct resolution:

- * Black and white and colour photos - 300 dpi
- * Graphs, drawings, etc - 800 dpi preferred; 600 dpi minimum
- * Combinations of photos and drawings (black and white and color) - 500 dpi

In addition to using figures in the text, upload each figure as a separate file in either .tiff or .eps format during submission, with the figure number.

Table captions should be written in the same format as figure captions; for example, “Table 1. Appearance styles.”. Tables should be referenced in the text unabbreviated as “Table 1.”

References:

Please ensure that every reference cited in the text is also present in the reference list (and viceversa). Any references cited in the abstract must be given in full. Unpublished results and personal communications are not recommended in the reference list, but may be mentioned in the text. Citation of a reference as “in press” implies that the item has been accepted for publication. Number citations consecutively in square brackets [1]. Punctuation follows the bracket [2]. Refer simply to the reference number, as in [3]. Use “Ref. [3]” or Reference [3]” at the beginning of a sentence: “Reference [3] was ...”. Give all authors’ names; use “et al.” if there are six authors or more. For papers published in translated journals, first give the English citation, then the original foreign-language citation.

Books

- [1] J. Clerk Maxwell, *A Treatise on Electricity and Magnetism*, 3rd ed., vol. 2. Oxford:Clarendon Press, 1892, pp.68-73.

Journals

- [2] Y. Yorozu, M. Hirano, K. Oka, and Y. Tagawa, “Electron spectroscopy studies on magneto-optical media and plastic substrate interface”, *IEEE Transl. J. Magn. Japan*, vol. 2, pp. 740-741, August 1987.

Conferences

- [3] Çolak I., Kabalci E., Bayindir R., and Sagiroglu S, “The design and analysis of a 5-level cascaded voltage source inverter with low THD”, *2nd PowerEng Conference*, Lisbon, pp. 575-580, 18-20 March 2009.

Reports

- [4] IEEE Standard 519-1992, Recommended practices and requirements for harmonic control in electrical power systems, *The Institute of Electrical and Electronics Engineers*, 1993.

Text Layout for Accepted Papers:

A4 page margins should be margins: top = 24 mm, bottom = 24 mm, side = 15 mm. Main text should be given in two column. The column width is 87mm (3.425 in). The space between the two columns is 6 mm (0.236 in). Paragraph indentation is 3.5 mm (0.137 in). Follow the type sizes specified in Table. Position figures and tables at the tops and bottoms of columns. Avoid placing them in the middle of columns. Large figures and tables may span across both columns. Figure captions should be centred below the figures; table captions should be centred above. Avoid placing figures and tables before their first mention in the text. Use the abbreviation “Fig. 1,” even at the beginning of a sentence.

Type size (pts.)	Appearance		
	Regular	Bold	<i>Italic</i>
10	Authors’ affiliations, Section titles, references, tables, table names, first letters in table captions, figure captions, footnotes, text subscripts, and superscripts	Abstract	
12	Main text, equations, Authors’ names, ^a		<i>Subheading (1.1.)</i>
24	Paper title		

Submission checklist:

It is hoped that this list will be useful during the final checking of an article prior to sending it to the journal's Editor for review. Please consult this Guide for Authors for further details of any item. Ensure that the following items are present:

- ❖ One Author designated as corresponding Author:
- E-mail address
- Full postal address
- Telephone and fax numbers

❖ All necessary files have been uploaded

- Keywords: a minimum of 4
- All figure captions (supplied in a separate document)
- All tables (including title, description, footnotes, supplied in a separate document)

❖ Further considerations

- Manuscript has been "spellchecked" and "grammar-checked"
- References are in the correct format for this journal
- All references mentioned in the Reference list are cited in the text, and vice versa
- Permission has been obtained for use of copyrighted material from other sources (including the Web)
- Color figures are clearly marked as being intended for color reproduction on the Web (free of charge) and in print or to be reproduced in color on the Web (free of charge) and in black-and-white in print.

Article Template Containing Author Guidelines for Peer-Review

First Author*, Second Author**‡, Third Author***

*Department of First Author, Faculty of First Author, Affiliation of First Author, Postal address

**Department of Second Author, Faculty of First Author, Affiliation of First Author, Postal address

***Department of Third Author, Faculty of First Author, Affiliation of First Author, Postal address

(First Author Mail Address, Second Author Mail Address, Third Author Mail Address)

‡Corresponding Author; Second Author, Postal address, Tel: +90 312 123 4567, Fax: +90 312 123 4567, corresponding@affl.edu

Received: xx.xx.xxxx Accepted:xx.xx.xxxx

Abstract- Enter an abstract of up to 250 words for all articles. This is a concise summary of the whole paper, not just the conclusions, and is understandable without reference to the rest of the paper. It should contain no citation to other published work. Include up to six keywords that describe your paper for indexing purposes. Define abbreviations and acronyms the first time they are used in the text, even if they have been defined in the abstract. Abbreviations such as IEEE, SI, MKS, CGS, sc, dc, and rms do not have to be defined. Do not use abbreviations in the title unless they are unavoidable.

Keywords- Keyword1; keyword2; keyword3; keyword4; keyword5.

2. Introduction

Authors should use any word processing software that is capable to make corrections on misspelled words and grammar structure according to American or Native English. Authors may get help by from word

processor by making appeared the paragraph marks and other hidden formatting symbols. This sample article is prepared to assist authors preparing their articles to IJET.

Indent level of paragraphs should be 0.63 cm (0.24 in) in the text of article. Use single column layout, double-spacing and wide (3 cm) margins on white paper at the peer review stage. Ensure that each new paragraph is clearly indicated. Present tables and figure legends in the text where they are related and cited. Number all pages consecutively; use 12 pt font size and standard fonts; Times New Roman, Helvetica, or Courier is preferred. Indicate references by number(s) in square brackets in line with the text. The actual authors can be referred to, but the reference number(s) must always be given. Example: "..... as demonstrated [3, 6]. Barnaby and Jones [8] obtained a different result"

IJET accepts submissions in three styles that are defined as Research Papers, Technical Notes and Letter, and Review paper. The requirements of paper are as listed below:

- Research Papers should not exceed 12 printed pages in two-column publishing format, including figures and tables.
- Technical Notes and Letters should not exceed 2,000 words.
- Reviews should not exceed 20 printed pages in two-column publishing format, including figures and tables.

Authors are requested write equations using either any mathematical equation object inserted to word processor or using independent equation software. Symbols in your equation should be defined before the equation appears or immediately following. Use "Eq. (1)" or "equation (1)," while citing. Number equations consecutively with equation numbers in parentheses flush with the right margin, as in Eq. (1). To make equations more compact, you may use the solidus (/), the exp function, or appropriate exponents. Italicize Roman symbols for quantities and variables, but not Greek symbols. Use an dash (–) rather than a hyphen for a minus sign. Use parentheses to avoid ambiguities in denominators. Punctuate equations with commas or periods when they are part of a sentence, as in

$$C = a + b \tag{1}$$

Section titles should be written in bold style while sub section titles are italic.

3. Figures and Tables

3.1. Figure Properties

All illustrations must be supplied at the correct resolution:

- Black and white and colour photos - 300 dpi
- Graphs, drawings, etc - 800 dpi preferred; 600 dpi minimum
- Combinations of photos and drawings (black and white and colour) - 500 dpi

In addition to using figures in the text, Authors are requested to upload each figure as a separate file in either .tiff or .eps format during submission, with the figure number as Fig.1., Fig.2a and so on. Figures are cited as “Fig.1” in sentences or as “Figure 1” at the beginning of sentence and paragraphs. Explanations related to figures should be given before figure. Figures and tables should be located at the top or bottom side of paper as done in accepted article format.



Figure 1. Engineering technologies.

Table captions should be written in the same format as figure captions; for example, “Table 1. Appearance styles.”. Tables should be referenced in the text unabbreviated as “Table 1.”

Table 1. Appearance properties of accepted manuscripts

Type size (pts.)	Appearance		
	Regular	Bold	<i>Italic</i>
10	Authors’ affiliations, Abstract, keywords, references, tables, table names, figure captions, footnotes, text subscripts, and superscripts	Abstract	
12	Main text, equations, Authors’ names, Section titles		<i>Subheading (1.1.)</i>
24	Paper title		

4. Submission Process

The *International Journal of Engineering Technologies* operates an online submission and peer review system that allows authors to submit articles online and track their progress via a web interface. Articles that are prepared referring to this template should be controlled according to submission checklist given in “Guide f Authors”. Editor handles submitted articles to IJET primarily in order to control in terms of compatibility to aims and scope of Journal.

Articles passed this control are checked for grammatical and template structures. If article passes this control too, then reviewers are assigned to article and Editor gives a reference number to paper. Authors registered to online submission system can track all these phases.

Editor also informs authors about processes of submitted article by e-mail. Each author may also apply to Editor via online submission system to review papers related to their study areas. Peer review is a critical element of publication, and one of the major cornerstones of the scientific process. Peer Review serves two key functions:

- Acts as a filter: Ensures research is properly verified before being published
- Improves the quality of the research

5. Conclusion

The conclusion section should emphasize the main contribution of the article to literature. Authors may also explain why the work is important, what are the novelties or possible applications and extensions. Do not replicate the abstract or sentences given in main text as the conclusion.

Acknowledgements

Authors may acknowledge to any person, institution or department that supported to any part of study.

References

- [1] J. Clerk Maxwell, *A Treatise on Electricity and Magnetism*, 3rd ed., vol. 2. Oxford:Clarendon Press, 1892, pp.68-73.
(Book)
- [2] H. Poor, *An Introduction to Signal Detection and Estimation*, New York: Springer-Verlag, 1985, ch. 4. (Book Chapter)
- [3] Y. Yorozu, M. Hirano, K. Oka, and Y. Tagawa, "Electron spectroscopy studies on magneto-optical media and plastic substrate interface", *IEEE Transl. J. Magn. Japan*, vol. 2, pp. 740-741, August 1987. (Article)
- [4] E. Kabalcı, E. Irmak, I. Çolak, "Design of an AC-DC-AC converter for wind turbines", *International Journal of Energy Research*, Wiley Interscience, DOI: 10.1002/er.1770, Vol. 36, No. 2, pp. 169-175. (Article)
- [5] I. Çolak, E. Kabalci, R. Bayindir R., and S. Sagiroglu, "The design and analysis of a 5-level cascaded voltage source inverter with low THD", *2nd PowerEng Conference*, Lisbon, pp. 575-580, 18-20 March 2009. (Conference Paper)
- [6] IEEE Standard 519-1992, Recommended practices and requirements for harmonic control in electrical power systems, *The Institute of Electrical and Electronics Engineers*, 1993. (Standards and Reports)

Article Template Containing Author Guidelines for Accepted Papers

First Author*, Second Author**‡, Third Author***

*Department of First Author, Faculty of First Author, Affiliation of First Author, Postal address

**Department of Second Author, Faculty of First Author, Affiliation of First Author, Postal address

***Department of Third Author, Faculty of First Author, Affiliation of First Author, Postal address

(First Author Mail Address, Second Author Mail Address, Third Author Mail Address)

‡Corresponding Author; Second Author, Postal address, Tel: +90 312 123 4567,

Fax: +90 312 123 4567, corresponding@affl.edu

Received: xx.xx.xxxx Accepted:xx.xx.xxxx

Abstract- Enter an abstract of up to 250 words for all articles. This is a concise summary of the whole paper, not just the conclusions, and is understandable without reference to the rest of the paper. It should contain no citation to other published work. Include up to six keywords that describe your paper for indexing purposes. Define abbreviations and acronyms the first time they are used in the text, even if they have been defined in the abstract. Abbreviations such as IEEE, SI, MKS, CGS, sc, dc, and rms do not have to be defined. Do not use abbreviations in the title unless they are unavoidable.

Keywords Keyword1, keyword2, keyword3, keyword4, keyword5.

1. Introduction

Authors should use any word processing software that is capable of making corrections on misspelled words and grammar structure according to American or Native English. Authors may get help from a word processor by making sure the paragraph marks and other hidden formatting symbols are visible. This sample article is prepared to assist authors in preparing their articles for IJET.

The indent level of paragraphs should be 0.63 cm (0.24 in) in the text of the article. Use single column layout, double-spacing and wide (3 cm) margins on white paper at the peer review stage. Ensure that each new paragraph is clearly indicated. Present tables and figure legends in the text where they are related and cited. Number all pages consecutively; use 12 pt font size and standard fonts; Times New Roman, Helvetica, or Courier is preferred. Indicate references by number(s) in square brackets in line with the text. The actual authors can be referred to, but the reference number(s) must always be

given. Example: "... as demonstrated [3,6]. Barnaby and Jones [8] obtained a different result ..."

IJET accepts submissions in three styles that are defined as Research Papers, Technical Notes and Letters, and Review paper. The requirements for paper are as listed below:

➤ Research Papers should not exceed 12 printed pages in two-column publishing format, including figures and tables.

➤ Technical Notes and Letters should not exceed 2,000 words.

➤ Reviews should not exceed 20 printed pages in two-column publishing format, including figures and tables.

Authors are requested to write equations using either any mathematical equation object inserted into the word processor or using independent equation software. Symbols in your equation should be defined before the equation appears or immediately following. Use "Eq. (1)" or "equation (1),"

while citing. Number equations consecutively with equation numbers in parentheses flush with the right margin, as in Eq. (1). To make equations more compact, you may use the solidus (/), the exp function, or appropriate exponents. Italicize Roman symbols for quantities and variables, but not Greek symbols. Use an dash (-) rather than a hyphen for a minus sign. Use parentheses to avoid ambiguities in denominators. Punctuate equations with commas or periods when they are part of a sentence, as in

$$C = a + b \quad (1)$$

Section titles should be written in bold style while sub section titles are italic.

6. Figures and Tables

6.1. Figure Properties

All illustrations must be supplied at the correct resolution:

- Black and white and colour photos - 300 dpi
- Graphs, drawings, etc - 800 dpi preferred; 600 dpi minimum
- Combinations of photos and drawings (black and white and colour) - 500 dpi

In addition to using figures in the text, Authors are requested to upload each figure as a separate file in either

Table 1. Appearance properties of accepted manuscripts

Type size (pts.)	Appearance		
	Regular	Bold	<i>Italic</i>
10	Main text, section titles, authors' affiliations, abstract, keywords, references, tables, table names, figure captions, equations, footnotes, text subscripts, and superscripts	Abstract-	<i>Subheading (1.1.)</i>
12	Authors' names,		
24	Paper title		

6.2. Text Layout for Accepted Papers

A4 page margins should be margins: top = 24 mm, bottom = 24 mm, side = 15 mm. The column width is 87mm (3.425 in). The space between the two columns is 6 mm (0.236 in). Paragraph indentation is 3.5 mm (0.137 in). Follow the type sizes specified in Table. Position figures and tables at the tops and bottoms of columns. Avoid placing them in the middle of columns. Large figures and tables may span across both columns. Figure captions should be centred below the figures; table captions should be centred above. Avoid placing figures and tables before their first mention in

.tiff or .eps format during submission, with the figure number as Fig.1., Fig.2a and so on. Figures are cited as "Fig.1" in sentences or as "Figure 1" at the beginning of sentence and paragraphs. Explanations related to figures should be given before figure.



Fig. 1. Engineering technologies.

Figures and tables should be located at the top or bottom side of paper as done in accepted article format. Table captions should be written in the same format as figure captions; for example, "Table 1. Appearance styles.". Tables should be referenced in the text unabbreviated as "Table 1."

the text. Use the abbreviation "Fig. 1," even at the beginning of a sentence.

7. Submission Process

The International Journal of Engineering Technologies operates an online submission and peer review system that allows authors to submit articles online and track their progress via a web interface. Articles that are prepared referring to this template should be controlled according to submission checklist given in "Guide f Authors". Editor handles submitted articles to IJET primarily in order to control in terms of compatibility to aims and scope of Journal. Articles passed this control are checked for

grammatical and template structures. If article passes this control too, then reviewers are assigned to article and Editor gives a reference number to paper. Authors registered to online submission system can track all these phases. Editor also informs authors about processes of submitted article by e-mail. Each author may also apply to Editor via online submission system to review papers related to their study areas. Peer review is a critical element of publication, and one of the major cornerstones of the scientific process. Peer Review serves two key functions:

- Acts as a filter: Ensures research is properly verified before being published
- Improves the quality of the research

8. Conclusion

The conclusion section should emphasize the main contribution of the article to literature. Authors may also explain why the work is important, what are the novelties or possible applications and extensions. Do not replicate the abstract or sentences given in main text as the conclusion.

Acknowledgements

Authors may acknowledge to any person, institution or department that supported to any part of study.

References

- [7] J. Clerk Maxwell, A Treatise on Electricity and Magnetism, 3rd ed., vol. 2. Oxford:Clarendon Press, 1892, pp.68-73. (Book)
- [8] H. Poor, An Introduction to Signal Detection and Estimation, New York: Springer-Verlag, 1985, ch. 4. (Book Chapter)
- [9] Y. Yorozu, M. Hirano, K. Oka, and Y. Tagawa, "Electron spectroscopy studies on magneto-optical media and plastic substrate interface", IEEE Transl. J. Magn. Japan, vol. 2, pp. 740-741, August 1987. (Article)
- [10] E. Kabalcı, E. Irmak, I. Çolak, "Design of an AC-DC-AC converter for wind turbines", International Journal of Energy Research, Wiley Interscience, DOI: 10.1002/er.1770, Vol. 36, No. 2, pp. 169-175. (Article)
- [11] I. Çolak, E. Kabalcı, R. Bayindir R., and S. Sagiroglu, "The design and analysis of a 5-level cascaded voltage source inverter with low THD", 2nd PowerEng Conference, Lisbon, pp. 575-580, 18-20 March 2009. (Conference Paper)
- [12] IEEE Standard 519-1992, Recommended practices and requirements for harmonic control in electrical power systems, The Institute of Electrical and Electronics Engineers, 1993. (Standards and Reports)

**INTERNATIONAL JOURNAL OF ENGINEERING TECHNOLOGIES (IJET)
COPYRIGHT AND CONSENT FORM**

This form is used for article accepted to be published by the IJET. Please read the form carefully and keep a copy for your files.

TITLE OF ARTICLE (hereinafter, "The Article"):

.....
.....
.....

LIST OF AUTHORS:

.....
.....
.....

CORRESPONDING AUTHOR'S ("The Author") NAME, ADDRESS, INSTITUTE AND EMAIL:

.....
.....
.....

COPYRIGHT TRANSFER

The undersigned hereby transfers the copyright of the submitted article to International Journal of Engineering Technologies (the "IJET"). The Author declares that the contribution and work is original, and he/she is authorized by all authors and/or grant-funding agency to sign the copyright form. Author hereby assigns all including but not limited to the rights to publish, distribute, reprints, translates, electronic and published derivatives in various arrangements or any other versions in full or abridged forms to IJET. IJET holds the copyright of Article in its own name.

Author(s) retain all rights to use author copy in his/her educational activities, own websites, institutional and/or funder's web sites by providing full citation to final version published in IJET. The full citation is provided including Authors list, title of the article, volume and issue number, and page number or using a link to the article in IJET web site. Author(s) have the right to transmit, print and share the first submitted copies with colleagues. Author(s) can use the final published article for his/her own professional positions, career or qualifications by citing to the IJET publication.

Once the copyright form is signed, any changes about the author names or order of the authors listed above are not accepted by IJET.

Authorized/Corresponding Author

Date/ Signature